ABSTRACT

Title of Document: **FUNCTIONAL INSIGHTS INTO HRG-1-MEDIATED HEME TRANSPORT**

Xiaojing Yuan, Doctor of Philosophy, 2012

Directed By: Associate Professor Dr. Iqbal Hamza,
Department of Animal and Avian Sciences

Heme is an essential cofactor involved in various biological processes including oxygen transport, xenobiotic detoxification, oxidative metabolism, gas sensing, circadian rhythm, signal transduction, microRNA processing and thyroid hormone synthesis. Heme is also an essential nutrient for parasites and is the major dietary iron source for humans. Despite our extensive understanding of the mechanisms of heme synthesis and degradation in eukaryotes, little is known as to how heme is transported and trafficked in eukaryotes. Recently, CeHRG-1 and CeHRG-4 were identified as the first *bona fide* heme importers/transporters using the heme auxotroph, *Caenorhabditis elegans*. To gain mechanistic insights into the heme transport function of HRG-1-related proteins, we conducted a structure-function analysis of CeHRG-1 and CeHRG-4 by exploiting yeast mutants that are genetically defective in

heme synthesis. Our studies reveal that HRG-1-related proteins transport heme across membranes through the coordinated actions of strategically placed amino acids that are topologically conserved in both, the worm and human proteins. To further dissect the functional elements that dictate their intracellular localization, we generated a series of chimeras by swapping the amino and carboxy terminal segments of CeHRG-1 and CeHRG-4. Our analysis in yeast and mammalian cells demonstrate that the C-terminal domains are essential for membrane localization of the protein, while the N-terminal domains are important for proper function, and plausibly multimerization of HRG-1-related proteins. Currently, there are no pharmacological means to aid in the study of the cellular and physiological roles of eukaryotic heme transporters. We, for the first time, developed and executed a high-throughput screen of 233,360 compounds, to identify potential antagonists of HRG-1-related proteins by utilizing parasite heme transporters as the primary screening bait. Subsequent study in parasites will provide novel drug candidates against helminths that infect humans, livestock, and plants, as well as against genetic disorders of heme and iron metabolism in humans. Taken together, results from our studies will significantly advance novel functional and therapeutic insights into HRG-1 mediated heme transport in health and disease.

FUNCTIONAL INSIGHTS INTO HRG-1-MEDIATED HEME TRANSPORT

By

Xiaojing Yuan

Dissertation submitted to the Faculty of the Graduate School of the
University of Maryland, College Park, in partial fulfillment
of the requirements for the degree of
Doctor of Philosophy
2012

Advisory Committee:
Dr. Iqbal Hamza, Chair
Dr. Ian Mather
Dr. Liqing Yu
Dr. Caroline Philpott
Dr. Eric Haag, Dean's Representative

Acknowledgements

I am indebted to the many people who supported and helped me overcome the obstacles and challenges I faced during my graduate studies. First and foremost, this dissertation would not have been possible without the continued guidance and support from my advisor, Dr. Iqbal Hamza. Dr. Hamza encouraged and challenged me while allowing me the room to be innovative throughout my studies. I would like to thank Dr. Hamza for all his help to improve my critical thinking and presentation skills. One simply could not wish for a better advisor.

I would also like to thank my committee members Dr. Ian Mather, Dr. Caroline Philpott, Dr. Lisa Taneyhill, Dr. Liqing Yu and Dr. Eric Haag for their valuable scientific discussions and for never accepting less than my best.

A special thank you to the members of the Hamza lab past and present. When I was a freshman in the lab, it was Abbhi, Anita, Caiyong, Scott, Jason, Jon and Caitlin who helped me to get started with my project. Thank you for all the discussions and standardizing of numerous of protocols. Tammy was always willing to help and she proofread this dissertation. Jason and Carine were wonderful benchmates and gave brilliant suggestions all the time. I must thank Tamika, Haifa and Caitlin for doing the worm and mammalian HRG-1 trafficking experiments and helped me when I was in Dallas. And the new lab members, Celine, Jianbing, Kate and Simon, have been very helpful. I could not have done my research without all your support.

I would like to thank the Animal and Avian Sciences department for providing me the opportunity to pursue my study and all the people for their help during the past five years. I want to express my special thanks to Dr. Olga Protchenko at the NIH. Olga trained me with all the yeast techniques. I also thank Dr. Richard Bruick's lab members and the high-throughput screen (HTS) facility people at University of Texas Southwestern Medical Center. They helped me a lot with the HTS experiments.

Finally, to my friends and family both here and abroad, thank you for your continued support and prayers throughout my educational journey. I know you didn't always understand what I was working on but your faith in me helped me through those rough patches.

Table of Contents

List of Tables

Chapter 4

List of Figures

Chapter 1

Chapter 3

Chapter 4

Abbreviations

ABC	ATP-binding cassette
AC_{50}	half maximal activity concentration
ALA	δ-aminolevulinic acid
ALAD	δ-aminolevulinate dehydratase
ALAS	δ-aminolevulinate synthase
BCRP	breast cancer resistance protein
BMDM	bone marrow derived macrophages
CFP	cyan fluorescence protein
COX	cytochrome c oxidase
CPgenIII	coproporphyrinogen III
CPOX	coproporphyrinogen oxidase
Ctr	copper transporter
CYC	cytochrome c
Cyt_{b5}	cytochrome b5
DRC	dose responsive curves
EP	erythrophagocytosis
ER	endoplasmic reticulum
ESP	Exome Sequencing Project
FECH	ferrochelatase
FLVCR	receptor for feline leukemia virus subtype C
Fpn	ferroportin
FPP	fluorescence protease protection
FRE	ferric reductase
GAL	galactokinase
GaPPIX	gallium protoporphyrin IX
GFP	green fluorescent protein
HA	hemagglutinin
Hap	heme activator protein
Hb	hemoglobin
HCP	heme carrier protein
HEK	human embryonic kidney
HERE	heme-responsive element
HIF	hypoxia inducible factor
HO	heme oxygenase
Hp	haptoglobin
HRG	heme responsive gene
HTS	high-throughput screen
IC_{50}	half maximal inhibitory concentration
ICS	intercistronic sequence
IMS	intermembrane space
IRE	iron-responsive elements
IRP	iron-responsive element-binding proteins
Isd	iron-regulated surface determinants

LB	Luria-Bertani
LC/MS	liquid chromatography–mass spectrometry
LHR	Leishmania heme hesponse
MARE	Maf recognition element
mCeHR	modified *C. elegans* Habitation and Reproduction
MDCK	Madin-Darby Canine Kidney
MFRN	mitoferrin
mrp	multidrug resistance protein
NGM	nematode growth medium
OD	optical density
OM	outer membrane
ORF	open reading frame
PBG	porphobilinogen
PBGD	porphobilinogen deaminase
PCFT	proton coupled folate transporter
PCR	polymerase chain reaction
PM	plasma membrane
PPgenIX	protoporphyrinogen IX
PPIX	protoporphyrin IX
PPOX	protoporphyrinogen oxidase
PUG	protoporphyrin uptake gene
RBC	red blood cells
SC	synthetic complete
SDS-PAGE	sodium dodecyl sulfate polyacrylamide gel electrophoresis
TMD	transmembrane domain
UROgenIII	uroporphyrinogen III
UROS	uroporphyrinogen synthase
UTR	untranslated region
XLSA	X-linked sideroblastic anemia
YFP	yellow fluorescent protein
YNB	yeast nitrogen base
YPD	yeast extract-peptone-dextrose
ZnMP	zinc mesoporphyrin IX

Chapter 1: Introduction

Iron deficiency is a major diet-related health problem that affects 60 to 80% percent of the world's population. In spite of the fact that iron is one of the Earth's most abundant metals, nearly two billion people are affected by iron-deficiency anemia. In developing countries, nutritional iron deficiency is often accompanied and exacerbated by malaria and hookworm infections. The malaria parasite, *Plasmodium falciparum*, causes anemia by destroying parasitized red blood cells, and sequestering iron to reduce host iron absorption. Hookworms cause anemia as they feed on blood from lacerated capillaries in the intestinal mucosa [1]. As a result, iron supplements should be considered in therapeutic treatments for both malaria and hookworm infections [2,3]. Two main factors contribute to the high incidence of iron deficiency anemia. At the pH of duodenum, Fe^{2+} oxidizes to Fe^{3+} and then precipitates to form ferric hydroxide or hydroxyl-iron dimers, which are absorbed poorly by the small intestine. In addition, plant compounds such as tannins and phytates can chelate free iron, therefore prevent iron absorption [4].

By contrast, heme (iron-protoporphyrin IX) is a more readily bioavailable iron source and contributes to two-third of body iron, even though heme constitutes only a third of total dietary iron [5]. This is because the plant compounds that interfere with iron absorption do not influence heme uptake and heme is soluble in the alkaline pH of the small intestine [6]. Heme is an essential cofactor for many proteins involved in various biological processes including oxygen transport, xenobiotic detoxification, oxidative metabolism, gas sensing, circadian rhythm, signal transduction, microRNA

processing and thyroid hormone synthesis [7,8,9,10,11,12]. Heme synthesis occurs via a highly conserved, eight-step pathway in most prokaryotes and eukaryotes. Cellular heme levels are tightly controlled by maintaining a balance between heme biosynthesis and heme degradation by the enzyme heme oxygenase. Additionally, intracellular and intercellular heme trafficking play a role in maintaining heme homeostasis. For example, a huge amount of heme is required during erythropoiesis, which may not be satisfied by the cell's internal capacity for heme synthesis but may require mobilization of heme from stored compartments. Another possibility is that heme may be redistributed from "heme-rich" tissues to tissues which have a large, transient requirement for heme during embryonic development. Although heme biosynthesis and its regulation have been well characterized, the mechanisms for heme transport in eukaryotes remain poorly understood. In addition, Trypanosomatid and helminth parasites lack part or all of the enzymes of the heme synthesis pathway, and acquire heme exogenously to sustain their survival [13,14,15]. Understanding heme transport will open a novel therapeutic way for anthelminthic drug development.

Heme homeostasis and erythropoiesis

Heme biosynthesis and regulation

Heme is synthesized in most eukaryotic cells through a series of eight highly conserved enzymatic steps (Fig. 1.1). In the human bone marrow, nearly 85% of synthesized heme is utilized for hemoglobin (Hb) production in erythrocytes.

Figure 1.1. The eukaryotic heme biosynthesis pathway. The first step of heme synthesis occurs in the mitochondrial matrix with the condensation of succinyl-CoA and glycine by ALAS to generate ALA. The mechanism of ALA transport across the outer membrane (OM) into the cytoplasm is unknown. ALA is converted to CPgenIII by four enzymatic reactions. CPgenIII is then transported back into the mitochondrial intermembrane space (IMS), possibly via ABCB6, where it is converted to PPgenIX by CPOX. The conversion of PPgenIX to PPIX is catalyzed by PPOX. The last step is the addition of Fe^{+2} by FECH to generate heme. The transporter responsible for heme transport across the OM into the cytoplasm remains unidentified. (Adapted from Schultz, I., *et al*.[16].)

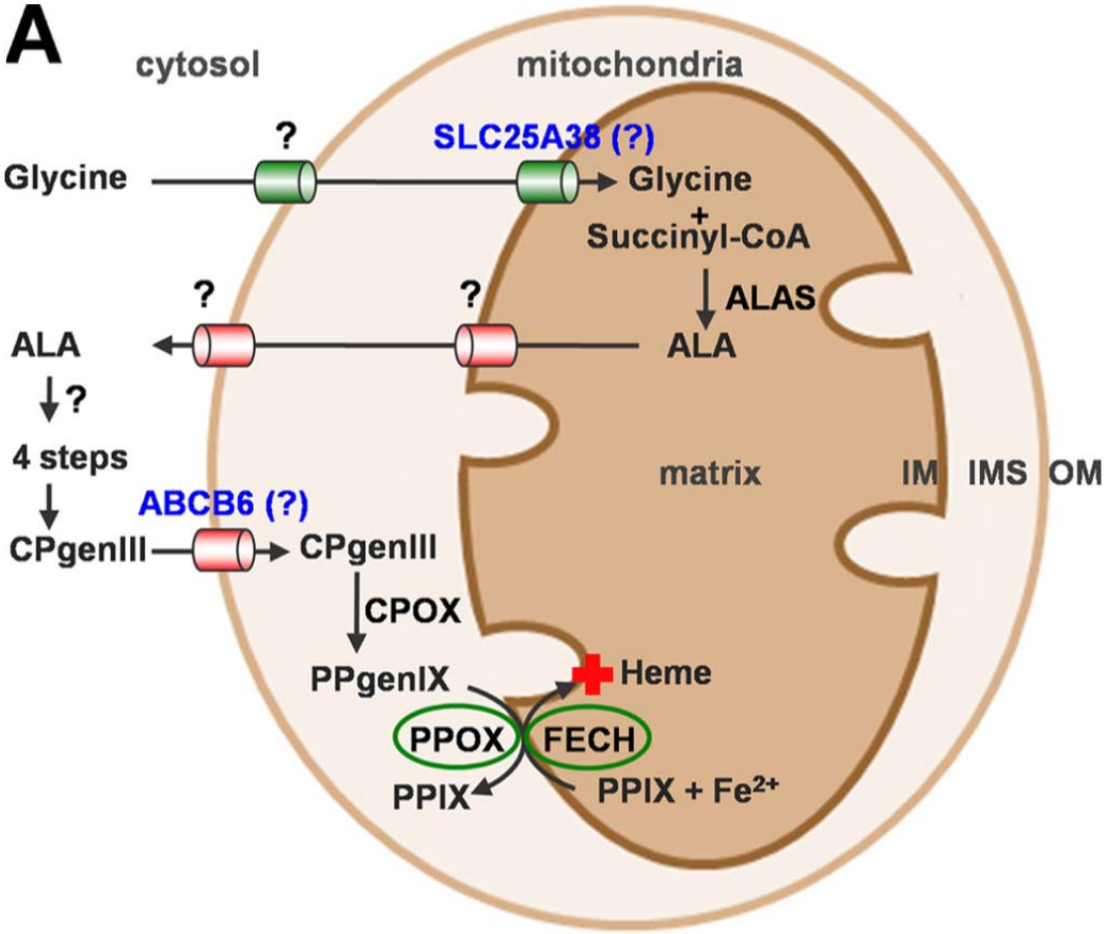
A
cytosol
mitochondria
?
SLC25A38 (?)
Glycine
Glycine
+
Succinyl-CoA
ALAS
?
?
ALA
ALA
?
4 steps
matrix
IM
IMS
OM
ABCB6 (?)
CPgenIII
CPgenIII
CPOX
PPgenIX
Heme
PPOX
FECH
PPIX
PPIX + Fe2+

Mutations in heme synthesis enzymes as well as porphyrin transporters have been associated with several variants of anemias and porphyrias [17].

The first step in the heme biosynthetic pathway is the condensation of glycine and succinyl CoA and to form 5-aminolevulinic acid (ALA). This step is catalyzed by ALA synthase (ALAS). In most vertebrates, there are two isoforms of ALAS, ALAS1 and ALAS2 [18,19,20]. ALAS1 (or ALAS–N) is expressed in all tissues, while ALAS2 (or ALAS–E) is expressed only in erythroid cells [21,22]. Mutations in ALAS2 have been shown to cause X-linked sideroblastic anemia (XLSA) due to reduced mitochondrial enzymatic activity [23]. ALA synthesis occurs in the matrix of mitochondria. Thus glycine must be transported from the cytosol into mitochondria. It has been recently reported that SLC25A38 is a mitochondrial glycine importer localized to the mitochondrial inner membrane. Mutations in SLC25A38 cause nonsyndromic congenital sideroblastic anemia in humans, whereas deficiencies in the SLC25A38 homolog, YDL119c, reduce ALA levels in yeast [24]. It has also been proposed that single-nucleotide polymorphisms of ALAS2 may have a modulatory effect on erythropoietic diseases [25].

ALA is transported out of mitochondria for the subsequent four steps of heme biosynthesis which occur in the cytosol. ALA dehydratase (ALAD) converts two molecules of ALA to porphobilinogen (PBG), an intermediate with a single pyrrole group. Porphobilinogen deaminase (PBGD) catalyzes the conversion of four molecules of PBG to an unstable polymer hydroxymethylbilane; uroporphyrinogen synthase (UROS) converts hydroxymethylbilane to uroporphyrinogen III (UROgenIII), a cyclic tetrapyrrole. In the next step, UROgenIII is decarboxylated by

uroporphyrinogen decarboxylase (UROD) to form coproporphyrinogen III (CPgenIII). CPgenIII is possibly transported through an ATP-binding cassette (ABC) protein, ABCB6, into mitochondria [26,27]. ABCB6 localizes to the mitochondrial outer membrane. Although the expression profile of ABCB6 mimics that of other heme biogenesis genes, it has not been reported that ABCB6 function is associated with blood defects in mice or humans [28]. Indeed, recent studies have shown that ABCB6 is dispensable for erythropoiesis and instead of mitochondria, it is localized in the endosomal/lysosomal compartment and in the plasma membrane of mature erythrocytes [29,30].

CPgenIII is converted by coproporphyrinogen oxidase (CPOX), an enzyme found in the mitochondrial intermembrane space, to form protoporphyrinogen IX (PPgenIX). The second to last step of the pathway is the oxidation of PPgenIX by protoporphyrinogen oxidase (PPOX) to form protoporphyrin IX (PPIX). In the final step, ferrochelatase (FECH) catalyzes the insertion of ferrous iron into the protoporphyrin IX (PPIX) ring to form protoheme or heme *b*. Heme *b* is modified at the C-2 and C-8 positions to form heme *a*, the form of heme that is found in cytochrome oxidases [31]. These modifications occur in two steps involving heme *o* synthase and heme *a* synthase. Heme *c* is found in cytochromes *c1* and cytochrome *c*. Heme *c* differs from heme *b* in that heme *c* binds proteins covalently through the two vinyl side chains [32]. The biosynthesis of heme, thus, also relies on the intracellular availability of iron. Ferrous iron enters the mitochondrial intermembrane space and is transported across the inner membrane and into the matrix by mitoferrin1 (MFRN1)

in erythroblasts [33,34] and mitoferrin2 (MFRN2) in proerythroblasts and nonerythroid cells [34,35,36].

Cells of different tissues have different heme requirements, and the pathway must be regulated accordingly. Erythroid precursors need to produce a greater amount of heme than other tissues for insertion into hemoglobin. In contrast to other cell types, heme produced in erythroid tissue is used to deliver oxygen to all tissues of the body. Therefore, erythroid precursors produce heme as long as iron is available. Upregulation of heme synthesis in erythrocytes at the transcriptional level is mainly achieved via erythroid-specific transcription factors. Differential transcriptional regulation is found in the first enzyme of the heme synthesis pathway, ALAS. ALAS1 is expressed ubiquitously, and is downregulated by heme [37,38,39]. The erythroid-specific isoform ALAS2, however, has a different regulation pattern than ALAS1. At the transcriptional level, *ALAS2* is upregulated during erythropoiesis through the binding of erythroid-specific factors, such as GATA-1 and NF-E1, to their target sequences [37]. At the post-transcriptional level, *ALAS2* is downregulated under low iron conditions by the IRP/IRE system [18]. Thus, erythroid levels of ALAS2 are directly linked to iron availability. This post-transcriptional regulation of ALAS2 allows cells to quickly adjust the heme synthesis pathway according to iron levels.

ALAD encodes the second enzyme in the heme synthesis pathway, and consists of eleven coding exons and two non-coding exons (1A and 1B). Differential regulation is achieved by utilizing two different promoters. The erythroid-specific promoter is located between exons 1 and 2, and contains GATA-1 binding sites.

Although the transcripts differ to allow for upregulation specifically in erythropoietic tissue, the resulting proteins are identical because the translational start site for both transcripts is in exon 2 [40]. The third and fourth genes in the pathway, PBGD and UROS, are transcriptionally regulated in a manner similar to ALAD by a housekeeping promoter in all cell types and an erythroid-specific promoter in erythroid tissue. Unlike ALAD, alternative splicing of PBGD leads to proteins that differ in the N-terminus [41,42,43]. Transcription of the next gene in the pathway, UROD, is also increased in erythroid tissues. However, the mechanism of regulation remains unclear, since it does not have an erythroid-specific promoter [44]. CPOX is the sixth gene in the heme synthesis pathway. The promoter of CPOX has a SP1-like element, a GATA-1 site, and a novel regulatory element, CPRE, which binds to erythroid-specific transcription factors like Klp1, to regulate transcription [45]. Interestingly, the CPRE element is also found in the human β-globin promoter, another gene that is upregulated in erythroid tissue [46]. The second to last gene, PPOX, is upregulated in erythroid cells due to two GATA sites contained within the first exon [47].

The final gene in the pathway, ferrochelatase (FECH), achieves differential expression in a manner similar to CPOX and PPOX. There is a single promoter which contains binding sites for SP1, NF-E2, and GATA-1. In K562 cells, a erythroleukemia cell line, the SP1 binding site was sufficient to drive erythroid expression of FECH [48]. It has also been shown that a point mutation in one of the SP1 binding sites disrupts proper transcription of the FECH mRNA and leads to erythropoietic protoporphyria [49]. In mouse embryonic stem cells, the NF-E2

binding site is necessary for both basal expression in pluripotent cells and erythroid-specific upregulation. The same study also demonstrated that the GATA-1 binding element acts as a repressor in pluripotent cells, but an enhancer during erythropoietic development [50]. FECH expression is also upregulated by iron sufficiency and hypoxia. The iron dependent regulation of FECH is due to an iron-sulfur cluster in its C-terminus [51]. It is induced by hypoxia due to two hypoxia inducible factor (HIF) binding sites in its promoter [52]. It is not surprising that the synthesis of heme is coordinated with iron and oxygen levels because they are all tightly linked during aerobic respiration.

Heme transport

Heme import

Although dietary uptake of heme constitutes a major source of iron, it has been difficult to study intercellular heme transport in eukaryotes due to its intricate link with heme biosynthesis [53]. Heme carrier protein 1 (HCP1/ SLC46A1) is a membrane protein expressed by enterocytes in the duodenum implicated in the absorption of heme in the intestine [54]. Functional studies in *Xenopus* oocytes expressing *HCP1*, revealed a 2-3 fold increase in heme uptake. Subsequent studies, however, have shown that SLC46A1 is in fact a folate/proton symporter and was renamed as the Proton Coupled Folate Transporter (PCFT/HCP-1) [55]. Loss-of-function missense mutations in HCP1 in humans are associated with hereditary folate

Figure 1.2. A schematic description of intracellular heme trafficking. Heme can be exported out of the cell or imported into the cell. The cell-surface FLVCR and the ABC transporter ABCG2 have been implicated in heme export in erythroid cells, whereas HRG-1 was identified as a heme importer. Question marks represent the presumptive heme trafficking pathways. *COX*, cytochrome c oxidase; *Cyt_{b5}, cytochrome b5*. (Adapted from Schultz, I., *et al*. [16])

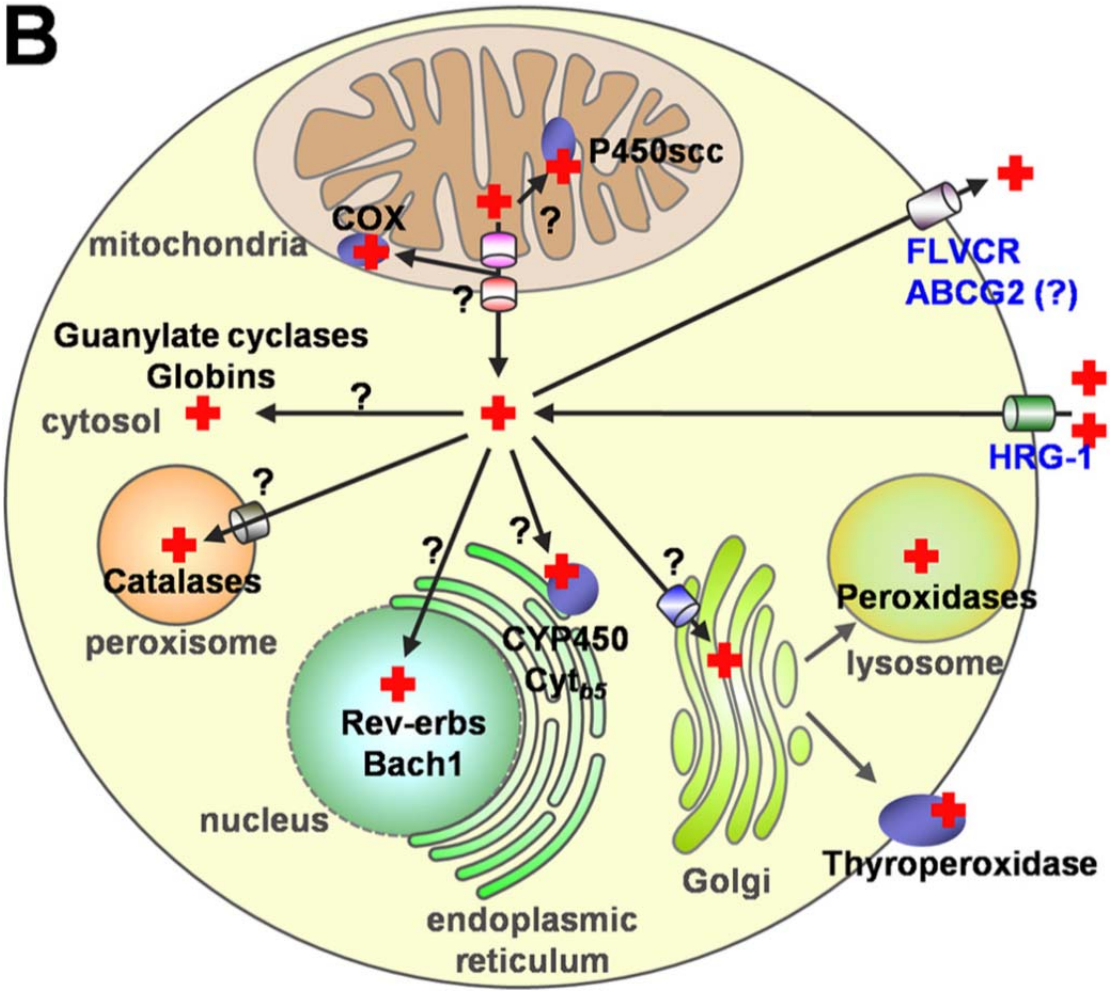
B
P450scc
COX
mitochondria
?
?
FLVCR
ABCG2 (?)
Guanylate cyclases
Globins
cytosol
?
HRG-1
?
Catalases
peroxisome
?
?
?
CYP450
Cyt$_{b5}$
Rev-erbs
Bach1
nucleus
endoplasmic
reticulum
Golgi
Peroxidases
lysosome
Thyroperoxidase

malabsorption with no apparent defects in erythropoiesis. RNA interference assays of *HCP1* in CaCo-2 cells reduced pH-dependent folate uptake by 60-80%. Folate transport by this protein was at least an order of magnitude higher than that observed with heme, suggesting that folate might be the physiological ligand for HCP-1. Interestingly, human patients with hereditary folate malabsorption carry a missense mutation in *HCP1* that leads to the formation of a non-functional protein. *HCP1*$^{-/-}$ erythroblasts are more prone to apoptosis and fail to differentiate [56]. Currently, it is unclear whether the erythropoietic defects observed in *HCP1*$^{-/-}$ animals are the direct result of inadequate dietary heme uptake or secondary to folic acid deficiency that *per se* is a major risk factor for developing megaloblastic anemia in humans [57].

Rao *et al* have demonstrated the roundworm *C. elegans* to be an excellent model for heme trafficking studies because it is a heme auxotroph that still requires intestinal uptake of dietary heme and subsequent dissemination throughout the organism for viability [15]. Genomic screens in *C. elegans* identified CeHRG-1 and CeHRG-4 as the first eukaryotic heme importers [58]. CeHRG-1 has orthologs in vertebrates, while CeHRG-4 is worm-specific. Transient knockdown of *hrg-1* in zebrafish resulted in hydrocephalus, yolk tube malformations and, most strikingly, anemia. Worm HRG-1 fully rescued all phenotypes observed due to knockdown of *hrg-1* in zebrafish [58]. The phenotypes resulting from knockdown of zebrafish *hrg-1* were restricted specifically to the erythroid lineage and did not impact other hematopoietic lineages. Additionally, significant heme-induced inward currents were observed in *Xenopus* oocytes injected with cRNA for CeHRG-1, CeHRG-4 as well as

the human homolog, hHRG-1, indicating heme-dependent transport across membranes [58].

Human HRG-1 mRNA was abundant in the brain, kidney, heart and skeletal muscle and in cell lines derived from duodenum, kidney, bone marrow and brain [58]. hHRG-1 localized to acidic endosomal and lysosomal organelles in HEK293 cells, and its affinity for heme decrease with increasing pH. Additionally, tyrosine (YxxxØ) and acidic-dileucine (DxxIL) based sorting motifs were found in the C-terminus of both *C. elegans* and human HRG-1 [58]. Yanatori and colleagues recently reported hHRG-1 localized to the plasma membrane and lysosomes in non-polarized HEp2 cells. In polarized MDCK cells, hHRG-1 was located to the basolateral membrane and a cytosolic organelle just under the apical membrane [59]. A recent study showed that hHRG-1 interacted with the c subunit of the vacuolar proton ATPase (V-ATPase) pump and enhanced endosomal acidification [60]. Together these suggest hHRG-1 plays a role in the transport of heme from the exoplasmic space or lumen of acidic endosome–lysosome compartments into the cytoplasm.

Recent expression analyses performed in *C. elegans* has identified two additional genes, MRP-5 and F22B5.4, that are required for proper intestinal heme transport in adult worms [61]. Both genes encode membrane proteins and may play a role in heme transport in *C. elegans* although their roles in vertebrate heme homeostasis are unknown.

Heme export

To date, two different plasma membrane exporters that recognize heme as a substrate have been identified. In mammals, FLVCR1 (feline leukemia virus, subgroup C receptor 1) was recently shown to be a cell surface heme exporter and *FLVCR1*$^{-/-}$ mice developed severe anemia, which was postulated to be due to the inability of macrophages and erythroblasts to export heme [62,63]. Mutations in FLVCR1 cause posterior column ataxia and retinitis pigmentosa due to dysregulation of heme homeostasis in a subpopulation of neurons in the retina and posterior columns of the spinal cord [64]. Interestingly, Tolosano *et al* have shown that in addition to full length FLVCR1 (FLVCR1a), there is another isoform, FLVCR1b, which is a shortened protein localized in mitochondria. Targeted deletion of FLVCR1a resulted in skeletal defects and vascular abnormalities but did not affect erythropoiesis, whereas knockdown of FLVCR1b impaired erythroid differentiation *in vitro*. Their results suggested FLVCR1b is a mitochondrial heme exporter. The physiological function of FLVCR1a remains unknown. A closely related homolog, FLVCR2, is reported to be a membrane-bound heme importer and may play a role in the extracellular endocytosis of heme. Knockdown of *FLVCR2* in human cells resulted in a significant decline in import of the fluorescent heme analog, zinc mesoporphyrin. Quantitative real-time PCR analysis found that *FLVCR2* transcripts can be detected in a wide range of human tissues including the fetal liver [65]. Recent studies have associated FLVCR2 with Fowler syndrome, a vascular disorder of the brain [66,67]. However, a physiological role for FLVCR2 in erythropoiesis is still unclear.

A second protein, breast cancer resistance protein (BCRP, also known as ATP-binding cassette transporter G2 or ABCG2) has been implicated in heme export in humans. Similar to ABCB6, ABCG2 is a member of the ATP-binding cassette transporter family that is expressed by hematopoietic progenitors [68]. Recent evidence indicates that ABCG2 binds directly to heme via an extracellular domain and delivers heme to extracellular chaperone proteins such as albumin [69]. In particular, the extracellular loop 3 of ABCG2 (ECL3) constitutes a porphyrin-binding domain, which strongly interacts with heme, hemin, and PPIX. Currently, the importance of ABCG2 in normal blood development is unknown. The expression level of ABCG2 is particularly high in the early stages of hematopoiesis, whereas that of FLVCR1 is high during erythropoiesis [68]. Thus, it has been hypothesized that these two heme exporters might have different roles or expression patterns depending on physiological conditions.

Heme intercellular trafficking

To date, several intercellular heme transport proteins have been identified in vertebrates; however, none of them directly contributes to erythropoiesis. Free, circulating heme binds to and is sequestered by a plasma protein, hemopexin, which delivers its bound heme to various cells types where it is degraded [53]. Hemopexin may also be responsible for the systemic delivery of intravenously administered heme to human patients suffering from blood disorders [70,71]. Another intercellular transport mechanism in vertebrates involves haptoglobin-mediated delivery of

circulating hemoglobin to monocytes and macrophages, leading to heme degradation and the recycling of iron [53]. Knockout studies in mice have revealed that whereas hemopexin and haptoglobin are proteins needed to buffer hemolytic stresses, they are not required for successful erythropoiesis [72].

Recently, HRG-3, a secreted protein in *C. elegans* was identified that is required for delivering heme from maternal intestine to developing embryo. Whereas deletion of HRG-3 had no obvious effect on adult worms, more than 30% of embryos from HRG-3 mutant mothers failed to hatch and all the hatched progeny were growth arrested at the first larval stage. These growth phenotypes were only observed when the mutant worms were grown under low heme conditions. Ectopic expression of HRG-3 in maternal intestinal tissues rescued heme-limited growth arrest of HRG-3 mutant worms, whereas expression in the embryos did not [73]. Collectively, this work demonstrates that HRG-3 binds to and delivers heme to the embryo from adult tissues. It is reasonable to speculate that during development and erythropoiesis, a heme chaperone is required to facilitate the targeted delivery and redistribution of heme between certain tissues and cell types, which could not be achieved by the liver-produced, high-affinity binding proteins, hemopexin or haptoglobin. Consequently, even though a HRG-3 mammalian homolog has not been discovered, a functional homolog of HRG-3 can be expected in mammals.

Heme degradation and recycling

Senescent red blood cells (RBCs) are constantly removed from the circulation by macrophages that also play a principal role in the breakdown of heme and the recycling of iron. Heme is released from lysed RBCs within phagolysosomes and is degraded by heme oxygenase-1 (HO-1) in the endoplasmic reticulum [33]. The first step is breakdown of heme by HO-1 into biliverdin, carbon monoxide and iron. The second step of the heme degradation pathway is the catalysis of biliverdin to bilirubin by biliverdin reductase. HO-1 also catalyzes the breakdown of free heme that is not bound to any protein, acting as a scavenger to prevent toxicity from free heme. Germline deletion of HO-1 leads to anemia in mice and published work suggests that HO-1 may play a cell-autonomous role in erythroblast differentiation [74]. Irradiated, wild-type recipient mice transplanted with HO-$1^{+/-}$ bone marrow cells have significantly fewer splenic erythroid precursors [75], indicating that HO-1 may be required for erythropoiesis both directly by promoting RBC maturation as well as indirectly by regulating systemic iron recycling. The degradation of heme in macrophages releases iron that is either stored as ferritin-bound iron or exported out of macrophages by the iron exporter, ferroportin-1 (FPN1, SLC40A1)[33].

Circulating iron is bound by the sequestration protein transferrin and the transferrin–iron complex can be internalized by the ubiquitously expressed transferrin receptor which permits cells to acquire iron for various functions [16,33]. The importance of heme degradation and iron recycling in erythropoiesis is underscored by findings that inactivation of the heme degradation machinery in mice is associated with anemias [74,76,77]. In particular, specific ablation of FPN1 in macrophages is also associated with the development of anemia, indicating that the erythropoietic

Figure 1.3. Proposed model of heme iron recycling following erythrophagocytosis. Senescent RBCs are specifically recognized and engulfed by BMDM inside an erythrophagosomal compartment. During this process, Nramp1 is recruited at the phagosomal membrane. After hemoglobin degradation, heme is transported through the phagosomal membrane via HRG-1. Once in the cytosol, heme can be transported outside the cell via FLVCR1. Additionally, cytosolic heme is degraded by HO-1. Freed heme iron is then recycled to the circulation via Fpn or is stored in the form of cytosolic ferritin.

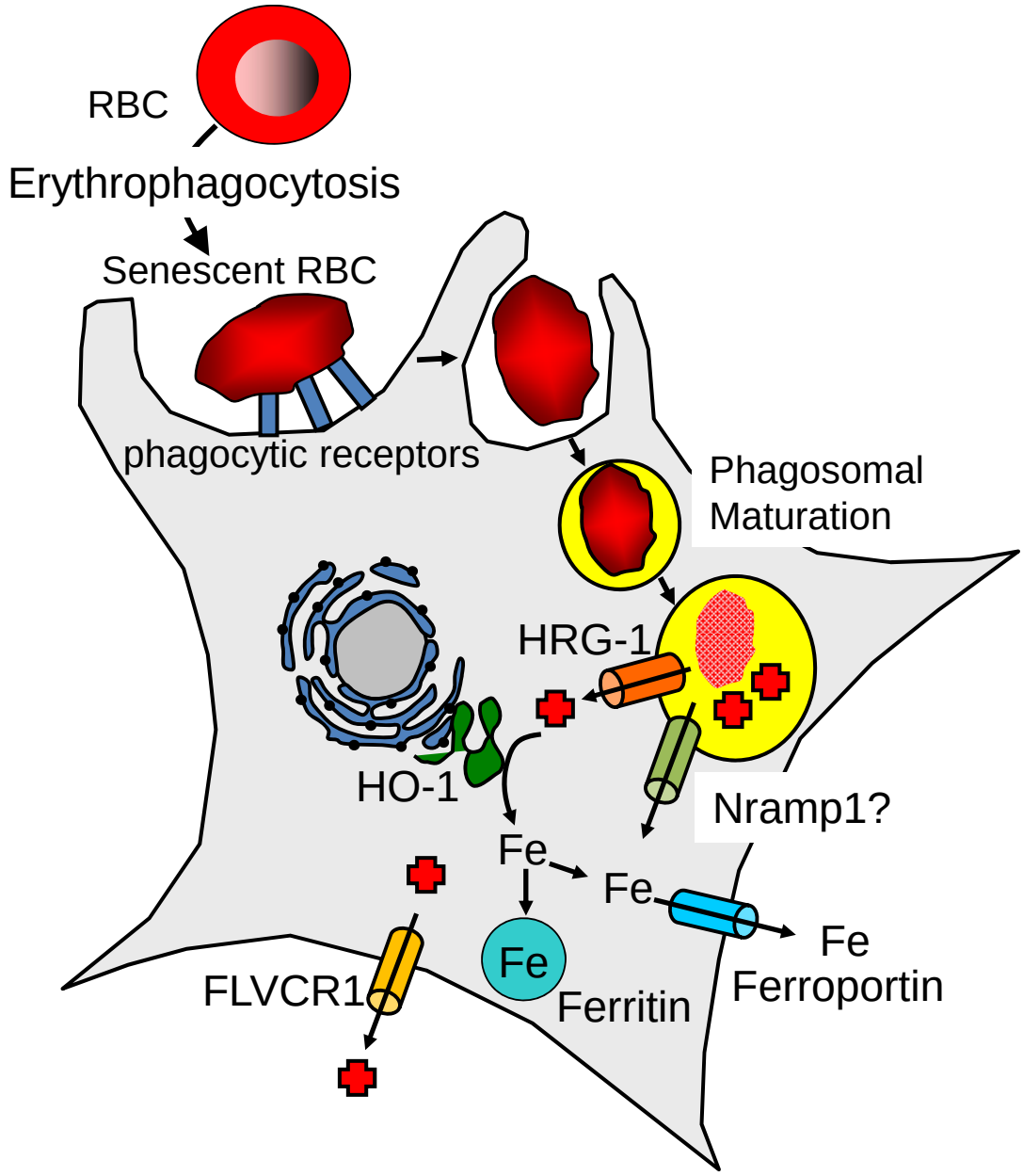
RBC
Erythrophagocytosis
Senescent RBC
phagocytic receptors
Phagosomal
Maturation
HRG-1
HO-1
Nramp1?
Fe
Fe
Fe
Ferritin
Fe
Ferroportin
FLVCR1

defects are not intrinsic to erythroblasts but rather associated with iron recycling by the reticuloendothelial system [76]. Interestingly, we and others have recently found that, in addition to lysosomal localization in HEK293 cells [58], the heme transporter HRG-1 is also recruited and colocalizes with Nramp1 at the erythrophagosomal membrane, surrounding ingested RBCs in bone marrow derived macrophages (BMDMs) (Fig. 1.3) (*C. White et al*, unpublished obsevations and [78]). However, the absence of HO-1 at this location indicates that during erythrophagocytosis (EP), at least a portion of heme released from degraded hemoglobin is mobilized by HRG-1 to the cytoplasm [78]. The cytosolic heme can then undergo intracellular redistribution including degradation by HO-1 for iron recycling, or be exported by FLVCR1.

Heme-regulated transcription and translation

Heme is a key regulator of several processes at the transcriptional level. Rajagopal *et al* identified 288 genes in *C. elegans* that are transcriptionally regulated by heme [58]. Heme may also promote erythroid differentiation by enhancing the expression of p18 and p21 which are negative regulators of the cell cycle. Adult hemoglobin is produced in erythroid tissue and consists of a heme molecule bound to a tetramer of two α-globin chains and two β-globin chains. In low heme conditions, it is necessary to downregulate globin chain production because aggregation of globins is toxic to an erythroid cell [79]. The transcriptional regulation of globin production by heme is mediated through Bach1, the first mammalian transcription factor shown to bind heme [80,81,82]. Bach1-Maf heterodimers bind to Maf recognition elements

(MAREs) and repress transcription when Bach1 is not bound to heme. As heme is sufficient, heme binding to Bach1 will result in its dissociation from DNA and export from the nucleus [83]. Bach1 has four cysteine proline (CP) heme regulatory motifs, which are responsible for heme binding. Deletion of these motifs inhibited Bach1 dissociation from MAREs upon the addition of excess heme. The heme degrading enzyme, HO-1, is similarly regulated by Bach1 [84]. In addition, hHRG-1 was also recently identified as a target of BACH1 in microarray expression analysis and ChIP-Seq experiments, further suggesting that HRG-1 may be an important player in erythropoiesis [85].

Heme is also involved in microRNA processing [12,86]. MicroRNAs are short RNAs that play a role in gene regulation at the transcriptional and post-transcriptional levels. This process is at least in part regulated by heme. A number of microRNAs are involved in different stages of erythropoiesis [87,88,89,90]. For example, an upstream regulatory element, which binds GATA-1 is required for the upregulation of a single pri-miRNA (precursor-RNA) that encodes both miR144 and miR451. Zebrafish depleted of miR451 showed impaired maturation of erythroid precursors, indicating that post-transcriptional regulation by microRNAs is essential for erythropoiesis [87].

In erythropoiesis, late-stage erythroblasts lose their nuclei to become reticulocytes. As they mature into erythrocytes over the next few days, they synthesize hemoglobin and other erythroid-specific proteins. Hemoglobin production must be coordinated with heme availability because aggregation of globin chains is toxic to the cell. As discussed above, globin chain production is regulated by heme at the transcriptional level by Bach1 binding to the promoters of the α-globin and β-

globin genes. However, mechanisms must exist to regulate globin production after the cell has lost its nucleus and transcriptional regulation is no longer possible. In reticulocytes, this regulation is achieved at the translational level by heme regulated eIF-2 (HRI) kinase [91,92]. In low heme conditions, when synthesis of globin chains needs to be downregulated, HRI is activated. Activated HRI phosphorylates serine 51 of the α-subunit of the initiation factor (eIF-2). eIF-2 is normally responsible for recruiting the initiator tRNA to the pre-initiation complex, but phosphorylation prevents eIF-2 from being utilized for translation, resulting in global reduction in mRNA translation. Although the mechanism that HRI uses for heme sensing remains to be elucidated, it was recently demonstrated that His119, His120, and Cys409 are the ligands for heme binding. Also, the proline residue adjacent to the Cys409 is important for heme Fe^{3+} complex binding [93].

Heme transport in pathogens

Heme uptake in bacterial pathogens

Compared to eukaryotes, heme uptake and transport have been well-characterized in bacteria. In pathogenic bacteria, iron is crucial to infect the host. As a defense mechanism against pathogens, the host must restrict access to iron and heme. This restriction of iron and heme to pathogens poses a serious problem that the bacteria must overcome for survival. While most bacteria secrete high-affinity, low-molecular weight chelators to sequester iron, some have the ability to fulfill their iron

requirements by utilizing host heme or heme-containing proteins, or by secreting hemophores (Fig. 1.4) [94].

Heme uptake systems are classified into two groups: *a)* those that involve direct binding of heme or hemoproteins by outer membrane receptors, and *b)* those that involve secretion of hemophores that bind the heme source and deliver it to specific receptors [94]. There are 29 outer membrane heme receptors that have been identified from different species of gram-negative bacteria. Although these receptors share between 21 to 90% homology when compared to each other, they all share a highly conserved amino acid motif FRAP(10X)H(XX)NPL(2X)E [95].

The outer membrane receptors can be divided into subgroups. A first subgroup of outer membrane receptors is not substrate-specific and binds either heme or heme-containing proteins. Such receptors are found in *Yersinia enterocolitica*, *Escherichia coli* and *Shigella* [94]. Outer membrane receptors, such as HemR in *Y. enterocolitica,* bind heme and actively transport it across the outer membrane into the bacterial periplasm. An intact Ton system, with the cytoplasmic membrane proteins ExbB and ExbD and membrane-anchored protein TonB, is required to provide energy for heme transport across the outer membrane. The TonB system uses a proton-motive force for the passage of heme into the periplasm. Heme is bound by a periplasmic heme binding protein such as HemT and then delivered to permeases on the cytoplasmic membrane, such as HemU and HemV in *Y. enterocolitica* [96]. Transport of heme across the cytoplasmic membrane requires expenditure of ATP. In the cytoplasm, HemS and HemO proteins process heme to release iron.

Figure 1.4. Heme acquisition by gram-negative bacteria. (A) Hemolysin secreted by bacterial cell degrades RBC, releasing Hb and heme. Once released, heme may be transported into the bacterial cell by different mechanisms i) direct binding of hemoglobin or heme to a specific TonB-dependent outer membrane receptor results in transport of heme into the periplasm. ii) Capture of hemoproteins such as hemoglobin or hemopexin by hemophores, which deliver these hemoproteins to a specific TonB-dependent outer membrane receptor. iii) Degradation of hemoproteins by either membrane bound or secreted bacterial proteases to release heme. (B) Heme bound by TonB-dependent outer membrane receptors is transported into the periplasm. TonB in association with the ExbB and ExbD proteins provides energy for this process. The transport of heme through the cytoplasmic membrane occurs via a system composed of a cytoplasmic membrane-associated permease and an ATPase. Heme oxygenase-like enzymes degrade heme in the cytoplasm. (Adapted from Severance *et al*. [53]).

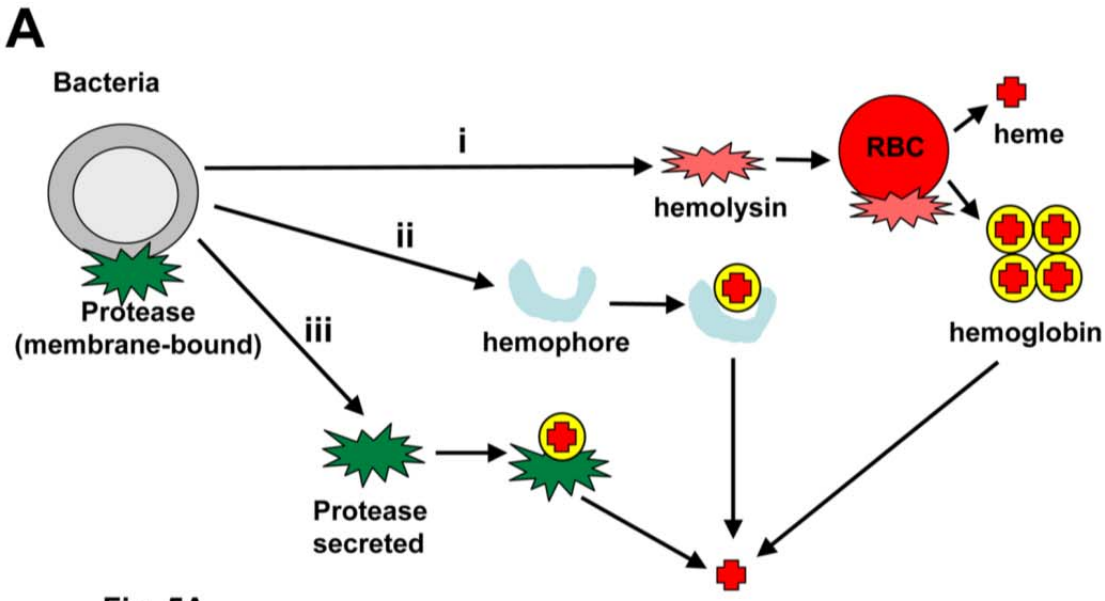
A
Bacteria
i
ii
iii
hemolysin
RBC
heme
hemoglobin
Protease
(membrane-bound)
hemophore
Protease
secreted

Fig. 5A

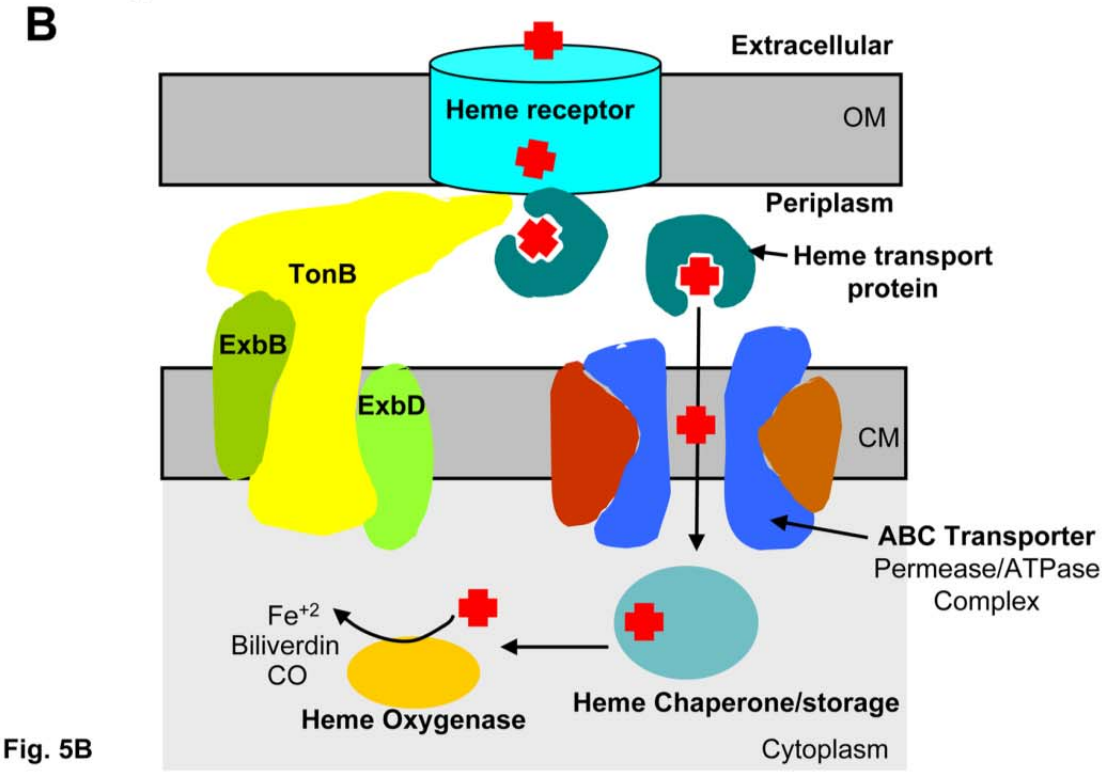
B
Extracellular
Heme receptor
OM
Periplasm
Heme transport
protein
TonB
ExbB
ExbD
CM
ABC Transporter
Permease/ATPase
Complex
Fe+2
Biliverdin
CO
Heme Oxygenase
Heme Chaperone/storage
Cytoplasm

Fig. 5B

The second subgroup of receptors is substrate-specific and binds only one or two sources of heme. These heme receptors are found in *Vibrio*, *Neisseria* and *Haemophilus* and these receptors have high affinity binding sites for one or two particular heme sources such as hemoglobin and or haptoglobin-hemoglobin (Hp-Hb) complexes [95]. The neisserial Hp-Hb and Hb receptor, HpuAB, is the only system with two outer membrane receptors, HpuA and HpuB. While HpuA is an outer membrane lipoprotein, HpuB is a TonB-dependent receptor that is similar to other TonB-dependent receptors. It has been shown that both proteins are required for Hb, Hpt-Hb and apo-haptoglobin binding. But it is not clear as to whether HpuA and HpuB have similar binding affinities for holo- versus apo-haptoglobin [95].

Several gram-negative bacteria secrete small extracellular proteins called hemophores. Hemophores are secreted by ABC transporters in a manner dependent on their carboxy-terminal secretion signal [97]. Hemophores bind heme and deliver it to specific outer membrane receptors. One of the best-studied systems is the HasA-HasR mediated heme uptake in *Serratia marcescens*. While usually the role of hemophores is to bind free heme or Hb-bound heme, the hemophore, HasA, secreted by HasDEF in *S. marcescens* extracts heme from hemoproteins. The free heme is then delivered to the outer membrane receptor HasR [98,99,100]. HasR can transport either free heme or heme from hemoglobin, but the presence of HasA promotes heme uptake to a greater extent. The mechanism of heme transfer to HasA from hemoglobin is not understood. It is thought that hemoglobin loses its heme moiety in solution, which is then bound by HasA [100,101]. Similar hemophore-mediated heme

acquisition systems have been identified in *Porphyromonas gingivalis* and the human pathogenic strain of *Escherichia coli* [102,103].

The only known bacterial system that utilizes heme bound to hemopexin is the HuxA hemophore system found in *Haemophilus influenzae* [104]. *H. influenzae* does not make heme and the *HuxABC* gene cluster found in these bacteria allows it to utilize hemopexin, a heme-binding blood plasma protein very efficiently. HuxA is actively secreted by HuxB and is absolutely required for the utilization of heme-hemopexin complexes [95].

Some gram-negative bacteria secrete proteases that degrade host hemoproteins to release heme. A heme binding protein in *E. coli* EB1 strain possesses proteolytic activity, as it is able to degrade hemoglobin [104]. *Porphyromonas gingivalis*, a gram-negative anaerobic bacterial pathogen, secretes a class of protease called gingipains [105]. Of the several gingipains, the lysine-specific cysteine protease Kgp has been shown to both bind and degrade hemoglobin, hemopexin and haptoglobin [63]. As heme is an essential nutrient for most pathogenic bacteria, the virulence of pathogenic bacteria can be affected by targeting heme uptake pathways. Mutations in heme-iron uptake genes in *Staphylococcus aureus* reduce its pathogenicity in the invertebrate animal model, *C. elegans* [106]. In *Bordatella pertussis*, the bacterial agent responsible for whooping cough in humans, heme utilization by the bacteria contributes to bacterial pathogenesis in a mouse infection model [107].

Heme uptake in fungal pathogens

While several bacterial heme uptake and transport systems have been well characterized, only recently have proteins involved in heme uptake been identified in primitive eukaryotes. In pathogenic yeast, *Candida albicans*, *RBT5* and *RBT51* have been identified as heme uptake genes. Rbt5 and Rbt51 are mannosylated GPI-anchored proteins, and Rbt5 is highly induced upon iron starvation [108]. Despite 70% homology between the two genes in *C. albicans*, RBT5 played a more important role than RBT51 in utilization of heme as an iron source. Disruptions in these genes did not reduce the virulence of *C. albicans* in murine models [109]. *C. albicans* possesses a heme-oxygenase enzyme (*CaHMX1*) that shares 25% identity with the human HO, and CaHMX1 is positively regulated by both heme and hemoglobin [110]. Whether heme iron utilization is essential for pathogenicity would be best addressed by using mutants such as *Cahmx1Δ* or *Cahmx1Δ* and *CaRbt5Δ* double mutants that are devoid of the ability to use the heme as an iron source [111]. Recent studies indicate that CaHMX1 plays a role in the pathogenesis of disseminated bloodstream infections by limiting the host immune response [112].

Heme transport in Trypanosomatids

Trypanosomes are parasitic protists that cause significant human and animal diseases worldwide, such as *Trypanosoma brucei* (sleeping sickness or African trypanosomiasis), *Trypanosoma cruzi* (Chagas' disease or American trypanosomiasis), and *Leishmania* spp.(leishmaniasis) [113]. The life cycle of these trypanosomatids is complex, presenting several developmental stages in different

hosts. They lack some or all components of the heme biosynthetic pathway and are dependent on the uptake of heme from their hosts [13,14].

Koreny *et al* proposed that the ancestor of all trypanosomatids is completely deficient in the ability to synthesize heme [114]. In some trypanosomatids like *Leishmania* spp., the pathway is partially rescued by genes encoding enzymes for the last three steps, possibly obtained by horizontal gene transfer from their host. *Leishmania* spp. can grow in media in which hemin is replaced by protoporphyrin IX, indicating that at least the last enzyme of the pathway, FECH, remains functional [13,115,116]. By contrast, trypanosomes lack all the enzymes for heme synthesis and *in vitro* cultivation of *Trypanosoma* requires the addition of heme compounds in the form of hemoglobin, hematin, or hemin to the medium [13,117]. *T. cruzi* proliferation is mediated almost exclusively by heme through unknown mechanisms. Treatment with SnPPIX, ZnMPIX and PdMPIX inhibit parasite proliferation, which is reverted by adding excess of heme [118]. A recent study reported TbHpHbR as a bloodstream stage-specific protein. TbHpHbR directs the internalization of heme carried by the haptoglobin-hemoglobin (Hp-Hb) complex into hemoproteins in order to optimize growth of bloodstream forms. However, TbHpHbR is only present in *T. brucei;* it is not found in the related kinetoplastids, *T. cruzi* or *Leishmania* [119].

Huynh *et al* recently identified *Leishmania* Heme Response-1 (LHR-1) as the first Trypanosomal heme transporter [120]. LHR-1 is a homolog of CeHRG-4 and is localized to the plasma membrane and endocytic compartments in the parasites. Episomal expression of LHR-1 increased the intracellular heme concentration of wild-type and single knockout *L. amazonensis* promastigotes, but was not sufficient

to allow recovery of viable parasites lacking both copies of the gene, suggesting it is an essential component for heme uptake and survival. Functional assays in yeast demonstrated that LHR-1 can transport heme directly [120]. The ATP-binding cassette protein LABCG5 was also recently proposed to mediate the salvage of heme released after lysosomal degradation of internalized hemoglobin in *L. donovani*. This intracellular process for heme salvage from degraded hemoglobin was proposed to be distinct from the pathway directly promoting porphyrin transport into the parasites [121].

Heme transport in parasitic worms

Helminthic infections are a huge burden to both public health and agriculture. More than two billion people are afflicted by helminthiasis, and agricultural losses due to plant-parasitic nematodes are estimated to be approximately eighty billion dollars annually [122,123]. Drug resistance is widespread, and there is a need to find new drug targets to eliminate these infectious agents [124]. Genomic analysis of heme biosynthetic enzymes has revealed that *C. elegans* lacks orthologs for these enzymes [15]. Heme biosynthetic enzyme activity measurements confirmed that *C. elegans* lack the ability to make heme [15]. We have additionally shown that other free-living nematodes such as *Panagrellus redivivus, Oscheius myriophila* and *Paragordius varius* and parasitic nematodes such as *Strongyloides stercoralis*, *Ancylostoma caninum*, *Haemonchus contortus*, *Trichuris suis* and *Ascaris suum* lack the enzymes that are required for heme biosynthesis [15]. However, genomic analysis

of these nematodes indicates that they encode abundant hemoproteins, suggesting the possibility that they must acquire heme from their environment. Like heme uptake in *C. elegans,* this process may involve homologs of HRG-1 [58].

Published reports have suggested a role for heme in the pathogenicity of different parasitic worms. Hookworm infections due to *Ancylostoma ceylanicum* are prevalent in developing countries and are associated with iron deficiency anemia. A recent study demonstrated the importance of host iron status as a key mediator of hookworm pathogenicity [125]. Animals fed a reduced iron diet leading to anemia had a significant reduction in the intestinal load of worms. This observation suggested that hookworms rely on host heme-iron for their growth and development and that treatment of hookworm infection with anthelminthic drugs in combination with iron supplements to prevent anemia might exacerbate the severity of infection. Since hookworms, like *C. elegans*, also lack the ability to make heme, another plausible explanation given by the authors was that animals fed a low-iron diet have reduced worm burden due to inadequate amounts of heme for hookworm metabolism [15,125].

Brugia malayi, a filarial nematode, is the causative agent of lymphatic filariasis that is endemic in Asia. Analysis of the of the *B. malayi* genome revealed the absence of the heme biosynthesis enzymes in these parasites [126]. Therefore, it is highly likely that these parasites obtain heme from their host or from *Wolbachia* (wBm), an intracellular endosymbiotic bacterium. *Wolbachia* has an intact heme pathway (except HemG, which may be substituted by a functional HemY) and a CcmB heme exporter, suggesting that the bacteria may be an important source of

heme for the nematode. Antibiotics that eliminate the endosymbiont have inhibitory effects on the development and fertility of the parasitic nematode and have been used to treat patients with filariasis. Since heme is important for the growth and development of the nematode, another potential drug target is the heme uptake pathway in *B. malayi* or the heme biosynthesis pathway of *Wolbachia* [127,128].

In summary, heme is essential for nearly all living organisms. Heme homoestasis is maintained through tight regulation of heme biosynthesis and degradation, as well as heme transport and trafficking. Understanding the mechanism of heme transport will significantly facilitate exploration of human genetic disorders of heme and iron metabolism, and open new paths for antiparasitic therapy.

Chapter 2: Materials and Methods

Plasmid Construction

To make yeast expression plasmids, the open reading frame (ORF) of CeHRG-1, CeHRG-4 and their hemagglutinin (HA) epitope-tagged versions were amplified by PCR from pcDNA3.1(+)zeo-CeHRG-1-HA and pcDNA3.1(+)zeo-CeHRG-4-HA[58], respectively, using gene specific primers containing BamHI and XbaI sites, digested, and ligated to pYES-DEST52 vector (Invitrogen) digested with the same enzymes. Codon optimized hHRG-1 ORF for yeast expression (yhHRG-1) was synthesized by Genscript (OptimumGene) and subcloned into pYES-DEST52 vector as described above. The ORF of hFLVCR2 (GenBank accession number BC019087) was PCR amplified from human FLVCR2 cDNA in pOTB7 (Clone ID 4866427, Open Biosystems) using gene specific primers and cloned into pYES-DEST52 vector as described above. Site-directed mutagenesis was performed on pcDNA3.1(+)zeo-CeHRG-1-HA and pcDNA3.1(+)Zeo-CeHRG-4-HA using the QuikChange XL Site-Directed Mutagenesis Kit following to the manufacturer's instructions (Stratagene). The sequences of primers used for generating mutations are listed in Appendix I. The sequences coding mutant proteins were sequenced and subcloned into pYES-DEST as described above.

Chimeras were generated from pcDNA3.1(+)zeo-CeHRG-1-HA, pcDNA3.1(+)zeo-CeHRG-4-HA and pcDNA3.1(+)zeo-hHRG-1-HA by fusion PCR.

The sequences of primers used for generating chimeras are listed in Appendix I. The chimeras were cloned into pcDNA3.1(+)zeo using 5' BamHI and 3' XhoI sites. The constructs were subsequently cloned into the pECFP-N1 vector using 5'XhoI and 3' BamHI sites, and subcloned into pYES-DEST vector using 5'BamHI and 3' XbaI sites.

For the HRG-1 small molecule antagonist screen, codon optimized ORFs of HRG-1 homologs from *Leishmania amazonesis* (yLHR-1), *Brugia malayi* (yBmHRG-1), *Ancylostoma ceylanicum* (yAceHRG-1), *Dirofilaria immitis* (yDiHRG-1), *Meloidogyne incognita* (yMiHRG-1), *Trypanosoma brucei* (yTbHR-1) and *Trypanosoma cruzi* (yTcHR-1) were synthesized by Genscript (OptimumGene) and subcloned into pYES-DEST52 vector using 5'BamHI and 3'XbaI sites. The yeast integrating plasmid pRS403 was used to generate integrated yeast cell lines. The GAL1 promoter/HRG-1 ORFs/CYC1 terminator expression cassette were amplified by PCR using 5'-NotI-GAL1/3'-SalI-CYC1tt primers from corresponding pYES-DEST52 constructs, and subcloned into the NotI/SalI sites of pRS403 vector.

Yeast Assays

Yeast Strains and Growth Media

The *S. cerevisiae* strains used in this study were derived from the W303 and YPH499 backgrounds (Appendix II). The *hem1*Δ(6D) and OPY102 strains were constructed as described elsewhere [129,130]. To construct *hem1*Δ *fre1*Δ

*fre2*Δ MET3-FRE1, plasmid pRS404-MET3-FRE1 was linearized with NdeI and integrated into the TRP1 locus of OPY102. Cells were maintained in YPD or appropriate synthetic complete (SC) media supplemented with 250 μM δ-aminolevulinic acid (ALA) (Frontier Scientific)[131].

To generated integrated yeast cells, pRS403 and the expression construct, pRS403-pGAL1-HRG-1 ORFs, were linearized at the unique NheI site in the HIS3 gene and transformed into the W303 strain using the lithium acetate method [132]. Integrated clones were screened on 2% w/v glucose SC -His plates, using yeast colony PCR for both sides of the integration site as described below. The primers used for PCR are listed in Appendix A; the expected product sizes were 1461 bp for 5'-B1-pRS403/3'-His3 primers and 1416 bp for 5'-His3/3'-A2-pRS403 primers. Integrated yeast lines were then tested by growing in 2% w/v raffinose SC (-His, +0.4% galactose) medium supplemented with different concentrations of GaPPIX. Isolated yeast stable lines were stored as frozen stocks containing 25% glycerol at -80ºC.

Yeast Colony PCR

To examine yeast integration, a colony was resuspended using a disposable plastic loop with 1 μl volume in 100 μl of 40 μM Tris base (no pH adjustment), 0.5 μM EDTA, 14 μM β-2-mercaptoethanol and 0.05% SDS. The cells were incubated at room temperature for 10 min followed by heating to 85–90°C for 10 min. After cooling to room temperature, the samples were centrifuged at 16,000g for 30 s.

Lysate (1µl) was used per 25 µl PCR reaction (94°C, 1 min preheat; 94°C, 3 min to denature the genomic DNA; and 30 cycles of 94°C for 30 s, 50°C for 30 s, 68°C for 3 min). 5 µl of the reaction product was then resolved on a 1% agarose gel.

Spot Growth Assay

The plasmids for HRG-1 wild-type and mutant expression were transformed into strain *hem1*Δ(6D) using lithium acetate method [132]. Transformants were selected on 2% w/v glucose SC (-Ura) plates supplemented with 250 µM ALA. Five or six transformed colonies were picked and streaked on 2% w/v raffinose SC (-Ura) plates supplemented with 250 µM ALA to deplete glucose for 48 hours. Prior to spotting, cells were cultivated in 2% w/v raffinose SC (-Ura) medium for 18 hours to deplete hemin. Cells were then suspended in water to an OD_{600} of 0.2. Ten-fold serial dilutions of each tranformant were spotted (10 µL /spot) onto 2% w/v raffinose SC (-Ura) plates supplemented with either 0.4% w/v glucose and 250 µM ALA (positive control), or 0.4% w/v galactose and different concentrations of hemin, incubated at 30°C for 3 days before imaging.

Ferrireductase Assay

The strain *hem1*Δ *fre1*Δ *fre2*Δ MET3-FRE1 was used for the ferrireductase assay. Yeast transformation and selection was performed as described above using

respective SC auxotrophic medium supplemented with 250 μM ALA. After being depleted of hemin in 2% w/v raffinose SC (-Ura, -Trp, -Met) medium for 12 hours, cells were suspended in 2% w/v raffinose SC (-Ura, -Trp) medium supplemented with 0.4% w/v galactose, 0.1 mM Na_2S and different concentrations of hemin to an OD_{600} of 0.3, cultivated in 96-well plates at 30°C, with shaking at 225 rpm for 16 hours and assayed for ferrireductase activity [133]. Cells were washed with washing buffer (2% BSA, 0.1% tween-20 in 2× PBS) three to four times to remove residual hemin in the medium, washed twice with reaction buffer (5% glucose, 0.05 M sodium citrate buffer, pH 6.5), suspended in reaction buffer and the OD_{600} determined using a plate reader (BioTek). Equal volume of assay buffer (2mM bathophenanthroline disulfonate (BPS), 2mM $FeCl_3$ in reaction buffer) was added to the cells (T = 0 min) and incubated at 30°C in the dark until red color developed. OD_{535} and OD_{610} were determined and ferrireductase activity (nmol / 10^6cells / min) was calculated as:

$$\frac{[(OD_{535(sample)} - OD_{610(sample)}) - (OD_{535(blank)} - OD_{610(blank)})] \times 45}{V_{cells} \times (OD_{600(sample)} - OD_{600(blank)}) \times T_{min}}$$

β-Galactosidase Reporter Assay

The plasmids for HRG-1 wild-type and mutant expression were co-transformed into strain *hem1*Δ(6D) with pCYC1-LacZ. Selection of transformants was performed as described above using appropriate SC auxotrophic medium supplemented with 250 μM ALA. Cells were depleted for hemin in 2% w/v raffinose SC (-Ura, -Trp) medium for 12 hours, and then were suspended in 10mL 2% w/v

raffinose SC (-Ura, -Trp) medium supplemented with 0.4% w/v galactose, and different concentrations of hemin to an OD_{600} of 0.1. Cells culture were cultivated at 30°C, with shaking at 225 rpm for 12 hours and assayed for β-galactosidase activity, as described elsewhere[134]. β-galactosidase activities were normalized to total protein concentration.

Immunoblotting

For western blotting experiments, yeast transformants were resuspended in lysis buffer (1% SDS, 8 M urea, 10 mM Tris-HCl pH 8.0, 10 mM EDTA) with protease inhibitors (1 mM phenylmethylsulfonyl fluoride, 4 mM benzamidine, 2 μg/mL leupeptin, and 1 μg/mL pepstatin) and 0.5 mm acid-washed glass beads. Cells were heated at 65°C for 10 min and disrupted using FastPrep-24 (MP Bio) for 3×30s at the 6.5m/s setting. Cell lysates were collected and the total protein concentration was quantified with the Bradford reagent (Bio-Rad). Protein samples were separated on 12% SDS-polyacrylamide gel and transferred to nitrocellulose membrane (Bio-Rad). For immunoblotting, the membranes were incubated with rabbit anti-HA (Sigma) as primary antibody at a 1:5,000 dilution for 16 hours at 4°C, followed by HRP-conjugated goat anti-rabbit antibody at a 1:10,000 dilution for 1 hour at room temperature. Signal was detected using SuperSignal chemiluminescence reagents (Thermo Scientific) in the Gel Documentation system (Bio-Rad).

Immunofluorescence

Yeast transformants were cultivated in 2% w/v raffinose SC (-Ura) medium supplemented with 0.4% w/v galactose and 250 μM ALA to mid-log phase, and then fixed with 4% formaldehyde for 1 hour at room temperature. Immunofluorescence microscopy was performed as described elsewhere [134]. Images were taken using a DM IRE2 epifluorescence microscope (Leica) connected to a Retiga 1300 cooled Mono 12-bit camera.

High-Throughput Screen

Yeast integration lines were streaked on 2% w/v raffinose SC –His plates from -80°C glycerol stocks, and incubated at 30°C for 3 days until colonies with pink color formed. The day before adding the compounds, a 10 to 20μL aliquot of yeast cells were collected from the plate and inoculated in 50mL 2% w/v raffinose SC –His liquid medium at 30°C, with shaking at 250 rpm for 24 to 30 hours. To prepare the assay culture, 2% w/v raffinose SC (–His, +0.4% galactose) medium supplemented with 2 to 20μM GaPPIX was loaded (35μL/well) into 384-well plates (Nunc) using a Multidrop reagent dispenser (TiterTek). The plates were then loaded with 0.7μL compound/well (5μM) using robotic liquid handlers (Beckman). Yeast cells were prepared by centrifuging the overnight liquid culture at 3,000g for 5 min and resuspending in 2% w/v raffinose SC (–His, +0.4% galactose) to an OD_{600} = 0.1. Yeast cells (35μL/well)were added to the preloaded 384-well plates and incubated in

a humidity container at 30°C without shaking. After 33-42 hours incubation, the OD_{600} was measured using a Synergy 2 plate reader (BioTek).

DRC assays were performed as described above with the following modifications. All the compounds were validated by LC/MS and prepared as fresh 10mM stocks in DMSO just before dispensation. Twelve different concentrations (0.1 nM to 30 μM) of the compounds were then prepared from the stocks in a master plate. Compounds (0.7μL/well) were loaded into 384-well plates using an Echo 555 liquid handler (Labcyte) and the OD_{600} was measured at multiple time points (0 h to 48 h).

Worm Assays

Worm Culture and Strains

C. elegans strains were maintained on nematode growth medium (NGM) agar plates seeded with OP50 bacteria at 20°C. Worm synchronization and cross were performed as described elsewhere [135]. The deletion strains *Δhrg-1* (tm3199) and *Δhrg-4* (tm2994) were obtained from the National Bioresource Project (Japan). The deletion strains were outcrossed eight times with the N2 Bristol strain before further study. A *Δhrg-1Δhrg-4* double deletion strain was generated by crossing *Δhrg-1* with *Δhrg-4;* homozygous mutant progeny and their wild-type brood mates were picked by single-worm PCR genotyping. A *Δhrg-1Δhrg-4unc-119* strain was generated by crossing the *Δhrg-1Δhrg-4* with the *unc-119 (ed3)* strain and maintained

in liquid mCeHR-2 medium supplemented with 20 μM hemin chloride [136]. For single-worm PCR, individual worms were lysed in 5 μL lysis buffer (50 mM KCl, 10 mM Tris-HCl, 2.5 mM MgCl2, 0.45% NP-40, 0.45% Tween-20, 0.01% gelatin, and 1mg/mL freshly prepared proteinase K) by freezing and heating (2 hours at -80°C, 1 hour at 65°C, and 30 min at 95°C). Worm lysates were subjected to PCR reactions with primers CeHRG-1_del_f and CeHRG-1_del_b to detect a 650 bp fragment of *hrg-1* in the *Δhrg-1* strain, and with primers CeHRG-4_del_f and CeHRG-4_del_b to detect a 450 bp fragment of *hrg-4* in the *Δhrg-4* strain (Appendix A).

Generation of Transgenic Worms

The rescue plasmid *Phrg-1::HRG-1-HA::ICS::GFP* was constructed by recombining the putative *hrg-1* promoter (~3 kb upstream of *hrg-1* gene, *Phrg-1*), the fused *hrg-1* gene (*HRG-1-HA::ICS::GFP*) and the 3'-UTR of *hrg-1* gene into a single destination vector, pDEST-R4-R3, using the Multisite Gateway system (Invitrogen). The entry clones of *hrg-1* promoter and 3'-UTR were constructed previously [58]. To make the fused *hrg-1* entry clone, *hrg-1* gene was amplified by PCR from N2 genomic DNA, tagged with the HA epitope, fused with the SL2 intercistronic sequence (ICS) and *gfp* gene, and cloned into the entry vector pDONR-221 by recombination using the Gateway BP Clonase kit (Invitrogen). Site-directed mutagenesis was performed on the rescue plasmid as described above. The promoter, coding region and 3'-UTR of all the rescue plasmids were sequenced before further analysis. The transgenic worms were generated by microparticle bombardment [137].

Rescue plasmids (10μg) were mixed with 5μg of the *unc-119* rescue plasmid pDP#MM016B and co-bombarded into *Δhrg-1Δhrg-4unc-119* worms using the PDS-1000 particle delivery system (Bio-Rad). At least two transgenic lines of each construct were analyzed for each experiment.

Worm Growth Assay on *ΔhemB E. coli*

The heme-deficient *E. coli* strain RP523 (*ΔhemB*) was a gift from Dr. Mark O'Brian at State University of New York at Buffalo [138]. Actively growing *ΔhemB* cells (grown overnight in Luria-Bertani (LB) medium supplemented with 1 μM hemin) were diluted at a ratio of 1:6 into fresh LB medium supplemented with different concentrations of hemin, cultivated for 5.5 hours, heat-inactivated at 65°C for 5 min, and diluted to a OD_{600} = 0.5 with corresponding LB medium. Each 35 mm NGM plate was seeded with 200μL cell culture.

Synchronized L1 larvae of worms grown on OP50 seeded NGM plates were transferred onto NGM plates seeded with *ΔhemB* grown with 50 μM hemin, and incubated at 20°C for 4 days (P_0). The P_0 worms were bleached when they reached gravid stage. Forty synchronized F_1 L1 larvae were transferred onto each *ΔhemB* plate and inoculated at 20°C for 3-5 days. Five F_1 gravid worms were placed onto each new appropriate *ΔhemB* plate and allow to lay eggs (F_2) for 12 hours. The growth of F_1 and F_2 worms was recorded by DIC imaging and COPAS BioSort (Union Biometrica, Holliston, MA) when the wild-type worms reached young adult stage. For COPAS BioSort, about 100 worms for each sample were analyzed for both length

(time of flight) and optical density (extinction). The settings for GFP measurement were gain=3.0, PMT voltage=600.

Worm ZnMP Uptake Assay

Worms were grown as described for the *ΔhemB* growth assay. F_1 worms were harvest at L4 stage from *ΔhemB* plates, washed twice with M9 buffer. Approximately 100 worms/well of F_1 worms were transferred to 12-well plates, inoculated in mCeHR-2 medium supplemented with 1.5 μM hemin chloride and different concentrations of ZnMP for 16 hours. ZnMP fluorescence intensity was scored using a DM IRE2 epifluorescence microscope (Leica) with a rhodamine filter and quantified by SimplePCI software [65,139].

Worm Immunoblotting

Worms were grown as described for the *ΔhemB* growth assay. F_1 worms were harvested at early gravid stage from *ΔhemB* plates, washed twice with M9 buffer, resuspended in lysis buffer (20 mM HEPES, pH 7.4, 0.5 % Triton X-100 and 150 mM NaCl) with Protease Inhibitor Cocktail Set III (Calbiochem) and Lysing Matrix D beads (MP Biomedicals), and disrupted using FastPrep-24 (MP Biomedicals) for 60s at the 6.5 m/s setting. The total protein concentration of worm lysates was quantified with the Bradford reagent (Bio-Rad) and subjected to immunoblotting analysis as described above.

Mammalian Assays

Cell Lines and Transfection

HEK293 and MDCK II cells were maintained in Dulbecco's modified medium with 10% fetal bovine serum, 1% penicillin-streptomycin, and glutamine. MDCK II cells were kindly provided by the Lippincott-Schwartz laboratory (NIH, Bethesda, Maryland). Transfections for immunoblotting were performed with Lipofectamine 2000 (Invitrogen), and those for immunofluorescence were performed with FuGENE 6 (Roche). For immunoblotting, HEK293 cells were seeded on tissue culture plates and transfected with Lipofectamine 2000 the next day at a confluence of 90%. Lipofectamine transfection was performed according to the manufacturer's protocol. Cells were harvested for immunoblotting two days after transfection. HEK293 cells for fluorescence microscopy were seeded on glass coverslips and transfected with FuGENE 6 the following day at a confluence of 50%. FuGENE 6 transfection was performed according to the manufacturer's protocol, and cells were fixed for microscopy two days after transfection. MDCK II cells were seeded on Corning transwell filters and allowed to form a monolayer. Before the cells had formed tight junctions they were transiently transfected using Lipofectamine 2000 according to the manufacturer's protocol. The formation of a monolayer was confirmed by trans-epithelial resistance readings in the range of 400-500 ohms. Rabbit anti-HA antibody (Sigma) was used for immunoblotting at a concentration of 1:2500 and for immunofluorescence at a concentration of 1:1000.

Immunoblotting of Mammalian Cell Lysate

Transiently transfected cells were lysed in buffer containing 1% Triton X-100, 20 mM Hepes pH 7.4 and 150 mM NaCl. Protein (35μg) was seperated on a 4-20% gradient SDS-PAGE gel and then transferred to nitrocellulose membrane (BioRad). Membranes were blocked with 5% nonfat milk for one hour, and then incubated for one hour in primary antibody in 5% milk. After six washes in phosphate-buffered saline with 0.05% Tween-20, blots were incubated with anti-rabbit horseradish peroxidase linked secondary antibody in 5% milk for 1 hour. Blots were washed again six times in phosphate buffered saline with 0.05% Tween-20, and then developed using Pico ECL reagents (Pierce).

Immunofluorescence in Mammalian Cells

Transiently transfected HEK293 or polarized MDCK II cells were fixed in 4% paraformaldehyde (PFA), quenched with 0.1M ethanolamine, and mounted on coverslips with Prolong Antifade (Invitrogen). HEK293 cells were stained before fixation with a plasma membrane marker (AlexaFluor633-conjugated wheat germ agglutinin) at 4 μg/ml for 5 minutes at 37^{o} C. HEK293 cells were co-transfected with Lamp-1 YFP and CFP tagged constructs. Lamp-1 YFP was a kind gift from Jennifer Lippincott-Schwartz. MDCK II cells were co-transfected with either the apical membrane marker, syntaxin-3 GFP, or the basolateral marker, NTCP GFP, and the HA tagged constructs. The MDCK II cells were then stained with anti-HA and AlexaFluor568-conjugated anti-rabbit antibodies (Invitrogen). Cells were examined

with a Leica 510 confocal microscope using argon and neon lasers and a 63x oil immersion lens.

Fluorescence Protease Protection Assay

The FPP Assay was carried out as previously described [73]. HEK293 cells were grown in LabTeK cover glass culture chambers (Nunc) and transfected with pECFP-N1 HRG-1 chimera constructs. Cultures were incubated for 24 hours and then the cells were washed three times with KHM buffer (20 mM HEPES, PH 6.5, 110 mM potassium acetate, and 2mM $MgCl_2$). Images of selected cells were recorded using a DMIRE2 epifluorescence microscope (Leica) connected to a Retiga 1300cooled Mono 12-bit camera. Time-lapse images were acquired before and after proteinase K (50mg/ml/3 minutes) digestion. Following this, the cells were treated with both 30 mM digitonin and proteinase K and images were recorded 1, 2 and 3 minutes after treatment.

Statistical Analysis

Statistical significance was calculated by using one-way ANOVA with the Student–Newman–Keuls multiple comparison test in GraphPad INSTAT version 3.01 (GraphPad, San Diego). Data values were presented as mean ± SEM. A p value < 0.05 was considered as significant.

Chapter 3: Topologically conserved residues direct heme transport in HRG-1-related proteins

Summary

Heme (iron protoporphyrin IX) is a macrocycle that not only plays an essential role as a prosthetic group in proteins but is an essential nutrient for parasites and is the major dietary iron source for humans [53,140]. Because hemes are essential but cytotoxic when present in excess, organisms must maintain appropriate levels of cellular heme. One means to accomplish this task is to regulate the synthesis and degradation of heme [16,141,142]. Another would be to regulate the trafficking and compartmentalization of heme [53]. While significant strides have been made in understanding the mechanisms and regulation of heme synthesis and degradation in eukaryotes, how heme is transported, trafficked, and compartmentalized within the cell remains poorly understood [53]. Studies of heme transporters in bacteria have provided the molecular underpinnings into protein function [143,144], but these transporters do not have identifiable homologs in animals.

By utilizing the free-living roundworm *Caenorhabditis elegans*, we previously identified HRG-1-related proteins, membrane-bound transporters which import heme [58]. HRG-1- related proteins have four paralogs in *C. elegans* - CeHRG-1, CeHRG-4, CeHRG-5, and CeHRG-6 which may function redundantly to ensure that the worm, a heme auxotroph, acquires an adequate supply of heme to sustain its growth and development [15,61]. Mammals, by contrast, have a single

homolog which is only ≈20% identical to CeHRG-1. Previous studies have demonstrated that both worm and human HRG-1 bind and transport heme, and that knockdown of *hrg-1* in zebrafish embryos results in severe anemia with concomitant defects in yolk tube extension and brain formation; phenotypes that are fully rescued by CeHRG-1 [58]. These studies predict that HRG-1-related proteins are essential for vertebrate development and have conserved functions across metazoa. To gain mechanistic insights into the heme transport function of HRG-1-related proteins, we conducted a structure-function analysis of CeHRG-1 and CeHRG-4 by exploiting yeast mutants that are unable to synthesize heme. Our studies reveal that HRG-1-related proteins transport heme across membranes through the coordinated actions of residues that are topologically conserved in the worm and human proteins. Our results imply that the mechanism for heme import employed by HRG-1-related proteins is ancient and predates vertebrate origins.

Results

CeHRG-1 and CeHRG-4 are both essential for heme homeostasis in *C. elegans*

To determine the *in vivo* localization of HRG-1-related proteins, we generated transgenic worms that expressed CeHRG-1 and CeHRG-4 tagged at the C-terminus with GFP. Both genes were expressed in the worm intestine with CeHRG-4 localized to the apical plasma membrane and CeHRG-1 primarily localized within an intracellular vesicular compartment (Fig. 3.1A). Metabolic labeling with the

Figure 3.1. Functional characterization of HRG-1-related proteins in *C. elegans*. (A) Transgenic worms stably expressing CeHRG-4::YFP or CeHRG-1::GFP translational fusions were cultivated in mCeHR-2 medium with 1.5 μM heme and 10 μM ZnMP for 16 hours with constant shaking. The localization of GFP variants (green) and ZnMP (red) was examined using a Zeiss 710 confocal microscope. Boxed regions in the upper images have been enlarged for clarity and shown at the bottom. (B) Schematic representation of *Δhrg-1* (tm3199) and *Δhrg-4* (tm2994). Open boxes represent open reading frames and grey boxes indicate untranslated regions. "+1" indicates the transcription start site. The deleted regions are represented by underline with the start and end indicated above. (C) Wild-type, *Δhrg-1*, *Δhrg-4* and *Δhrg-1Δhrg-4* worms were synchronized, placed on NGM plates seeded with RP523 bacteria grown at 50 μM hemin (P0), synchronized again and transferred to RP523 plates of low (1 μM) and high (50 μM) hemin (F1) and follow the growth for two subsequent generations. Representative images of F2 progeny are shown. Scale bar, 50 μm. (D) Worms in (C) were measured by COPAS BioSort. Each dot represents an individual worm: wild-type (green), *Δhrg-1* (orange), *Δhrg-4* (blue) and *Δhrg-1Δhrg-4* (red). Time of flight and extinction indicate the length and the optical density of worms, respectively.

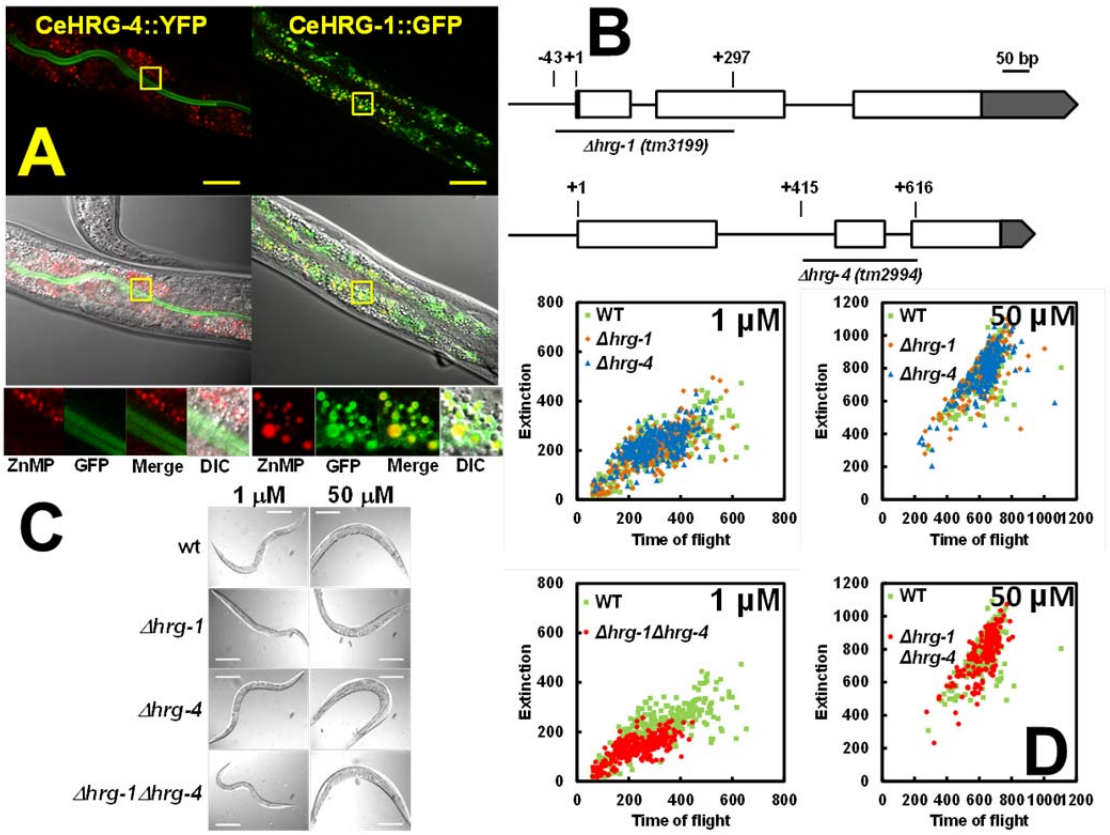
CeHRG-4::YFP
CeHRG-1::GFP
A
ZnMP
GFP
Merge
DIC
ZnMP
GFP
Merge
DIC
B
-43+1
+297
50 bp
Δhrg-1 (tm3199)
+1
+415
+616
Δhrg-4 (tm2994)
WT
Δhrg-1
Δhrg-4
1 μM
50 μM
Extinction
Time of flight
C
1 μM
50 μM
wt
Δhrg-1
Δhrg-4
Δhrg-1Δhrg-4
WT
Δhrg-1Δhrg-4
D

fluorescent heme analog zinc mesoporphyrin (ZnMP) revealed that CeHRG-1 localized to vesicular membranes containing ZnMP fluorescence. These localization studies are consistent with our previous genetic knockdown experiments in worms which showed that ZnMP accumulated in vesicles when CeHRG-1 was depleted, while RNAi of CeHRG-4 reduced ZnMP entry into the intestine.

To delineate the function of HRG-1-related proteins, we analyzed worms with a genetic deletion in *hrg-1* and *hrg-4*. As shown in Fig. 3.1B, *Δhrg-1* (tm3199) contains a 341 bp deletion which results in the loss of exon 1 (including 43 bp upstream of the ATG start codon), intron 1, and a portion of exon 2. By contrast, *Δhrg-4* (tm2994) has a 202 bp deletion which eliminates part of intron 1, exon 2, and intron 2. PCR amplification of the genomic DNA from *Δhrg-1* and *Δhrg-4* confirmed the presence of these deletions (Appendix III). Analysis by RT-PCR from RNA extracted from *Δhrg-1* strain revealed no discernible product, although a ≈450 bp fragment was amplified in RNA samples obtained from the *Δhrg-4* deletion strain (Appendix III A). DNA sequencing of the 450 bp product revealed that a truncated CeHRG-4 protein containing the first two TMDs and six additional amino acids followed by several stop codons could be synthesized if the *Δhrg-4* mRNA were to be translated (Appendix III B). Together, these results suggest that the *Δhrg-1* strain is a null mutant whereas the *Δhrg-4* strain could be a hypomorph.

Since CeHRG-1 and CeHRG-4 are highly upregulated when worms are grown with low environmental heme, we analyzed the deletion mutants for heme-dependent phenotypes [145]. Neither *Δhrg-1* nor *Δhrg-4* showed any obvious phenotypes compared to wild-type broodmates when fed with RP523, a mutant *E. coli* strain that

does not synthesize heme [73]. Feeding worms RP523 cultivated in different concentration of heme permits external control of heme levels within the worm via dietary manipulations. Because the *C. elegans* genome contains multiple paralogs of HRG-1-related proteins which may function redundantly, we generated a *Δhrg-1Δhrg-4* double mutant strain. Unlike the single mutants, the *Δhrg-1Δhrg-4* mutant worms were significantly growth retarded in low heme corresponding to a delay of up to three larval stages during development (Fig. 3.1 C, D). Most importantly, this growth delay was fully suppressed when double mutant worms were fed a heme-replete diet (Fig. 3.1 C, D). These genetic studies affirm that both *hrg-1* and *hrg-4* are essential for heme homeostasis in *C. elegans* when worms are maintained under minimal dietary heme conditions. Moreover, the additive phenotypes observed in the *Δhrg-1Δhrg-4* double mutants indicate that the aberrant mRNA generated in *Δhrg-4* worms has little or no function.

Expression of HRG-1-related Proteins in *Saccharomyces cerevisiae hem1*Δ Strain

Our genetic investigations of *C. elegans* clearly indicate that CeHRG-1 and CeHRG-4 function in a concerted manner to maintain heme homeostasis in the worm. The presence of multiple paralogs of HRG-1-related proteins in *C. elegans* hinders a systematic investigation of the mechanisms employed by individual HRG-1-related proteins within the animal. To circumvent this complication, we sought to recapitulate the heme auxotrophy of *C. elegans* in a simpler, defined system. We exploited *S. cerevisiae*, because this single cell eukaryote does not contain HRG-1-

related protein homologs and utilizes exogenous heme poorly even in the absence of endogenous heme synthesis [130,136]. A forward genetic screen in yeast had recently identified the porphyrin transporter Pug1p using sensitive, functional assays established to assess heme transport activity in *hem1*Δ strain, a yeast mutant that is deficient in *HEM1* which encodes for 5-aminolevulinate synthase, the first enzyme of the heme synthesis pathway [130]. HRG-1-related proteins tagged at the C-terminus with a HA epitope was expressed in *hem1*Δ under the control of the inducible *GAL1* promoter, which was induced by adding galactose and repressed by adding glucose. When both CeHRG-1 and CeHRG-4 are expressed in yeast, their proteins migrated at the predicted molecular weights, similar to our earlier expression analysis in mammalian cell lines (Fig. 3.2A) [58]. Indirect immunofluorescence microscopy indicated that CeHRG-4-HA localized primarily on the plasma membrane, while CeHRG-1-HA was found on the yeast vacuolar membrane, a membrane compartment equivalent to the mammalian lysosome (Fig. 3.2B). These studies are consistent with expression studies of CeHRG-1 and CeHRG-4 proteins in worms (Fig. 3.1B) and mammalian cells [58].

CeHRG-1 and CeHRG-4 Mediate Heme Transport in Yeast

A *hem1Δ* yeast mutant is unable to grow unless it is supplemented with either ALA, the product of the 5-aminolevulinate synthase enzyme, or an excess of exogenous heme (supplemented as hemin chloride) in the growth medium. We used

Figure 3.2. Improved hemin utilization in yeast strains overexpressing HRG-1-related proteins. (A) Immunoblotting was performed on transformants overexpressing C-terminus HA-tagged CeHRG- 4 or CeHRG-1 in the *hem1*Δ(6D) strain. Predicted molecular mass of HRG-1-related proteins was detected as indicated by filled circles. Asterisks indicate putative dimers. (B) Same yeast transformants were subjected to indirect immunofluorescence microscopy. For clarity, the boxed regions in the left images have been enlarged to show the intracellular localization of HRG-1-related proteins. Scale bar, 5 μm. (C) The *hem1*Δ(6D) strain transformed with empty vector pYES-DEST52, CeHRG-4, CeHRG-1 and their HA-tagged versions were cultivated overnight in SC medium without ALA and spotted in serial dilutions on 2% raffinose SC (-Ura, +0.4% galactose) plates supplemented with indicated concentrations of hemin (positive control: +0.4% glucose, +250μM ALA, negative control: - ALA, -hemin). Plates were incubated at 30°C for 3 days prior to imaging. (D) The *hem1*Δ*fre1*Δ*fre2*ΔMET3-FRE1 strain was transformed with empty vector pYES-DEST52 and plasmids for HRG-1-related protein expression. Transformants were ALA-starved for 12 hours, grown in 2% raffinose SC (-Ura, -Trp, +0.4% galactose) medium supplemented with indicated concentration of hemin for 16 hours, and assayed for ferric reductase activity. (E) The *hem1*Δ(6D) strain co-transformed with pCYC1-LacZ and empty vector or plasmids expressing HRG-1- related proteins was ALA-starved for 12 hours, and grown in 2% raffinose SC (-Ura, -Trp, +0.4% galactose) medium supplemented with indicated concentration of hemin for 12 hours, lysed and β-galactosidase activity was measured. Error bars represent the standard error of the mean (SEM) from three independent experiments. *** $p < 0.001$.

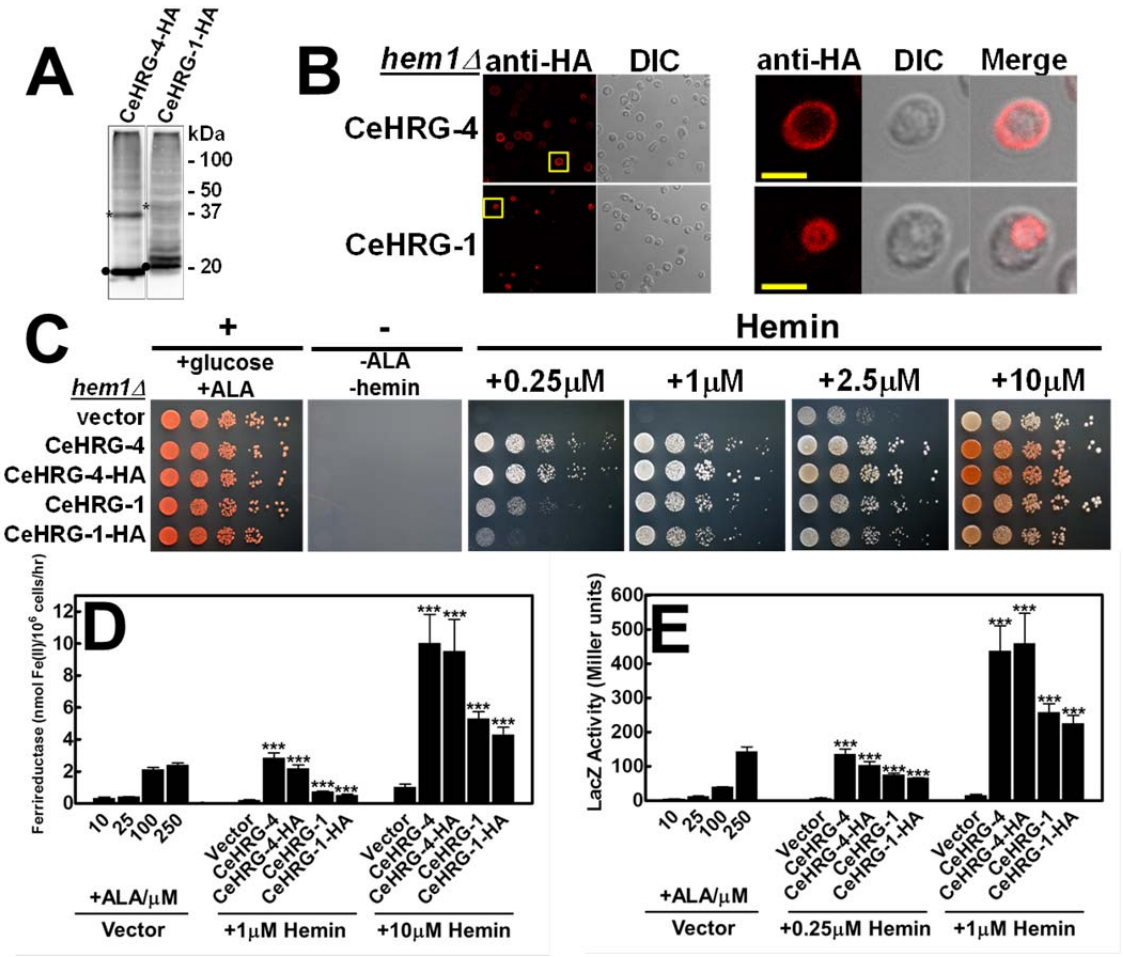
A
CeHRG-4-HA
CeHRG-1-HA
kDa
100
50
37
20
B
hem1Δ
anti-HA
DIC
Merge
CeHRG-4
CeHRG-1
C
+
-
Hemin
+glucose
+ALA
-ALA
-hemin
+0.25μM
+1μM
+2.5μM
+10μM
hem1Δ
vector
CeHRG-4
CeHRG-4-HA
CeHRG-1
CeHRG-1-HA
D
Ferrireductase (nmol Fe(II)/10^6 cells/hr)
10
25
100
250
Vector
CeHRG-4
CeHRG-4-HA
CeHRG-1
CeHRG-1-HA
+ALA/μM
Vector
+1μM Hemin
+10μM Hemin
E
LacZ Activity (Miller units)
+0.25μM Hemin
+1μM Hemin

three independent assays established in *hem1Δ* yeast mutants [130]. (a) First, we determined rescue of growth of *hem1Δ* strain transformed with a plasmid expressing HRG-1-related proteins and grown on agar plates containing varying concentrations of heme (Fig. 3.2C). The degree of growth rescue and the heme concentration indicates relative uptake of heme by HRG-1-related proteins. (b) Second, we measured the activity of a heme-dependent enzyme, ferric reductase [130,133], as an indicator of intracellular heme concentrations in a *hem1Δfre1Δfre2ΔMET3-FRE1* strain (Fig. 3.2D). This strain lacks both native genes for *FRE1* and *FRE2*, the major surface reductases which are sensitive to regulation by iron and copper, but has one of these ferric reductases (Fre1p) present under the control of the inducible *MET3* promoter. Thus, any perturbations in cellular heme levels due to expression of the HRG-1-related proteins, are reflected in a concomitant change in the ferric reductase enzyme activity [130,133]. (c) Third, we measured changes in the regulatory pools of heme by determining β-galactosidase activity from a *CYC1::lacZ* promoter-reporter fusion (Fig. 3.2E). Here, *lacZ* expression is dependent on Hap1-5. Hap1 is a transcription factor that binds heme and activates *CYC1* expression in response to cellular changes in heme [146,147]. Thus, the level of β-galactosidase activity in *CYC1::lacZ* expressing HRG-1-related proteins reflects the availability of regulatory pools of intracellular heme to activate the *CYC1* promoter.

The *hem1Δ* strain transformed with pYES-DEST52 vector alone did not grow unless supplemented with 2.5 to 10 μM heme. By contrast, cells overexpressing CeHRG-1 and CeHRG-4, either with or without a HA epitope tag, showed a significant improvement in growth at both 0.25 μM and 1 μM heme (Fig. 3.2C). The

imported heme was incorporated into cellular hemoproteins, because yeast expressing CeHRG-4 and CeHRG-1 showed >10-fold and 5-fold increase in ferrireductase activity, respectively (Fig. 3.2D). Furthermore, cells expressing HRG-1- related proteins had elevated cytoplasmic heme because CeHRG-4 and CeHRG-1 expression increased the activity of *CYC1::LacZ* reporter by 10 to 20-fold (Fig. 3.2E). In addition, CeHRG-5 and CeHRG-6 also significantly and consistently enhanced the heme-dependent growth of the *hem1Δ* strain confirming our *in silico* observations that these putative paralogs transport heme. (Fig. 3.3). Together, these studies unequivocally demonstrate that multiple HRG-1- related proteins transport heme in the worm and lend validity to the use of the yeast as a heterologous system to dissect the mechanism of HRG-1-related protein activity.

Identification of conserved heme-binding ligands in HRG-1-related proteins

Although multiple sequence alignments reveal only 27% identity and 41% similarity between CeHRG-1 and CeHRG-4, an examination of the two protein sequences using membrane topology modeling revealed highly conserved amino acids that are located within the protein's predicted secondary structure that may function as axial ligands (H, Y or C) for heme (Fig. 3.4A). CeHRG-1 and CeHRG-4 are predicted to contain four transmembrane domains (TMDs) and both the amino and carboxyl terminus reside in the cytoplasm [58]. Conserved residues in CeHRG-1 include H88 and H90 in TMD2, H135 in the second predicted exoplasmic (E2) loop, and in the carboxyl terminus a FARKY motif, a cluster of aromatic and basic amino acids which could

Figure 3.3. Worm HRG-1 homologs function as heme importers in yeast *hem1*Δ strain. The *hem1*(6D) strain was transformed with empty vector pYES-DEST52, and c-terminus HA-tagged HRG-1 proteins. Spot growth assay were performed with indicated conditions. Plates were incubated at 30°C for 3 days prior to imaging.

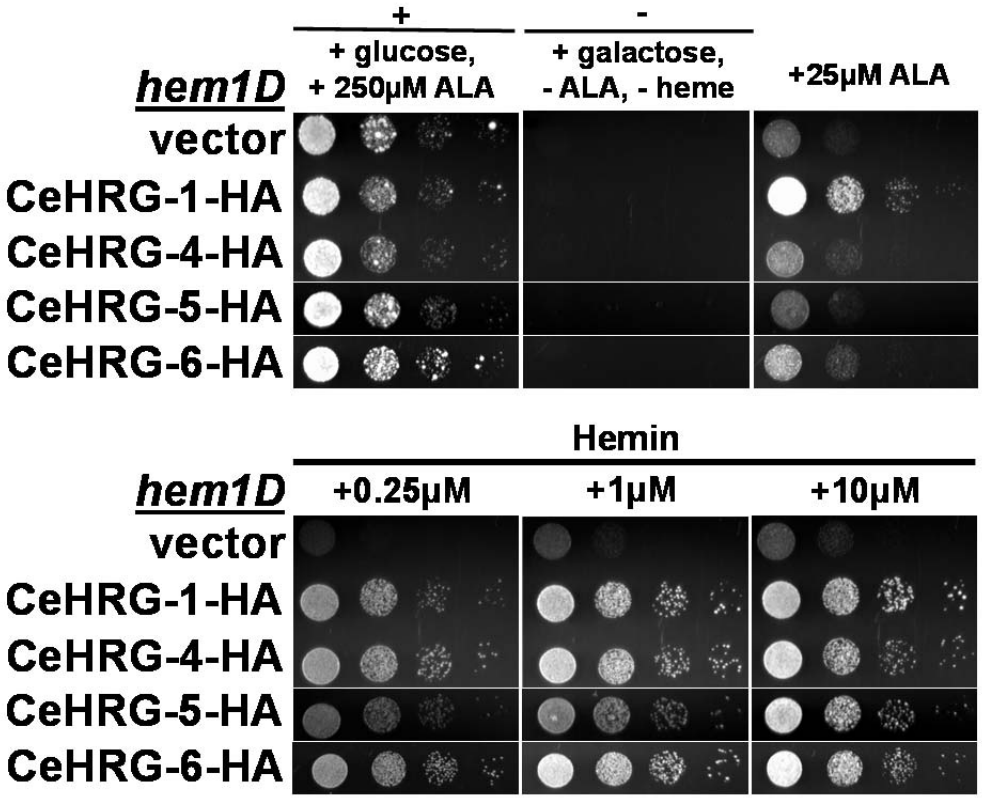
+
-
+ glucose,
+ 250μM ALA
+ galactose,
- ALA, - heme
+25μM ALA
hem1D
vector
CeHRG-1-HA
CeHRG-4-HA
CeHRG-5-HA
CeHRG-6-HA
Hemin
hem1D
+0.25μM
+1μM
+10μM
vector
CeHRG-1-HA
CeHRG-4-HA
CeHRG-5-HA
CeHRG-6-HA

Figure 3.4. Heme transport analysis of wild-type and mutant CeHRG-4. (A) Putative topology of CeHRG-4 and CeHRG-1 predicted by TMHMM 2.0 and SOSUI. The amino and carboxyl-termini are cytoplasmic, C1 is the cytoplasmic loop and E1 and E2 are the exoplasmic loops. Potential heme interacting residues are shaded in red. (B) The *hem1*Δ(6D) strain was transformed with empty vector pYES-DEST52, CeHRG-4-HA and its mutants. Spot growth assay were performed with indicated conditions. Plates were incubated at 30°C for 3 days prior to imaging. (C) The *hem1*Δ*fre1*Δ*fre2*ΔMET3-FRE1 strain was transformed with empty vector pYES-DEST52, CeHRG-4 and its mutants. Ferric reductase assays were performed with indicated concentrations of hemin. Ferric reductase activity (nmol / 10^6cells / min) was measured and normalized to the activity of vector. (D) The *hem1*Δ(6D) strain cotransformed with pCYC1-LacZ and empty vector pYES-DEST52, CeHRG-4 or its mutants. β-galactosidase activity was measured. Error bars represent the standard error of the mean (SEM) from three independent experiments. * $p < 0.05$, ** $p < 0.01$, *** $p < 0.001$.

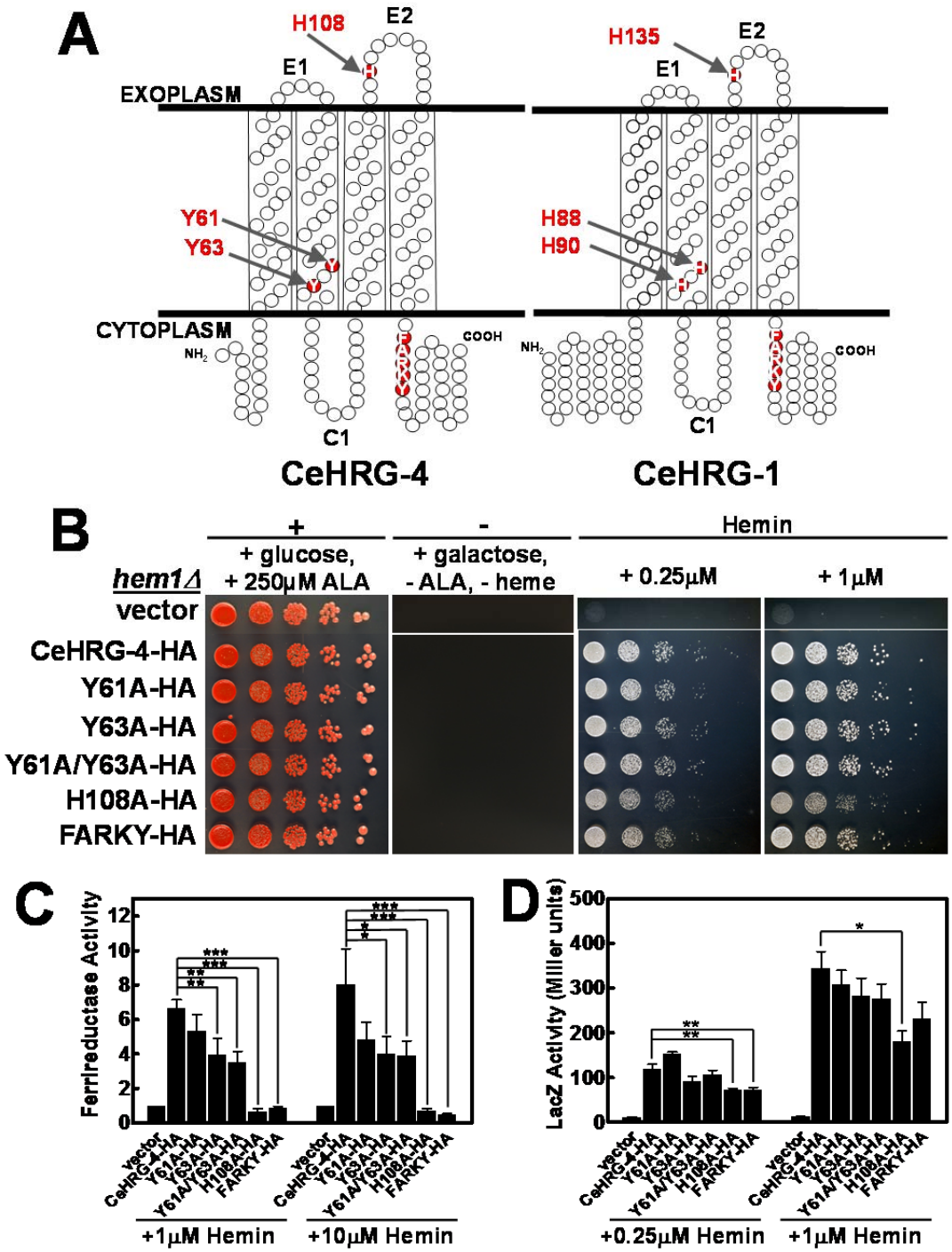
A
H108
E2
E1
EXOPLASM
Y61
Y63
CYTOPLASM
NH2
COOH
C1
CeHRG-4
H135
E2
E1
H88
H90
NH2
COOH
C1
CeHRG-1
B
+
-
Hemin
+ glucose,
+ 250μM ALA
+ galactose,
- ALA, - heme
+ 0.25μM
+ 1μM
hem1Δ
vector
CeHRG-4-HA
Y61A-HA
Y63A-HA
Y61A/Y63A-HA
H108A-HA
FARKY-HA
C
Ferrireductase Activity
12
10
8
6
4
2
0
vector
CeHRG-4-HA
Y61A-HA
Y63A-HA
Y61A/Y63A-HA
H108A-HA
FARKY-HA
+1μM Hemin
+10μM Hemin
D
LacZ Activity (Miller units)
500
400
300
200
100
0
+0.25μM Hemin
+1μM Hemin

Figure 3.5. Sequence alignment of CeHRG-1 and CeHRG-4. Pairwise sequence alignment was performed on CeHRG-1 and CeHRG-4 using EMBOSS Needle. Predicted transmembrane domains are shown as boxed region (TMD 1 - 4). Conserved amino acids shared by CeHRG-1 and CeHRG-4 are shaded in gray. Potential heme interacting motifs (red) and worm HRG-1 specific residues (green) are indicated by asterisks.


TMD 1
CeHRG-1 1 MHQIYSSDVSSITSKSSIAKAEIIIMEEEQQRQSC---CTWFHSIKVQIWIAW--LGVSA
CeHRG-4 1 ----------MTAE---NRGFCQLIC---H---INVRIGWTIFGIVF
E1 loop
TMD 2
CeHRG-1 56 GVMAGTVFAIQ-YQNWIAVTMCFISSGFATLVLHLHLAYKKTQMAGW-SET-RIRCIAAV
CeHRG-4 29 GISAILTYAIKFH-NWSATATTAIATLFACETLYLYWALKKNTIVNWKSSTFQL----MI
TMD 3
E2 loop
TMD 4
CeHRG-1 113 GATVSFISFIAMVFCLV---VAGIEHQ---TLDKQGIMGANLWIAAVWFFMTSKWSALTW
CeHRG-4 84 WPNV-FIGLILGLLGCLVCYIIAGITHQGAGSI--QAYGENLWFTGSWSLVITKW---TW
CeHRG-1 167 R---FARKYRAFCEESQPL--LAAAPPEYSV------TI--
CeHRG-4 138 QNAFFARKY---------LNKIGTASEDGDIDDDDVEVIKS

interact and orient heme side chains (Fig. 3.4A and Fig. 3.5). It is noteworthy that the potential His heme ligands in the TMD2 of CeHRG-1 are substituted with Tyr (Y61 and Y63) in CeHRG-4 (Fig. 3.4A). Tyr, which preferentially binds ferric iron, forms heme ligands with a lower redox potential than His and the coordination stabilizes heme and prevents it from carrying out oxidative chemistry [148,149].

CeHRG-4 Function Requires a Histidine in the E2 Loop and the FARKY Motif in the C-terminus

To examine the role of specific residues for CeHRG-4 functions, we replaced Y61, Y63, H108 and FARKY with alanines (Fig. 3.4A and Fig. 3.5). Immunoblotting and fluorescence microscopy studies revealed comparable expression and localization of the mutant and wild-type proteins (Fig. 3.6). Heme-dependent growth of transformed *hem1Δ* strain showed reduced growth only for the H108A mutant (Fig. 3.4B). By contrast, ferrireductase assays revealed a significant reduction in the activity for Y63, H108 and FARKY mutants, although only mutations in H108 and the FARKY motif resulted in severe attenuation (Fig. 3.4C). Although β-galactosidase assays confirmed that substitutions of H108 and FARKY with Ala in CeHRG-4 significantly decreased cytoplasmic heme levels at low heme, the Y63A mutant had consistently reduced activity but was statistically not significant (Fig. 3.4D). We found that the Y61A mutant did not alter the activity of heme-dependent reporters in any of the assays. The observation that only the H108A mutant showed impaired growth of *hem1Δ* strain may reflect the reduced sensitivity of the growth

Figure 3.6. Localization and expression of CeHRG-4-HA and mutants in yeast. (A) Indirect immunofluorescence microscopy was conducted on *hem1*(6D) strain transformed with empty vector pYES-DEST52, CeHRG-4-HA and mutants. Rabbit anti-HA was used as the primary antibody, and an AlexaFluo568-conjugated goat anti-rabbit antibody was used as the secondary antibody. Boxed regions were enlarged for clarity. Scale bar, 5 μm. (B) Immunoblotting was performed on transformants of CeHRG-4-HA and its mutants in the *hem1*(6D) strain. Predicted molecular mass of CeHRG-4 was detected as indicated by filled circles. Asterisks indicated putative dimers. The endogenous expression level of phosphoglycerate kinase 1 (PGK1) was used as loading control (15 μg total protein / lane).

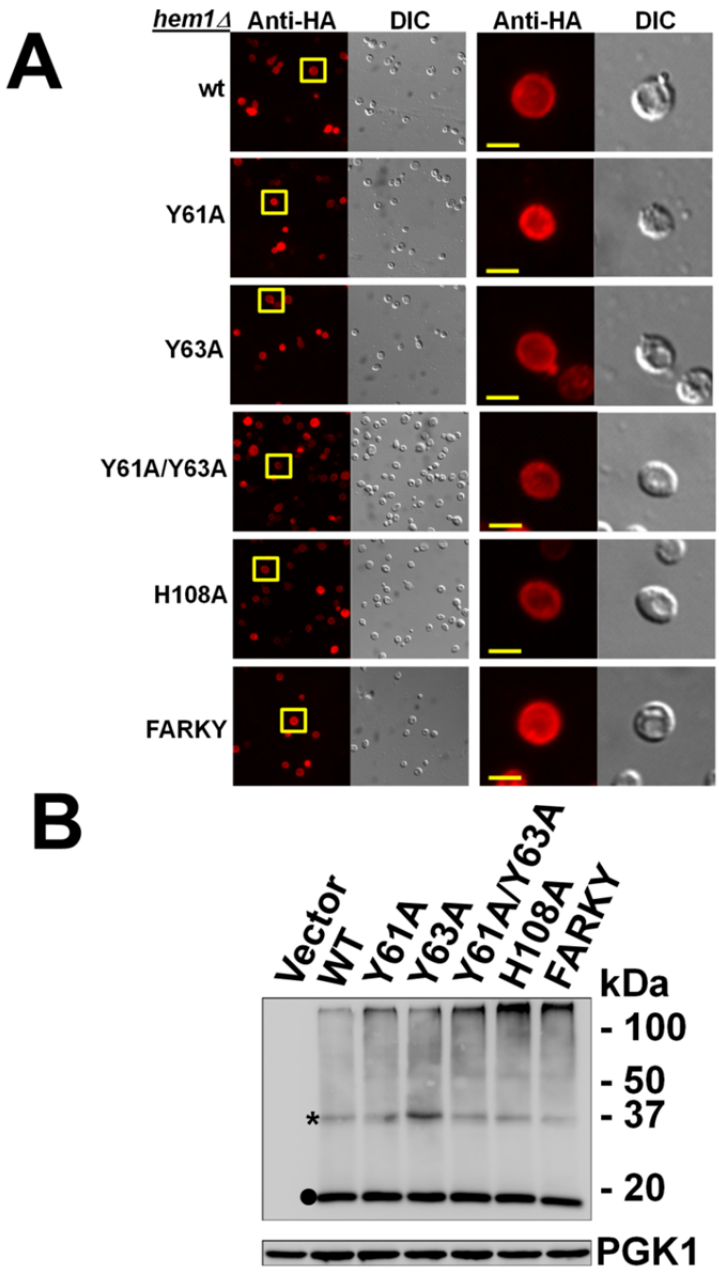
A
hem1Δ
Anti-HA
DIC
Anti-HA
DIC
wt
Y61A
Y63A
Y61A/Y63A
H108A
FARKY
B
Vector
WT
Y61A
Y63A
Y61A/Y63A
H108A
FARKY
kDa
- 100
- 50
- 37
- 20
*
PGK1

assay to residual heme transport activity in other mutants (Fig. 3.4B versus 3.4C, D). Collectively, these results strongly implicate H108 and the FARKY motif, and to a lesser extent Y63, in heme transport by CeHRG-4.

CeHRG-1 Function Requires a Histidine in TMD2 and the C-terminus FARKY Motif

Based on the primary amino acid sequence homology and secondary structure prediction of CeHRG-1 and CeHRG-4, we set out to establish whether select conserved amino acids were essential for heme transport by CeHRG-1 (Fig. 3.4A and Fig. 3.5). Mutations in H90 and the FARKY motif resulted in a dramatic reduction in growth compared to wild-type CeHRG-1 at low and high heme (Fig. 3.7A). By contrast, mutating H135 in the putative E2 loop resulted only in a slight growth delay even though each of the mutants were expressed and localized to the yeast vacuolar membrane (Fig. 3.8). Consistent with the growth assays, substitutions of H90 and FARKY with alanine resulted in significant reduction in ferrireductase and β-galactosidase activities in low and high heme conditions (Fig. 3.7B and C). As observed in the growth assay, the H135A mutant showed reduction in ferrireductase and β-galactosidase activities at low heme which was alleviated by increasing the heme concentrations. As observed for the Y61A mutant of CeHRG-4, the equivalent H88A mutant showed no obvious defects indicating that this ligand does not compensate in the H90A mutant. Our results suggest that, under heme deplete conditions, CeHRG-1 predominantly requires H90 in the predicted TMD2 and the C-

terminus FARKY motif, and to a lesser extent H135 in the predicted E2 loop, for heme transport.

To determine whether other potential heme-binding ligands (H, Y, or C) conserved in HRG-1-related proteins may compensate as secondary ligands in the site-directed mutants, we mutagenized H14 and H40 in the N-terminus, H41 and Y67 in the E1 loop, and C97 and C127 in a highly conserved CLV motif within TMD3, of CeHRG-4 and CeHRG-1, respectively (Fig. 3.5 and Fig. 3.9). Mutating each of these residues to Ala did not significantly alter the function of either CeHRG-1 or CeHRG-4 suggesting the predominant heme ligands in both proteins are the His in the E2 loop, the His or Tyr in TMD2 and FARKY motif in the C-terminus.

H90A has dominant-negative effects on CeHRG-1 function in *C. elegans*.

Because *C. elegans* contains multiple paralogs of HRG-1-related proteins, and as neither *Δhrg-1* nor *Δhrg-4* single mutants have obvious phenotypes, we generated *hrg-1* transgenic worms in the *Δhrg-1Δhrg- 4* double mutant strain to verify our yeast results *in vivo*. The constructs were created by putting *hrg-1* and *gfp* under the control of the *hrg-1* promoter (~3 kb upstream of *hrg-1* gene, *Phrg-1*) separated by the SL2 intercistronic sequence (ICS) from *rla-1* (Fig. 3.10A). In the transgenic worms, the *HRG-1::ICS::GFP* transgene is transcribed as a single polycistronic mRNA, but yields two separate proteins: HRG-1 and GFP. Thus, GFP fluorescence is indicative of transgene expression. The CeHRG-1 and H88A mutant transgenic worms did not show growth improvement when expressed in the present of low

Figure 3.7. Heme transport analysis of wild-type and mutant CeHRG-1. (A) The *hem1*Δ(6D) strain was transformed with empty vector pYES-DEST52, CeHRG-1-HA and its mutants. Spot growth assay were performed with indicated conditions. Plates were incubated at 30°C for 3 days prior to imaging. (B) The *hem1*Δ*fre1*Δ*fre2*ΔMET3-FRE1 strain was transformed with empty vector pYES-DEST52, CeHRG-1 and its mutants. Ferric reductase assay were performed with indicated concentrations of hemin. Ferric reductase activity (nmol / 10^6cells / min) was measured and normalized to the activity of vector. (C) The *hem1*Δ(6D) strain co-transformed with pCYC1-LacZ and empty vector pYES-DEST52, CeHRG-1 or its mutants. β-galactosidase activity was measured. Error bars represent the standard error of the mean (SEM) from three independent experiments. * $p < 0.05$, ** $p < 0.01$, *** $p < 0.001$.

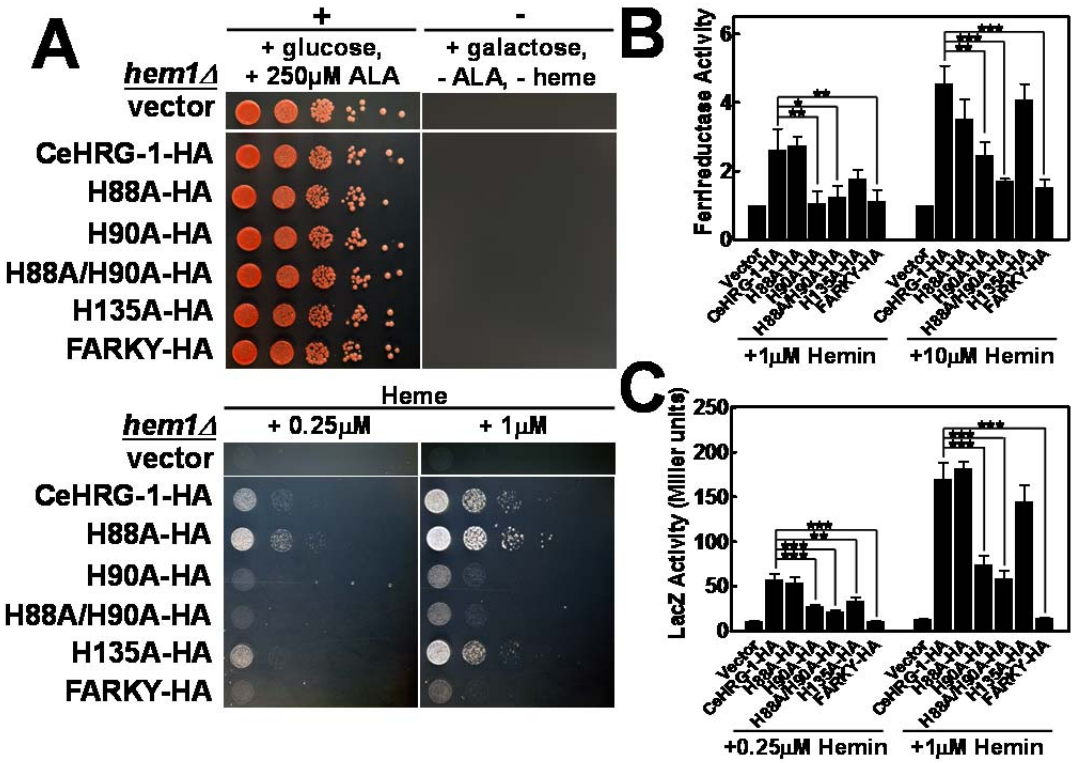
A
+
-
+ glucose,
+ 250μM ALA
+ galactose,
- ALA, - heme
hem1Δ
vector
CeHRG-1-HA
H88A-HA
H90A-HA
H88A/H90A-HA
H135A-HA
FARKY-HA
Heme
+ 0.25μM
+ 1μM
B
Ferrireductase Activity
+1μM Hemin
+10μM Hemin
C
LacZ Activity (Miller units)
+0.25μM Hemin
+1μM Hemin

Figure 3.8. Localization and expression of CeHRG-1-HA and mutants in yeast. (A) Indirect immunofluorescence microscopy was conducted on *hem1*(6D) strain transformed with empty vector pYES-DEST52, CeHRG-1-HA and mutants. Rabbit anti-HA was used as the primary antibody, and an AlexaFluo568-conjugated goat anti-rabbit antibody was used as the secondary antibody. Boxed regions were enlarged for clarity. Scale bar, 5 μm. (B) Immunoblotting was performed on transformants of CeHRG-1-HA and its mutants in the *hem1*(6D) strain. Predicted molecular mass of CeHRG-1 was detected as indicated by filled circles. Asterisks indicated putative dimers. The endogenous expression level of phosphoglycerate kinase 1 (PGK1) was used as loading control (30 μg total protein / lane).

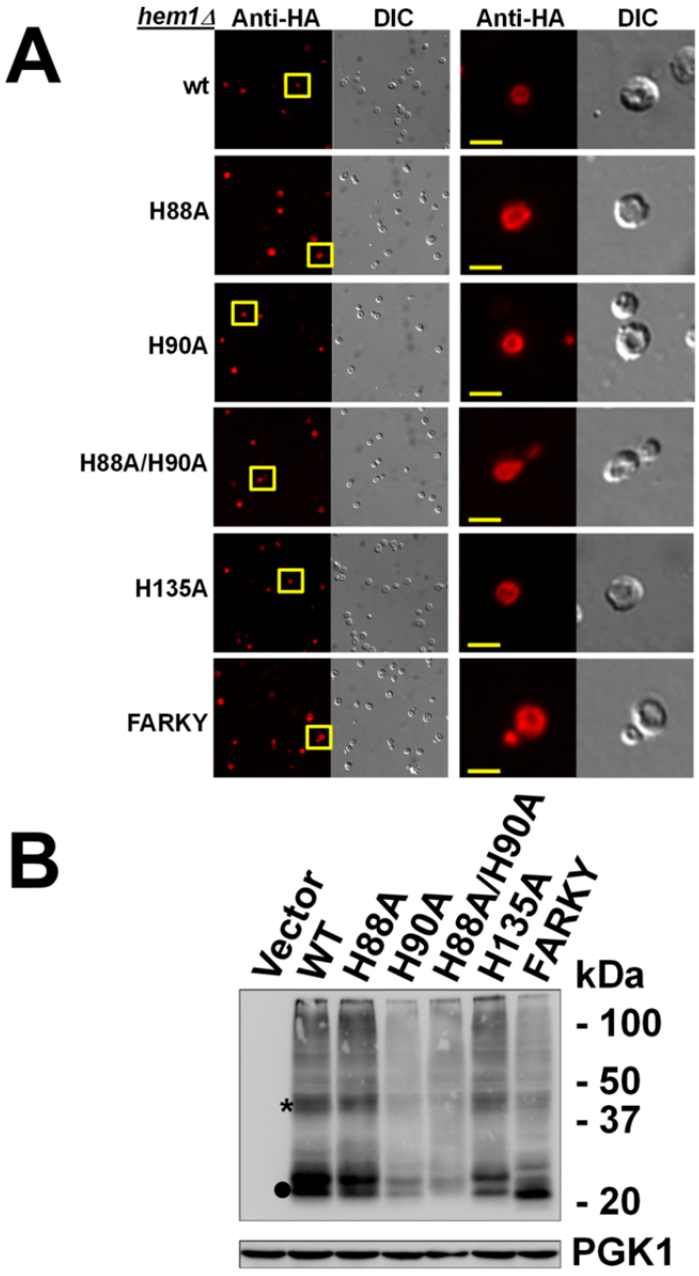
A
hem1Δ
Anti-HA
DIC
Anti-HA
DIC
wt
H88A
H90A
H88A/H90A
H135A
FARKY
B
Vector
WT
H88A
H90A
H88A/H90A
H135A
FARKY
kDa
- 100
- 50
- 37
- 20
*
PGK1

Figure 3.9. Mutagenesis of worm specific potential heme ligand did not affect HRG-1 function. The *hem1*Δ(6D) strain transformed with empty vector pYES-DEST52, CeHRG-4-HA, CeHRG-1-HA and alanine substitutions of histidines/tyrosines at the amino-terminus, E1 loop, and a CLV motif in TMD3. Spot growth assay were performed with indicated conditions. Plates were incubated at 30°C for 3 days prior to imaging.

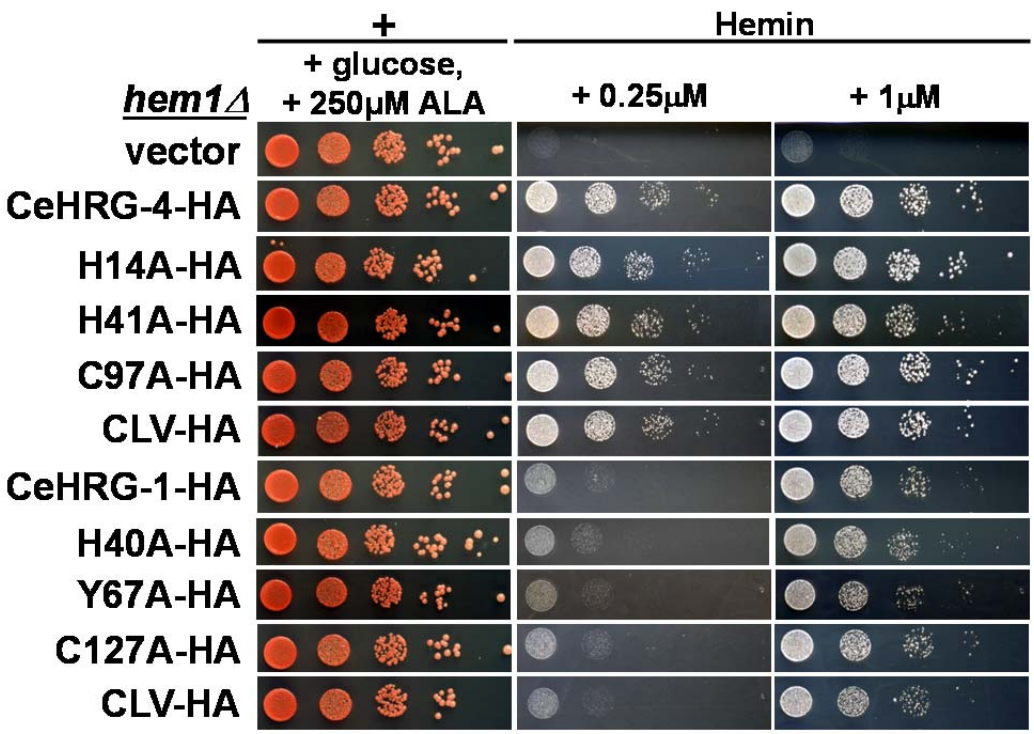
+
Hemin
hem1Δ
+ glucose,
+ 250μM ALA
+ 0.25μM
+ 1μM
vector
CeHRG-4-HA
H14A-HA
H41A-HA
C97A-HA
CLV-HA
CeHRG-1-HA
H40A-HA
Y67A-HA
C127A-HA
CLV-HA

Figure 3.10. H90A has dominant-negative effects on CeHRG-1 function in *C. elegans.* (A) The rescue plasmid *Phrg-1::HRG-1-HA::ICS::GFP* was constructed by recombining the putative *hrg-1* promoter (~3 kb upstream of *hrg-1* gene, *Phrg-1*), the fused *hrg-1* gene (*HRG-1-HA::ICS::GFP*) and the 3'-UTR of *hrg-1* gene into a single destination vector, pDEST-R4-R3, and was bombarded into the *Δhrg-1Δhrg-4unc-119* strain to generate *hrg-1* transgenic worms. *hrg-1* transgenic worms were synchronized, placed on NGM plates seeded with RP523 bacteria grown at 50 μM hemin (P0), synchronized again and transferred to RP523 plates of low (1 μM) and high (50 μM) hemin (F1) and the growth followed for two subsequent generations. Representative images of F1 and F2 progeny are shown. Scale bar, 50 μm. (B) The sizes of worms in (A) were measured by COPAS BioSort. Time of flight (TOF) indicate the length of worms, n>200. (C) Worms were grown as described in *ΔhemB* growth assay. Approximately 100 worms/well of F_1 worms were transferred to 12-well plates, inoculated in mCeHR-2 medium supplemented with 1.5 μM hemin chloride and 10 μM of ZnMP for 16 hours. ZnMP fluorescence intensity was scored by a DMIRE2 epifluorescence microscope (Leica). (D) The mean fluorescence intensities of ZnMP in (C) were quantified by SimplePCI, n=50. (E) Worms were grown as described in *ΔhemB* growth assay. F_1 worms were harvest at young gravid stage from *ΔhemB* plates, washed twice with M9 buffer, resuspended in lysis buffer with protease inhibitor cocktail set III and Lysing Matrix D beads, and disrupted using FastPrep-24 (MP Bio) for 60s at the 6.5 m/s setting. The total protein concentration of worm lysates was quantified with the Bradford reagent (Bio-Rad) and subjected to immunoblotting (50μg / lane).

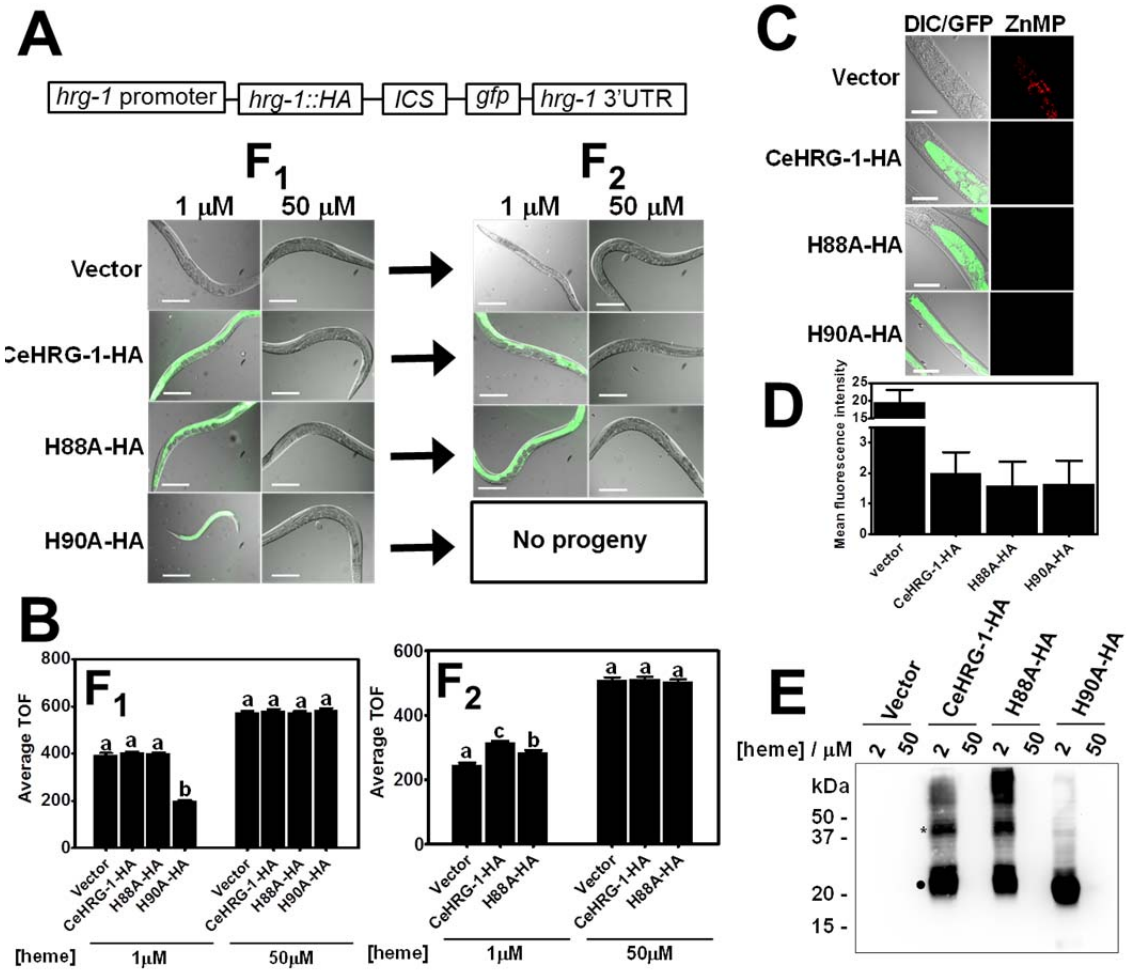
A
hrg-1 promoter
hrg-1::HA
ICS
gfp
hrg-1 3'UTR
F1
F2
1 μM
50 μM
Vector
CeHRG-1-HA
H88A-HA
H90A-HA
No progeny
B
F1
F2
Average TOF
[heme]
1μM
50μM
C
DIC/GFP
ZnMP
D
Mean fluorescence intensity
E
[heme] / μM
kDa
50 -
37 -
20 -
15 -

heme, which might be due to the modest phenotype of the *Δhrg-1Δhrg-4* double mutant strain. However, expression of the H90A mutant exhibited a severe growth arrest phenotype in the F1 progeny of *Δhrg-1Δhrg-4* worms fed with RP523 grown with 2 μM heme compared to the vector or wild-type control. This growth phenotype was fully suppressed with 50 μM heme (Fig. 3.10A, B). This result suggests that in addition to being a dysfunctional heme transporter, as revealed in the yeast growth assay, the H90A mutant exerts a dominant negative effect that's observable only at low heme.

To further investigate heme transport mediated by CeHRG-1 in *C. elegans*, we measured ZnMP uptake in these transgenic worms. From our previous RNAi results [58], we expected that worms expressing CeHRG-1 or the H88A mutant would have reduced fluorescence signal in *Δhrg-1Δhrg-4* double mutant background, as they can disperse the vesicular accumulated ZnMP into the cytosol; and expression of the H90A mutant would have equal or increased ZnMP signal comparing to vector, as H90A is a non-functional or dominant-negative heme transporter. Surprisingly, as for the wild-type, the H90A mutant transgenic worms also showed reduced ZnMP fluorescence signal (Fig. 3.10C, D). Because HRG-1-related proteins are multimeric, we speculate that the reduced ZnMP fluorescence concomitant with growth retardation could be because the H90A mutant may hetero-multimerize with other HRG-1 paralogs and thus disrupt heme import into the intestine. Recent studies showed the H32R mutation in ferroportin (FPN1) has a dominant negative effect in the flatiron mouse [150]. This is because the H32R mutant multimerizes with the wild-type protein and interferes with its plasma membrane localization, thereby

preventing iron export. Indeed, immunoblotting results show that, unlike wild-type CeHRG-1 or H88A mutant, the H90A mutant migrates primarily as a monomer, raising the possibility that it has the potential to interfere with multimerization of other HRG-1 paralogs (Fig. 3.10E).

A Conserved Histidine in TMD2 is Essential for Heme Transport by Human HRG-1

The human homolog of HRG-1-related proteins is only ≈20% identical to CeHRG-1 even though worm and human proteins colocalize to the endolysosomal compartment, and bind and transport heme, implying that these proteins are functional orthologs [58]. To verify whether the results of our mechanistic studies of worm HRG-1-related proteins can be extended to humans, we expressed hHRG-1 in *hem1Δ*yeast. Immunoblotting of lysates from yeast cells expressing hHRG-1-HA revealed hHRG-1 migrating at the predicted molecular weight, albeit the steady-state protein level was significantly lower than CeHRG-1 and CeHRG-4 (Fig. 3.11B). To optimize the expression of hHRG-1 in yeast, we generated a synthetic open-reading frame (yhHRG-1) which was modified for codon usage bias; the Codon Adaptation Index (CAI) was upgraded from 0.51 to 0.90 for maximal expression in *S. cerevisiae*. Steady state proteins levels for optimized yhHRG-1-HA were at least ten-fold greater than the unoptimized hHRG-1-HA (Fig. 3.11B). This difference in expression was concomitant with the significantly greater ability of yhHRG-1-HA to rescue the growth of *hem1Δ*yeast (10,000 fold for yhHRG-1-HA versus 10 fold for hHRG-1-HA

compared to vector control), stimulate Fre1p enzymatic activity, and induce *CYC1::lacZ* reporter activity (Fig. 3.11D-F). Indirect immunofluorescence microscopy indicated that similar to CeHRG-1, the human homolog also localized primarily to the yeast vacuole (Fig. 3.11C). Despite low identity at the amino acid sequence level between the human and worm proteins, several features are remarkably conserved in HRG-1-related proteins. Namely, both homologs localized to similar endocytic compartments, showed similarity in four predicted TMDs, and possess conserved amino acids that were topologically preserved. Potential ligands at the corresponding position in hHRG-1 were H56 in TMD2, H100 in the E2 loop, and YAHRY in the C-terminus (Fig. 3.11A). As proof-of-principle, we generate a H56A mutant in hHRG-1. The mutant protein expressed and localized to the vacuole but had significantly reduced function consistently in all three assays irrespective of heme concentrations (Fig. 3.11B-F). These results strongly support our proposition that the overall mechanism for heme transport by HRG-1-related proteins is likely conserved between worms and humans.

In collaboration with Dr. Mark Fleming at Harvard Medical School, we have identified a C to T single base variant (pt EA023) of the human *HRG-1* gene in African American population, which results in a P36L substitution in the E1 exoplasmic loop between TMD1 and TMD2 (Fig. 3.11A). The individuals heterozygous for P36L are anemic (Unpublished observations). Although the possibility that those patients are compound heterozygous with polymorphisms in other genes cannot be excluded, our yeast growth assay indicated the P36L variant was unable to rescue growth of the *hem1*Δ yeast strain on media with low heme (Fig.

3.12). This result suggests the P36L substitution in hHRG-1 results in a dysfunctional protein and consequently anemia due to either haploinsufficiency or a dominant negative effect. Furthermore, our previous work has shown moderate knockdown of *HRG-1* in zebrafish leads to mild anemia (MO1), while severe depletion causes lethality and growth defects (MO2), suggesting that lowering the expression of HRG-1 can directly result in anemia (8). To evaluate whether additional human polymorphisms in *HRG-1* caused a reduction in heme transporter activity, we searched the NHLBI Exome Sequencing Project (ESP) and found three variants, G73S, S82L and W115C. In contrast to P36L, these variants were only present in European Americans (0.0309%, 0.0309% and 0.0279%, respectively) but not in African Americans. Interestingly, P36 and W115 are highly conserved residues in vertebrates, whereas G73 and S82 seem to be dispensable (Fig. 3.12A). Yeast growth assay indicated an inability of the W115C variant to transport heme, while G73S and S82L had no obvious effect on hHRG-1 heme transport activity (Fig. 3.12B). In the future, it would be important to evaluate whether these hHRG-1 variants can rescue the anemia phenotype in zebrafish *hrg-1* morphants.

We next determined whether the assays employed to determine the heme import function of hHRG-1 can be extended to FLVCR2, another transporter recently postulated to be a heme importer in human cells [65]. hFLVCR2 was abundantly expressed in *hem1Δ* yeast, localized primarily to the plasma membrane and intracellular vesicles (Fig. 3.12 A, B). Yeast expressing hFLVCR2 showed 2-fold increase in ferrireductase activity, indicating elevated heme in the secretory pathway (Fig. 3.13 C). However, hFLCVR2 did not enhance heme-dependent growth of

Figure 3.11. Heme transport analysis of wild-type and mutant hHRG-1. (A) Putative topology of hHRG-1 predicted by TMHMM 2.0 and SOSUI. The amino and carboxyl-termini are cytoplasmic, C1 is the cytoplasmic loop and E1 and E2 are the exoplasmic loops. Potential heme interacting residues are shaded in red. (B) Immunoblotting was performed on transformants overexpressing c-terminus HA epitope tagged hHRG-1 or yeast codon-optimized yhHRG-1 and its H56A mutant (yH56A-HA) in the *hem1*Δ(6D) strain. Predicted molecular mass of hHRG-1 was detected as indicated by filled circles. The endogenous expression level of phosphoglycerate kinase 1 (PGK1) was used as loading control (30 μg total protein / lane). (C) Immunofluorescence microscopy results of yhHRG-1-HA and yH56A-HA mutant in the *hem1*Δ(6D) strain. Rabbit anti-HA was used as the primary antibody, and an AlexaFluo568-conjugated goat antirabbit antibody was used as the secondary antibody. Scale bar, 5 μm. (D) The *hem1*Δ(6D) strain was transformed with empty vector pYES-DEST52, hHRG-1 and its mutants. Spot growth assay were performed with indicated conditions. Plates were incubated at 30°C for 3 days prior to imaging. (E) The *hem1*Δ *fre1*Δ *fre2*Δ MET3-FRE1 strain was transformed with empty vector pYES-DEST52, hHRG-1 and its mutants. Ferric reductase assay were performed with indicated concentrations of hemin. Ferric reductase activity (nmol / 10^6 cells / min) was measured and normalized to the activity of vector. (F) The *hem1*Δ(6D)) strain co-transformed with pCYC1-LacZ and empty vector pYES-DEST52, CeHRG-1 or its mutants. β-galactosidase activity was measured. Error bars represent the standard error of the mean (SEM) from three independent experiments. * $p < 0.05$, ** $p < 0.01$, *** $p < 0.001$.

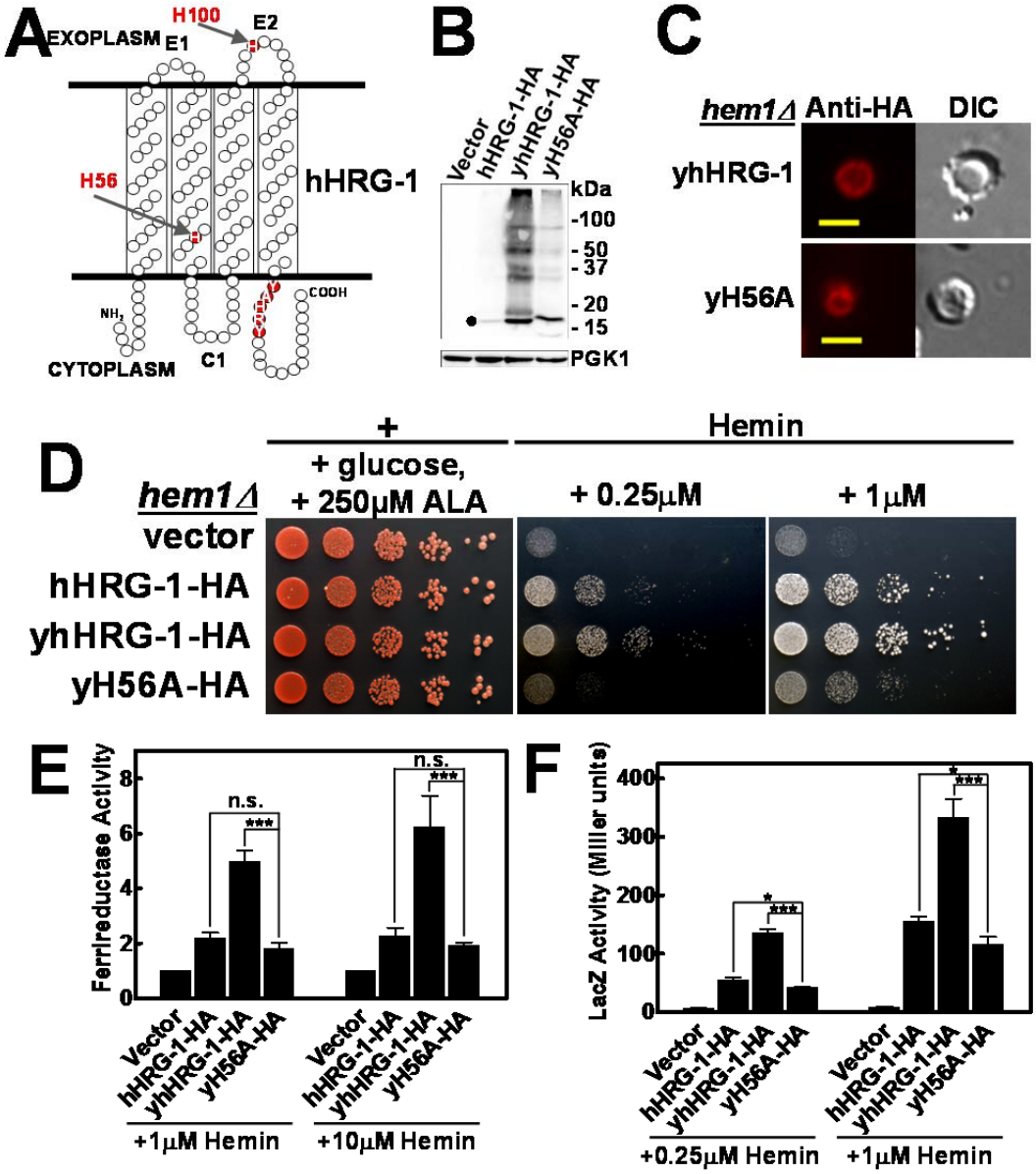
A
EXOPLASM
H100
E2
E1
H56
hHRG-1
NH2
COOH
CYTOPLASM
C1
B
Vector
hHRG-1-HA
yhHRG-1-HA
yH56A-HA
kDa
-100
-50
-37
-20
-15
PGK1
C
hem1Δ
Anti-HA
DIC
yhHRG-1
yH56A
D
+
Hemin
+ glucose,
+ 250μM ALA
+ 0.25μM
+ 1μM
hem1Δ
vector
hHRG-1-HA
yhHRG-1-HA
yH56A-HA
E
Ferrireductase Activity
n.s.
***
Vector
hHRG-1-HA
yhHRG-1-HA
yH56A-HA
+1μM Hemin
+10μM Hemin
F
LacZ Activity (Miller units)
*
***
+0.25μM Hemin
+1μM Hemin

Figure 3.12. Heme transport analysis of hHRG-1 variants. (A) Multiple sequence alignment of vertebrate HRG-1 orthologues. Asterisks indicate polymorphic positions in human HRG-1. (B) The *hem1*Δ(6D) strain transformed with empty vector pYES-DEST52, hHRG-1-HA and hHRG-1 variants identified in human population. Spot growth assay were performed with indicated conditions. Plates were incubated at 30°C for 3 days prior to imaging.

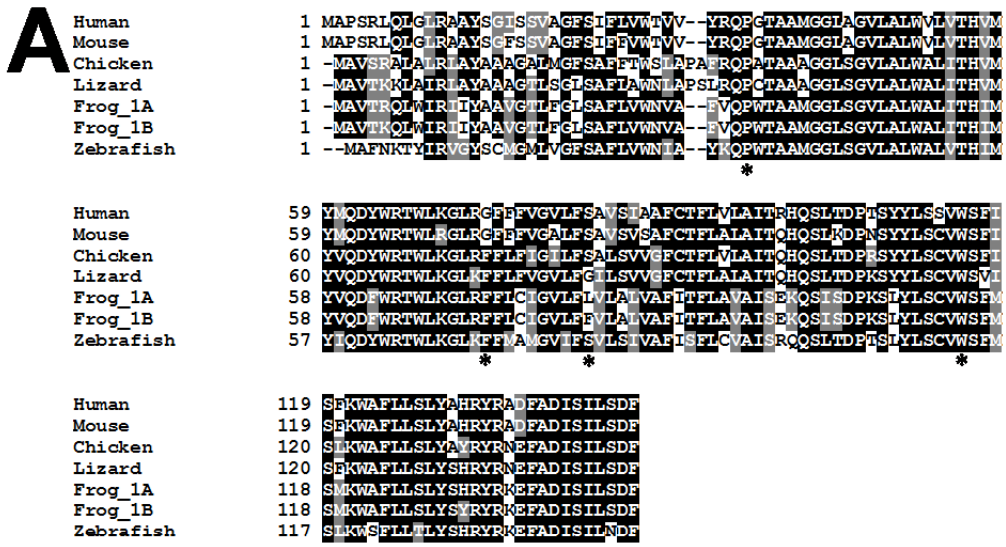
A
Human 1 MAPSRLQLGLRAAYSGISSVAGFSIFLVWTVV--YRQPGTAAMGGIAGVLALWVLVTHVM
Mouse 1 MAPSRLQLGLRAAYSGFSSVAGFSIFFVWTVV--YRQPGTAAMGGIAGVLALWVLVTHVM
Chicken 1 -MAVSRALALRLAYAAAGAIMGFSAFFTWSLAPAFRQPATAAAGGLSGVLALWALITHVM
Lizard 1 -MAVTKKLALRLAYAAAGTLSGLSAFIAWNLAPSLRQPCTAAAGGLSGVLALWALITHVM
Frog_1A 1 -MAVTRQLWIRIIYAAVGTLFGLSAFLVWNVA--FVQPWTAAMGGLSGVLALWALITHIM
Frog_1B 1 -MAVTKQLWIRIIYAAVGTLFGLSAFLVWNVA--FVQPWTAAMGGLSGVLALWALITHIM
Zebrafish 1 --MAFNKTYLRVGYSCMGMLVGFSAFLVWNIA--YKQPWTAAMGGLSGVLALWALVTHIM
Human 59 YMQDYWRTWLKGLFGFFFVGVLFSAVSIAAFCTFLVLAITRHQSLIDPTSYYLSSVWSFI
Mouse 59 YMQDYWRTWLRGLFGFFFVGALFSAVSVSAFCTFLALAITCHQSLKDPNSYYLSCVWSFI
Chicken 60 YVQDYWRTWLKGLRFFLFIGILFSALSVVGFCTFLVLAITCHQSLIDPRSYYLSCVWSFI
Lizard 60 YVQDYWRTWLKGLKFFLFVGVLFGILSVVGFCTFLALAITCHQSLIDPKSYYLSCVWSVI
Frog_1A 58 YVQDFWRTWLKGLRFFLCIGVLFLVLALVAFITFLAVAISEKQSISDPKSTYLSCVWSFM
Frog_1B 58 YVQDFWRTWLKGLRFFLCIGVLFFVLALVAFITFLAVAISEKQSISDPKSTYLSCVWSFM
Zebrafish 57 YIQDYWRTWLKGLKFFMAMGVTFSVLSIVAFISFLCVAISRQQSLIDPTSTYLSCVWSFM
Human 119 SFKWAFLLSLYAHRYRADFADISILSDF
Mouse 119 SFKWAFLLSLYAHRYRADFADISILSDF
Chicken 120 SLKWAFLLSLYAYRYRNEFADISILSDF
Lizard 120 SFKWAFLLSLYSHRYRNEFADISILSDF
Frog_1A 118 SMKWAFLLSLYSHRYRKEFADISILSDF
Frog_1B 118 SMKWAFLLSLYSYRYRKEFADISILSDF
Zebrafish 117 SLKWSFLLTLYSHRYRKEFADISILNDF
B
+
Hemin
+250μM ALA, +glucose
+0.25μM
+1μM
hem1Δ
Vector
hHRG-1-HA
P36L-HA
G73S-HA
S82L-HA
W115C-HA

Figure 3.13. Overexpression of hFLVCR2 did not increase heme uptake in yeast *hem1*Δ strain. (A) Immunofluorescence microscopy results of hFLVCR2 in the *hem1*(6D) strain. Rabbit anti-HA was used as the primary antibody, and an AlexaFluo568-conjugated goat anti-rabbit antibody was used as the secondary antibody. Scale bar, 5 μm. (B) Immunoblotting was performed on transformants overexpressing c-terminus HA epitope tagged CeHRG-4, CeHRG-1 or hFLVCR2 in the *hem1*(6D) strain. Predicted molecular mass were detected as indicated by filled circles (15 μg / lane). (C) The *hem1*Δ*fre1*Δ*fre2*ΔMET3- FRE1 strain was transformed with empty vector pYES-DEST52, CeHRG-4, CeHRG-1 and hFLVCR2. Ferric reductase assay were performed with indicated concentrations of hemin. Ferric reductase activity (nmol / 10^6cells / min) was measured and normalized to the activity of vector. (D) The *hem1*Δ(6D) strain transformed with empty vector pYES-DEST52, CeHRG-4, CeHRG-1 and hFLVCR2. Spot growth assay were performed with indicated conditions. Plates were incubated at 30°C for 3 days prior to imaging. Error bars represent the standard error of the mean (SEM) from three independent experiments. * $p < 0.05$, ** $p < 0.01$, *** $p < 0.001$.

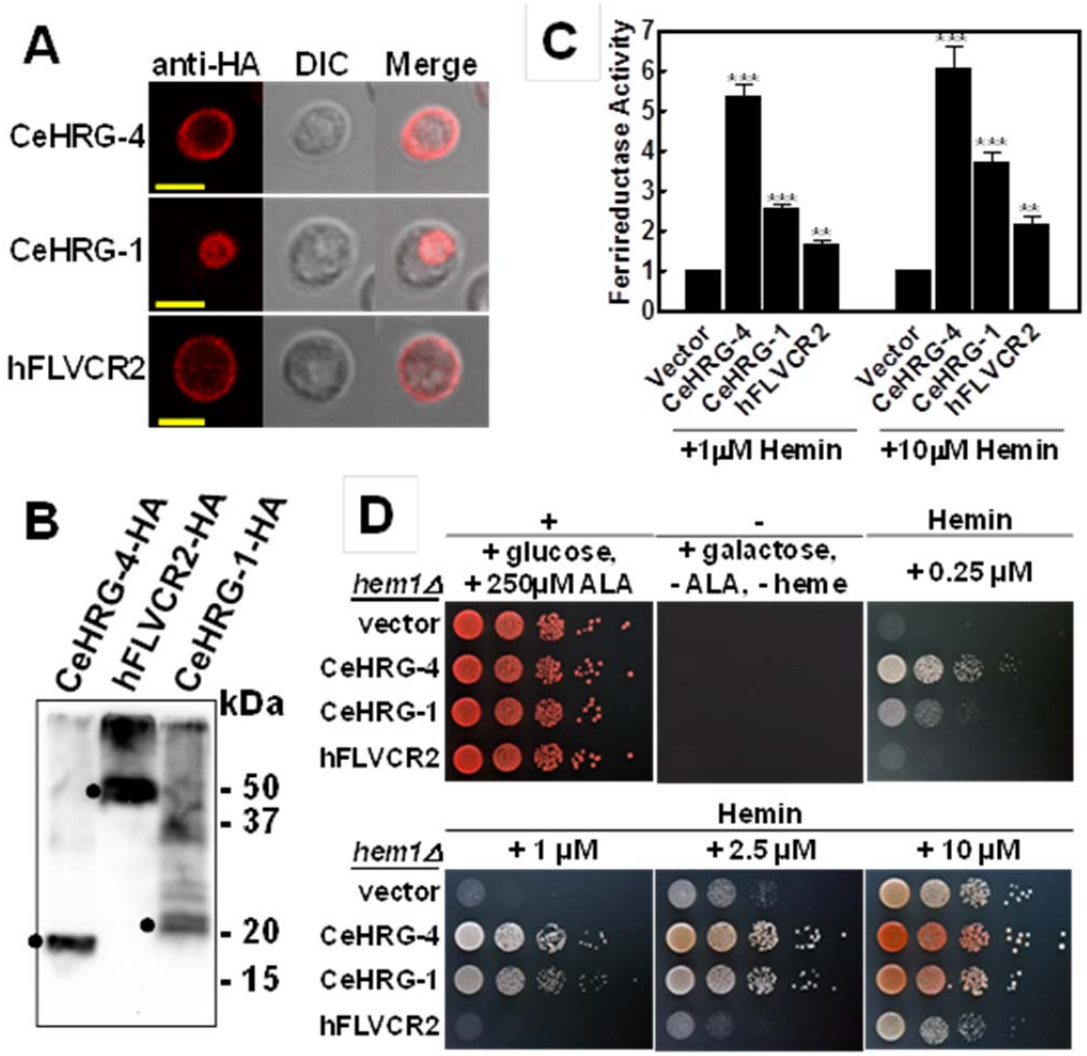
A
anti-HA
DIC
Merge
CeHRG-4
CeHRG-1
hFLVCR2
C
Ferrireductase Activity
0
1
2
3
4
5
6
7
***
***
**
***
***
**
Vector
CeHRG-4
CeHRG-1
hFLVCR2
Vector
CeHRG-4
CeHRG-1
hFLVCR2
+1μM Hemin
+10μM Hemin
B
CeHRG-4-HA
hFLVCR2-HA
CeHRG-1-HA
kDa
- 50
- 37
- 20
- 15
D
+
-
Hemin
+ glucose,
+ 250μM ALA
+ galactose,
- ALA, - heme
+ 0.25 μM
hem1Δ
vector
CeHRG-4
CeHRG-1
hFLVCR2
Hemin
hem1Δ
+ 1 μM
+ 2.5 μM
+ 10 μM
vector
CeHRG-4
CeHRG-1
hFLVCR2

hem1Δ yeast compared to vector, even at 10 μM heme (Fig. 3.13D). These results suggest that, under our assay conditions, hFLVCR2 does not function as a plasma membrane heme importer.

C-terminal chimeras of HRG-1-related proteins reveal structures required for localization

Both CeHRG-1 and hHRG-1 proteins have predicted tyrosine and acidic dileucine based sorting motifs on their C-terminal regions (Fig. 3.14A). The YxxØ motif is involved in rapid internalization of the proteins from the plasma membrane. This sorting motif has also been implicated in the targeting of transmembrane proteins to the lysosomes and sorting of proteins to the basolateral membrane in polarized cells [151]. The dileucine-based sorting signal plays an important role in sorting a number of type I, type II, and multispanning membrane proteins. Like the tyrosine motif, the D/ExxLL motif is also involved in the internalization of proteins from the plasma membrane and targeting of proteins to the lysosomes. Furthermore, our protease protection assays indicated that the C-terminus of HRG-1-related proteins is cytoplasmic (unpublished observations).

In order to systematically identify the portion of HRG-1 dictating localization from function, we synthesized several fusion chimeras by swapping the N and C terminal segments of HRG-1-related proteins (Fig. 3.14B) and examined their subcellular localization in HEK293 cells and polarized MDCK II cells. The results

Figure 3.14. Topology of N- and C-terminal chimera constructs of CeHRG-1, CeHRG-4 and hHRG-1. (A) Predicted topology of CeHRG-4, CeHRG-1, hHRG-1 with residues essential to heme transport marked in grey, tyrosine sorting motifs in red and dileucine motifs in blue. (B) Schematic of chimera constructs. CeHRG-1 is shown in blue, CeHRG-4 in green, and hHRG-1 in red. The transmembrane domains for each are indicated by rectangles. The chimeras of CeHRG- 1, CeHRG-4, and hHRG-1 are shown with the transmembrane region shaded in light grey.

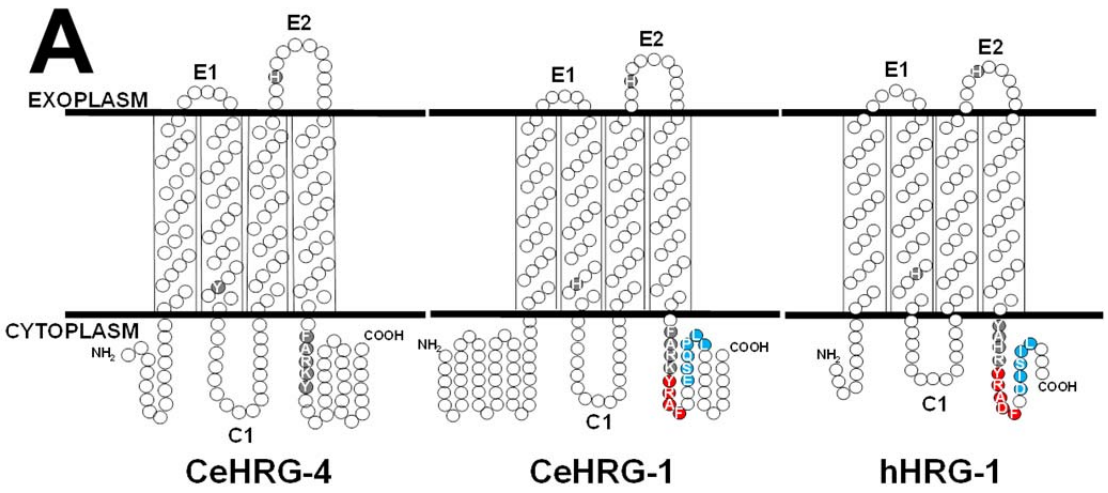
A
EXOPLASM
CYTOPLASM
E1
E2
C1
NH2
COOH
CeHRG-4
CeHRG-1
hHRG-1

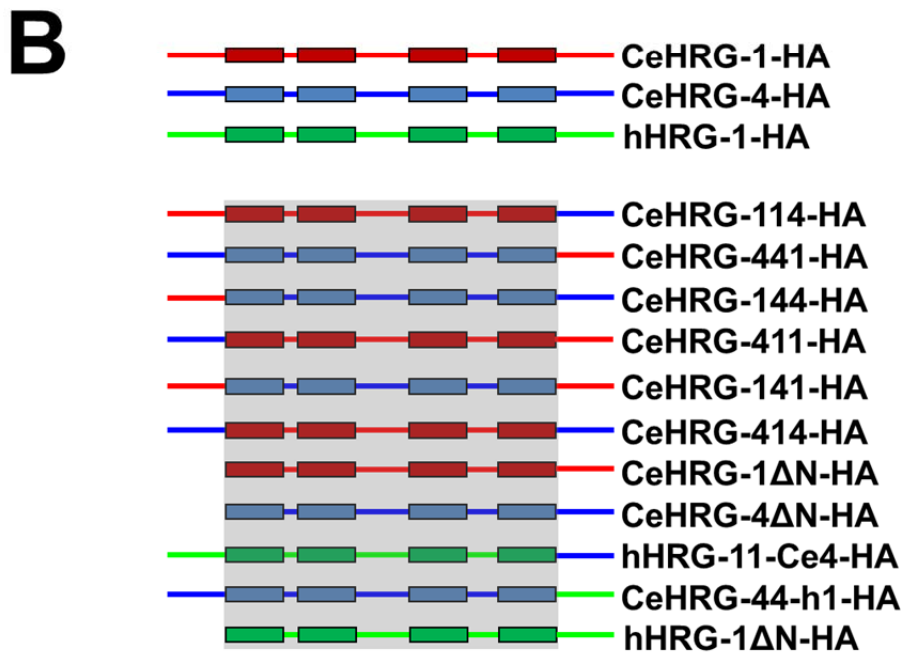
B
CeHRG-1-HA
CeHRG-4-HA
hHRG-1-HA
CeHRG-114-HA
CeHRG-441-HA
CeHRG-144-HA
CeHRG-411-HA
CeHRG-141-HA
CeHRG-414-HA
CeHRG-1ΔN-HA
CeHRG-4ΔN-HA
hHRG-11-Ce4-HA
CeHRG-44-h1-HA
hHRG-1ΔN-HA

are summarized in Appendix IV. In short, when the C-terminus of CeHRG-1 was replaced with the C-terminal domain of CeHRG-4, CeHRG-114-CFP was seen on the plasma membrane of HEK293 cells, consistent with the localization of CeHRG-4-CFP. Conversely, CeHRG-441-CFP, a construct generated by replacing the C-terminal domain of CeHRG-4 with the CeHRG-1 C-terminal domain, localized to the endosomal-lysosomal membranes as CeHRG-1-CFP. C-terminal domain chimeras of hHRG-1 and CeHRG-4 exhibited similar results. By contrast, swapping neither the N-terminal domains nor the transmembrane domains of HRG-1-related proteins changed their membrane localization. Similarly, when expressed in polarized MDCK II cells, CeHRG-4-CFP localized to the apical surface whereas CeHRG-1-CFP and hHRG-1-CFP were detected in vesicular compartments immediately underneath the apical surface. Swapping the C-terminal domains of these proteins resulted in an equivalent exchange of the localization of each chimeric protein. These findings indicate that the C-terminal domains of HRG-1-related proteins dictate proper intracellular localization and trafficking.

HRG-1 chimeras show heme transport activity

In order to correlate the intracellular localization of these chimeras with heme transport activity, we exploited the previously established functional assays in yeast [129,130]. HRG-1-related proteins transport heme thereby rescuing the growth of the *hem1*Δ yeast strain, a heme auxotroph, at low heme concentrations [152]. *hem1*Δ yeast, transformed with different chimeras, were assessed for growth; HRG-1-related

protein C-terminal chimeras showed growth that were comparable to wild-type HRG-1-related proteins. However, yeast transformed with CeHRG-411-HA, CeHRG-1ΔN-HA and hHRG-1ΔN-HA showed significantly decreased growth at 0.25 μM heme compared to wild-type CeHRG-1-HA and hHRG-1-HA (Fig. 3.15). These studies indicated that although the N-terminal domains of CeHRG-1 or hHRG-1 may not affect localization, they play an essential role in the heme transport function of these proteins. To further assay the effect of these chimeras on the regulatory pool of cytoplasmic heme, we performed β-galactosidase activity assays using the *CYC::lacZ* promoter-reporter fusion. As previously reported, wild-type HRG-1-related proteins transformed yeast show increased β-galactosidase activity compared to yeast transformed with the pYES-DEST52 empty vector [152]. Yeast transformed with C-terminal chimeras also showed a significant increase in LacZ activity compared to vector, similar to the changes observed in the growth of *hem1*Δ transformed yeast (Fig. 3.16). We observed a lack of activity for the CeHRG-1ΔN-HA, and a more modest decrease in β-galactosidase activity of the CeHRG-411-HA chimera and hHRG-1ΔN-HA. The decreased activity observed in these N-terminal chimeras can not be solely explained by protein degradation because the expression of CeHRG-411-HA is much higher than wild-type CeHRG-1-HA in yeast (Fig. 3.17). Taken together, these studies revealed that the N-terminal domains might be essential for HRG-1 heme uptake function.

Analysis of the N-terminal domain revealed that although it does not affect the localization of HRG-1-related proteins, it is necessary for the function of CeHRG-1. It is possible that the N-terminal domain may play a role in heme transport by

Figure 3.15. N-terminal chimeras of worm and human HRG-1 have impaired heme transport activity in *hem1Δ S. cerevisiae*. *hem1*Δ yeast cells were transformed with pYES-DEST52 (vector), HA-tagged wild-type HRG-1-related proteins and domain-swapping chimeras. Expression of all C-terminal and transmembrane domain chimeras rescued *hem1*Δ growth, similarly to what was seen with the wild-type proteins. Yeast cells transformed with CeHRG-411-HA, CeHRG-1ΔN-HA or hHRG-1ΔN-HA did not grow at 0.25 μM heme.

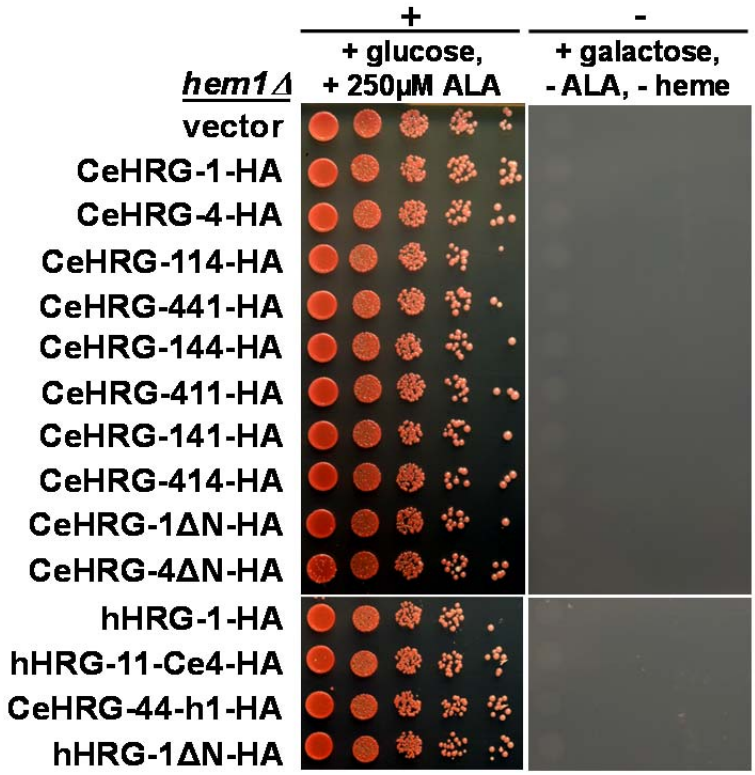
+
-
+ glucose,
+ 250μM ALA
+ galactose,
- ALA, - heme
hem1Δ
vector
CeHRG-1-HA
CeHRG-4-HA
CeHRG-114-HA
CeHRG-441-HA
CeHRG-144-HA
CeHRG-411-HA
CeHRG-141-HA
CeHRG-414-HA
CeHRG-1ΔN-HA
CeHRG-4ΔN-HA
hHRG-1-HA
hHRG-11-Ce4-HA
CeHRG-44-h1-HA
hHRG-1ΔN-HA

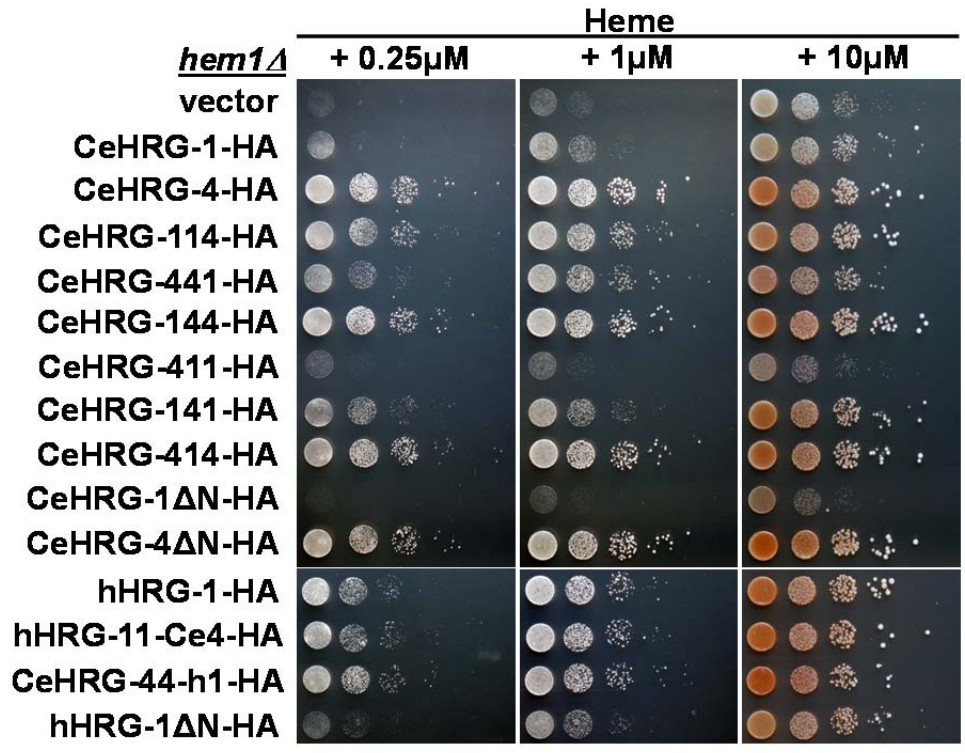
Heme
hem1Δ
+ 0.25μM
+ 1μM
+ 10μM
vector
CeHRG-1-HA
CeHRG-4-HA
CeHRG-114-HA
CeHRG-441-HA
CeHRG-144-HA
CeHRG-411-HA
CeHRG-141-HA
CeHRG-414-HA
CeHRG-1ΔN-HA
CeHRG-4ΔN-HA
hHRG-1-HA
hHRG-11-Ce4-HA
CeHRG-44-h1-HA
hHRG-1ΔN-HA

Figure 3.16. The N-terminus is required for CeHRG-1 transport heme in yeast. β-galactosidase activity was assayed in yeast cells co-transformed with pCYC-LacZ and pYES-DEST52 (vector), CeHRG-1-HA, CeHRG-4-HA or the chimeras listed. LacZ activity was assayed in 0.25 μM and 1 μM heme.

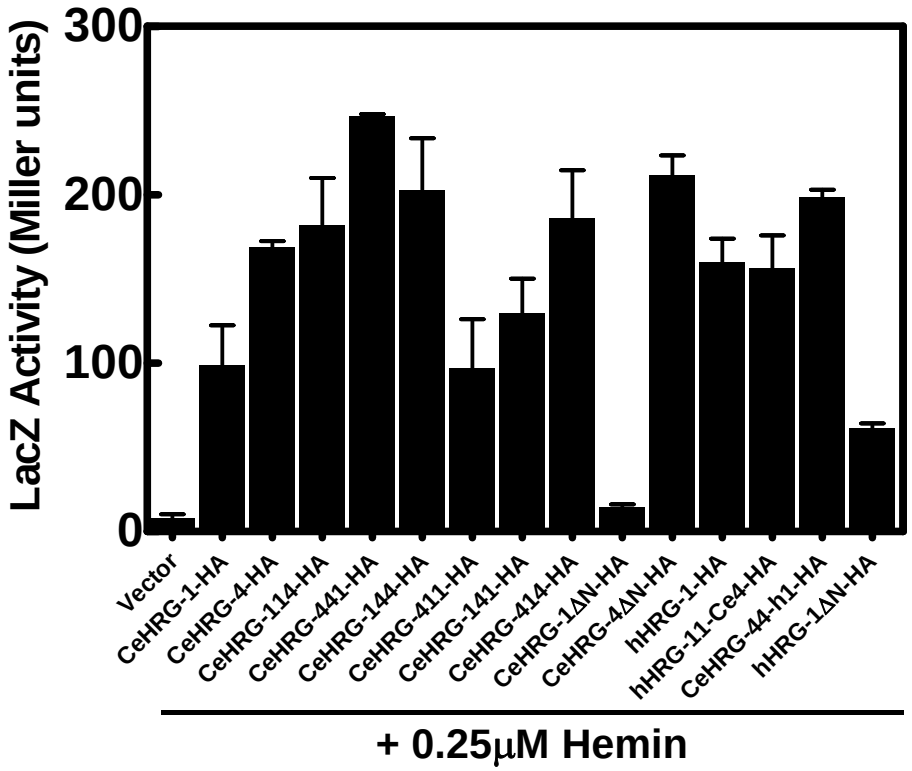
LacZ Activity (Miller units)
300
200
100
0
Vector
CeHRG-1-HA
CeHRG-4-HA
CeHRG-114-HA
CeHRG-441-HA
CeHRG-144-HA
CeHRG-411-HA
CeHRG-141-HA
CeHRG-414-HA
CeHRG-1ΔN-HA
CeHRG-4ΔN-HA
hHRG-1-HA
hHRG-11-Ce4-HA
CeHRG-44-h1-HA
hHRG-1ΔN-HA
+ 0.25μM Hemin

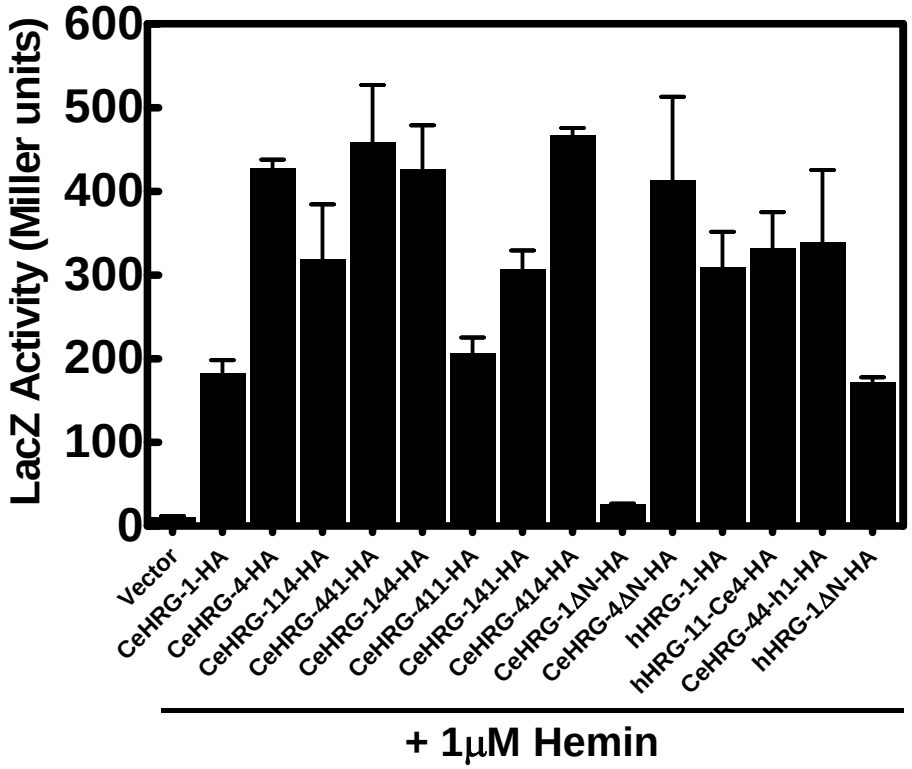
LacZ Activity (Miller units)
600
500
400
300
200
100
0
Vector
CeHRG-1-HA
CeHRG-4-HA
CeHRG-114-HA
CeHRG-441-HA
CeHRG-144-HA
CeHRG-411-HA
CeHRG-141-HA
CeHRG-414-HA
CeHRG-1ΔN-HA
CeHRG-4ΔN-HA
hHRG-1-HA
hHRG-11-Ce4-HA
CeHRG-44-h1-HA
hHRG-1ΔN-HA
+ 1μM Hemin

Figure 3.17. CeHRG-1 and CeHRG-4 chimeras show varied multimeric patterns. (A) HEK293 cells were transfected with CeHRG-1-HA, CeHRG-4-HA and chimeras, and analyzed by immunoblotting for the C-terminal HA tag. (B) Immunoblot of HRG-1 chimeras expressed in *hem1*Δ yeast strain, analyzed by immunoblotting for the C-terminal HA tag. Phosphoglycerate kinase 1 (PGK1) was shown as an internal loading control.

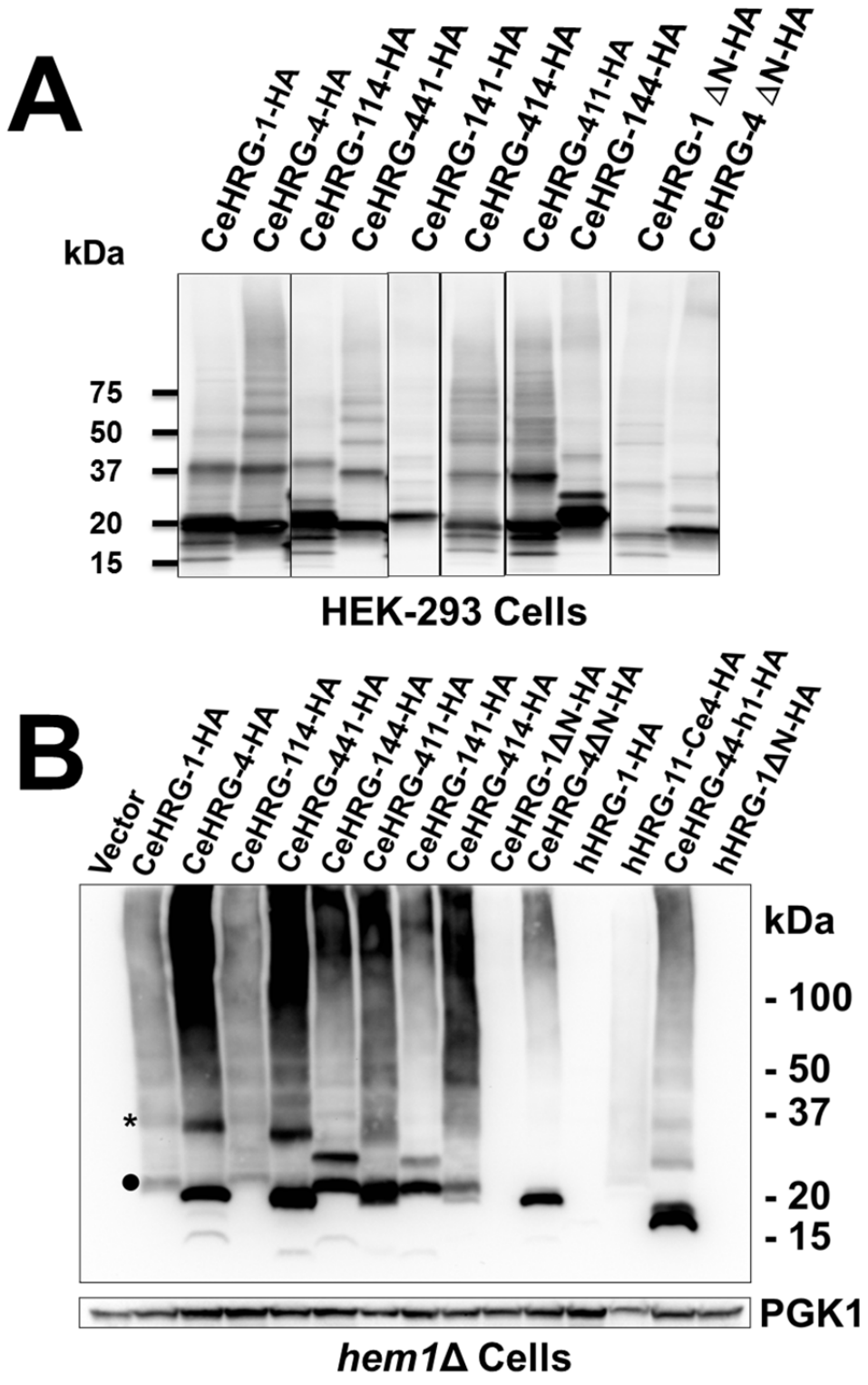
A
CeHRG-1-HA
CeHRG-4-HA
CeHRG-114-HA
CeHRG-441-HA
CeHRG-141-HA
CeHRG-414-HA
CeHRG-411-HA
CeHRG-144-HA
CeHRG-1 ΔN-HA
CeHRG-4 ΔN-HA
kDa
75
50
37
20
15
HEK-293 Cells
B
Vector
CeHRG-1-HA
CeHRG-4-HA
CeHRG-114-HA
CeHRG-441-HA
CeHRG-144-HA
CeHRG-411-HA
CeHRG-141-HA
CeHRG-414-HA
CeHRG-1ΔN-HA
CeHRG-4ΔN-HA
hHRG-1-HA
hHRG-11-Ce4-HA
CeHRG-44-h1-HA
hHRG-1ΔN-HA
kDa
- 100
- 50
- 37
- 20
- 15
*
PGK1
hem1Δ Cells

regulating protein-protein interactions such as HRG-1 multimerization. To further delineate the N-terminal domains' specific role in heme uptake, we examined the multimeric patterns of chimeras in mammalian and yeast cells. Interestingly, chimeras with the N-terminal domain of CeHRG-4 (CeHRG-441, 411 and 414) migrated as higher molecular weight multimers that was comparable to wild-type CeHRG-4, whereas chimeras with the N-terminal domain of CeHRG-1 (CeHRG-114, 144 and 141) migrated as wild-type CeHRG-1 oligomers (Fig. 3.17). These results indicate that the N-terminal domains of HRG-1-related proteins might be essential for protein folding or multimerization. Thus, the decreased heme transport activities of CeHRG-1ΔN-HA, CeHRG-411-HA and hHRG-1ΔN-HA observed in yeast assays could be a consequence of aberrant multimerization and/or lower protein stability.

DISCUSSION

Our genetic studies in worms reveal a definitive growth phenotype only when both *hrg-1* and *hrg-4* are deleted (Fig. 3.1C and D). Results from the *hem1Δ* yeast growth assays clearly demonstrate that, in addition to CeHRG-1 and CeHRG-4, two additional paralogs exist for heme transport in *C. elegans*. This is not surprising given that worms are solely dependent on environmental heme for growth and development. Thus, multiple backup systems exist in worms that ensure adequate heme is acquired for sustenance and transfer to their progeny [73]. From an experimental standpoint, these backup systems, however, occlude a thorough mechanistic analysis of HRG-1-related proteins using the *C. elegans* model. To recapitulate the heme auxotrophy of

worms, we exploited the *hem1Δ* yeast strain which is unable to synthesize heme and lacks the ability to utilize exogenous heme at low concentrations. In the current study, we employed independent functional assays in yeast to probe the molecular characteristics of heme transport by HRG-1- related proteins [130]. Our results reveal that, despite sharing only 27% identity and localizing to different subcellular compartments, the overall mechanism for heme transport employed by CeHRG-1 and CeHRG-4 are similar. We attribute the greater activity of CeHRG-4 in utilizing exogenous heme in the yeast reporter assays to its plasma membrane localization. By contrast, although CeHRG-1 predominantly localizes to the vacuolar membrane, it still has significant ability to utilize exogenous heme. It is conceivable that, as observed in mammalian cells [58], a portion of CeHRG-1 traffics to the plasma membrane.

Based on data from our assays, we propose a mechanistic model for heme import by HRG-1-related proteins. A histidine in the E2 loop on the extracellular/luminal side binds and transfers heme to a histidine (or a tyrosine at the synonymous position in CeHRG-4) in TMD2 within the channel. The heme is subsequently translocated to the cytoplasmic side facilitated by the FARKY (YAHRY in humans) motif in the C-terminal tail. The aromatic and positively charged amino acids in this motif may serve as heme ligands and stabilize or orient the vinyl and propionic acid side chains. A precedent for such a mechanism was recently established for the *Helicobacter hepaticus* CcsBA, a multi-pass ten transmembrane channel [153]. Heme is transported from the cytoplasm into the bacterial periplasm by CcsBA, a cytochrome *c* synthetase, by first binding to two histidines, defined as a

weak heme binding site within the TMDs, followed by translocation to a periplasmic heme binding region comprising two histidines and a WWD domain [153]. This mechanism of heme transfer prevents oxidation of the heme-iron and allows for proper orientation of the heme for covalent bond formation with the reduced apocytochrome. Our previous studies show that HRG-1-related proteins migrate as dimers and trimers on nondenaturing PAGE, raising the possibility that HRG-1-related protein functions as a multimer [58]. Thus, optimal transport function may be dependent on the cumulative contribution from individual heme-binding ligands from each subunit. Such a situation is observed with the three TMD copper transporter Ctr1 which functions as a symmetric trimer to form a channel lined with ligands for copper binding and transport [154].

Based on the degree of functional rescue in the yeast reporter assays for each mutant of the HRG- 1-related proteins, we postulate that a hierarchy may exist for binding heme amongst the ligands. HRG-1-related proteins may contain dual binding sites or heme translocation: a weak low affinity site followed by a high affinity primary substrate binding site. This concept is supported by the recent crystal structure of the LeuT leucine transporter and biochemical characterization of CcsBA heme transporter [153,155,156,157]. Both proteins possess a low affinity, transiently occupied substrate binding site that works in conjunction with a high affinity primary binding site to promote substrate movement and conformational gating.

Site-directed mutation reveals that H90 in CeHRG-1 (H56 in hHRG-1) is replaced by a synonymous Y63 in CeHRG-4 in TMD2. Although both His and Tyr are heme-binding ligands, replacing His with a Tyr as a ligand in hemoproteins

decreases the reactivity of heme possibly because of the increased anionic character of the phenolic group in Tyr which preferentially stabilizes oxidized heme (ferric and ferryl-oxo) [148,149]. Primary amino acid sequence alignments of putative HRG-1-related proteins from other species reveal that the His in TMD2 is highly conserved in the majority of species examined. However, in a small number of HRG-1 homologs, the His is substituted by a Tyr, as in the case of the HRG-1 homolog from the human pathogen *Leishmania amazonensis* which functions as a heme transporter [120]. *C. elegans* is a heme auxotroph and must acquire heme from the environment to sustain growth and development. Under physiological conditions, this soil-dwelling bacterivorous nematode likely ingests heme from multiple sources to maximize heme utilization through the concerted actions of both, CeHRG-1 and CeHRG-4 in the worm intestine. In its natural habitat, CeHRG-4 on the intestinal plasma membrane might encounter oxidized heme more readily than CeHRG-1 which might transport heme derived from the digestion of ingested hemoproteins in the lysosome, an organelle equivalent to the yeast vacuole, a storage compartment for iron, and plausibly, heme [158,159].

What drives translocation of heme through the HRG-1-related transporters? One possible mechanism could be heme concentration gradients generated by interactions of the transporter with downstream binding partner(s). In Gram positive bacteria, heme transfer from IsdA to IsdC, cell-wall anchored proteins in *Staphylococcus aureus*, is driven by kinetics and transient stereospecific weak "handclasp" interactions [160,161]. This is in stark contrast to Gram negative bacteria which utilize high affinity protein-protein interactions for heme transfer

[143,144,162]. Another mechanism could involve coupling with an energetically favorable flow or counterflow of ion gradients generated by primary transporters, a feature characteristic of permeases. Indeed, a recent study demonstrated that human HRG-1 associates with the V-ATPase proton pump [60], suggesting the possibility that a proton gradient generated by V-ATPases may drive heme transport, similar to the endocytic calcium transporters in yeast [163].

Is the mechanism for heme transport by HRG-1-related proteins shared with other metazoan heme transporters? FLVCR2, a member of the major facilitator superfamily, was recently reported to import heme in mammalian cells [65]. Although we did not observe heme import in our assay conditions, given the high degree of homology between FLVCR2 and the heme effluxer FLVCR1 [62,164,165], it is possible that FLVCR2 may export heme. This explains the increased ferrireductase activity observed in yeast expressing FLVCR2. As an effluxer, FLVCR2 should transport heme to the luminal side of the intracellular compartments. Thus the secretory pathway had elevated heme, even though the heme content was decreased in whole cell. These results with FLVCR2 are similar to our unpublished results with MRP-5, a heme exporter identified in *C. elegans*. Hemopexin facilitates heme export by FLVCR1 by binding to a 69 amino acid peptide (residues 132-201), which contains two exoplasmic loops and two TMDs [166]. *In silico* examination of the membrane topology of FLVCR2 predicts a 12 TMD protein with several strategically placed, evolutionarily conserved, heme-binding ligands in the exoplasmic and cytoplasmic loops and within the TMDs. Genetic studies have unequivocally demonstrated that FLVCR1 is essential for development; FLVCR1-

null mice lack definitive erythropoiesis and are embryonic lethal [63]. A structure-function analysis of FLVCR heme transporters will lay the groundwork for establishing whether the overall mechanism for heme transport identified for HRG-1-related proteins is also conserved in FLVCR. Although the physiological role for heme import by hHRG-1 in humans is still unclear, concurrent genetic studies with the mouse equivalent of *Hrg-1* will shed significant insight on the biological role of heme transporters in mammalian growth and development.

In addition to the functional residues we identified that are critical for heme transport, non-canonical tyrosine and dileucine based sorting motifs were indentified in both CeHRG-1 and hHRG-1 (Fig. 3.14). These motifs determine internalization and sorting to endosomal-lysosomal vesicles within the cytoplasm [151]. FPP assays revealed the C-terminal domains of HRG-1-related proteins indeed reside in the cytoplasm. Furthermore, swapping the C-terminal domains of CeHRG-1 or hHRG-1 with CeHRG-4 resulted in reversal of protein localization. Our studies revealed plasma membrane localization for CeHRG-114-GFP and endo-lysosomal localization for CeHRG-441. These findings indicate that the C-terminal domains of CeHRG-1, CeHRG-4 and hHRG-1 are required for proper protein localization. The sorting motifs identified in the cytoplasmic C-terminal domains of CeHRG-1 and hHRG-1 likely play a role in protein retrieval and sorting to the endolysosomal compartments. Further studies will be required to determine how and what regulates the intracellular localization of HRG-1-related proteins, and how this is tied to their function in *C. elegans* and mammals.

Chapter 4: High-Throughput Screen for Modulators of Heme Transporters

Summary

Neglected tropical diseases (NTDs) infect approximately 1.4 billion of the world's population, mainly in underdeveloped countries. NTDs are a group of 13 parasitic and bacterial infections, in which >90% infections are caused by a diverse group of parasitic worms or Trypanosomatids [167,168,169,170]. However, due to the lack of research funding support and general genome complexity compared to those of model organisms, little progress has been made in developing effective treatment agents [171,172]. To sustain their growth and reproduction, parasites exhibit distinct adaptations that allow them to acquire nutrients unidirectionally from the host. An example is the heme acquisition pathway exploited by Trypanosomatid and helminth parasites, suggesting a unique antiparasitic clinical target [13,14,118,120].

We have identified HRG-1 and HRG-4 as the first heme importers/transporters using the genetically tractable organism *C. elegans* [58]. Subsequent analysis of human and *Leishmania* HRG-1 orthologs revealed conserved pathways for cellular heme trafficking across species [120]. Currently, there are no pharmacological tools to aid in the study of the cellular and physiological roles of these eukaryotic heme transporters. Here, we report the development and validation of a cell-based, high-throughput screening (HTS)-compatible screen for small

molecule antagonists of HRG-1-related proteins using a simple growth assay in yeast. Because parasitic nematodes and the kinetoplastids also acquire heme from the environment, it is anticipated that compounds identified in this screen can be used to establish the feasibility of targeting the heme transport pathway for the treatment of helminth infections, Trypanosomiasis, intestinal nematodes, kinetoplastid diseases, lymphatic filariasis, onchocerciasis, and Leishmaniasis, as well as human genetic disorders of heme and iron metabolism.

Results

HRG-1-related proteins transport the toxic heme analog GaPPIX in wild-type yeast

We have utilized yeast as a model to investigate HRG-1-mediated heme uptake. Growth of the heme deficient yeast strain *hem1*Δ can be rescued by expressing HRG-1-related proteins in the presence of low heme [152]. We further revealed that ectopic expression of HRG-1-related proteins confers uptake of not only heme, but also heme analogs, in yeast. As shown in Fig. 4.1A, wild-type yeast expressing either HA-tagged or untagged CeHRG-4 are extremely sensitive to the toxic heme analog, gallium protoporphyrin IX (GaPPIX). Dose-response growth curves demonstrate that CeHRG-4-expressing yeast have >2,000-fold lower relative IC50 (half maximal inhibitory concentration) value for GaPPIX than yeast transformed with the vector alone (Fig. 4.1B). Because gallium cannot undergo oxidation-reduction reactions like iron, mis-incorporation of GaPPIX into

Figure 4.1. HRG-4 transport the toxic heme analog GaPPIX in wild-type yeast. (A) Transformed wild-type w303 yeast were serially diluted and plated on 2% raffinose SC (-Ura, +0.4% galactose) plates supplemented with no or 1μM GaPPIX to determine growth after 3 days. (B) Transformed wild-type w303 yeast cells were inoculated at 0.1 OD_{600} in 10 mL of 2% raffinose SC (-Ura, +0.4% galactose) medium and the indicated concentrations of GaPPIX, 30^{o} C with shaking at 225rpm for 16h prior to determining growth. The relative IC50 (mean ± SEM) for Vector was 61.77 μM and CeHRG-4 was 0.029 μM.

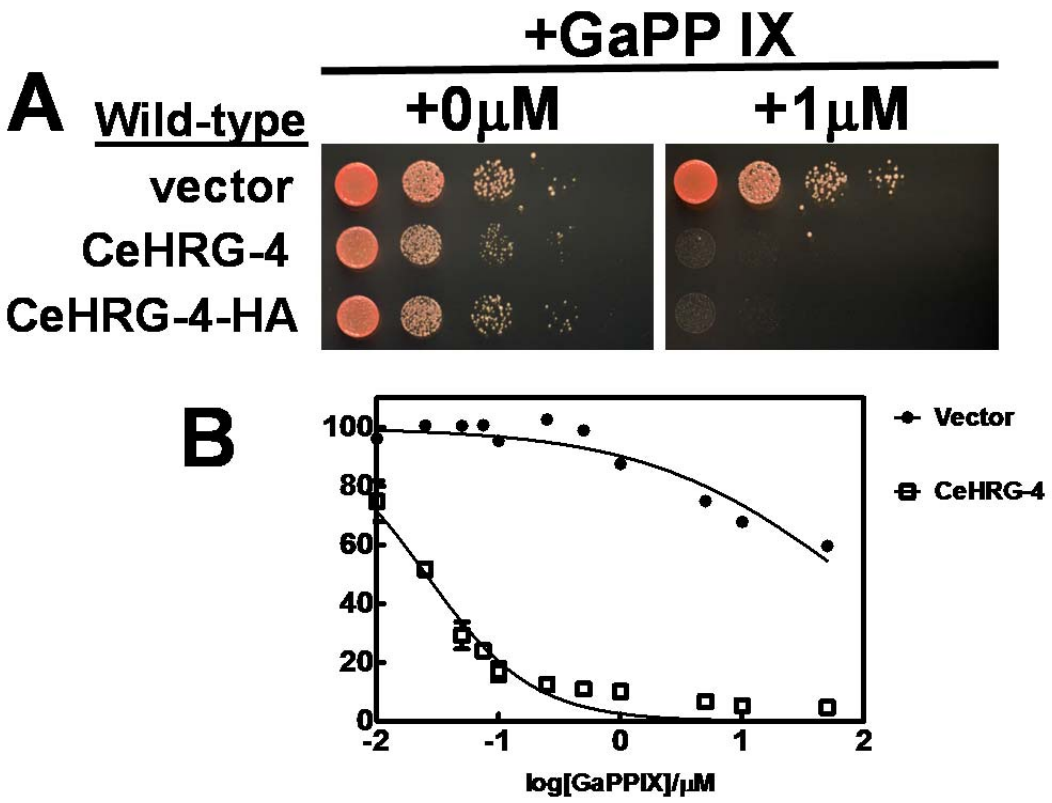
A
+GaPP IX
Wild-type
+0μM
+1μM
vector
CeHRG-4
CeHRG-4-HA
B
100
80
60
40
20
0
-2
-1
0
1
2
log[GaPPIX]/μM
Vector
CeHRG-4

hemoproteins is cytotoxic [15]. As we have demonstrated in *C. elegans*, GaPPIX toxicity in HRG-4 expressing yeast can be alleviated by addition of excess heme which effectively competes with GaPPIX for uptake [58].

High-throughput screen development

To identify small molecule antagonists of the HRG-1 heme transporters in an HTS-compatible format, a simple yeast growth assay was developed based on the observation that ectopically expressed HRG-1-related proteins confers uptake of heme and the toxic heme analog, GaPPIX in yeast. To avoid additional steps of yeast transformation and consequent data variation, yeast strains stably integrated with HRG-1-related proteins were generated. Putative HRG-1-related proteins antagonists are easily identified when the lethality of GaPPIX on yeast growth is blocked as assessed by optical absorbance (Fig. 4.2).

To develop a robust and reproducible protocol for the HTS assay in 384-well plate format, various control parameters including yeast density and incubation time, well volume, sealing methods, humidification, shaking effect and GaPPIX concentration needed to be optimized. For CeHRG-4 expressing yeast cells, adding 0.3 μM or 1 μM GaPPIX was sufficient to fully inhibit cell growth (Fig. 4.3). High concentrations of GaPPIX (≥ 30 μM) occasionally precipitated, an effect exacerbated by shaking. We used 1 μM GaPPIX in the HTS for identification of the CeHRG-4 antagonists. Standard growth curves of other worm HRG-1 paralogs were performed using the optimized conditions. Because CeHRG-1 is primarily localized to the vacuolar membranes in yeast, these cells are resistant to GaPPIX toxicity. To

circumvent this problem, we utilized the plasma membrane CeHRG-1 chimera, CeHRG-414, as a substitute (Fig. 4.3). Yeast expressing each of the four worm HRG-1 paralogs was sensitive to GaPPIX toxicity, permitting us to potentially identify small molecule antagonists which may have transporter selectivity and aiding in chemically dissecting the significance of redundant heme transporters in *C. elegans*.

Although the compounds in the chemical library were dissolved in DMSO, under the assay conditions, 1% DMSO had negligible effects on cell growth and was consequently chosen as the negative control (Fig. 4.3). We next evaluated two positive controls: (1) Addition of excess heme to compete with GaPPIX for uptake by CeHRG-4. Heme did not fully restore cell growth due in part to the toxicity of excess heme itself and the propensity of heme/GaPPIX to precipitate at high concentrations (Fig. 4.4). To prevent heme aggregation, several solvents were tested, including 0.3N NH_4OH (pH 8.0), DMSO, 20 or 40 mM MES buffer (pH 6.1) and 0.05% Tween 20, though none of the solvents provided significant improvement. (2) Alternatively, 0.4% glucose (dissolved in DMSO) was used to suppress expression from the GAL1 promoter driving CeHRG-4 expression. Though this control does not mimic the mechanism of rescue we sought, cell growth was fully restored (Fig. 4.4).

To test whether the optimized assay parameters could be scaled for HTS, a series of experiments were performed to evaluate signal-to-background ratio, variation within and between plates, and day-to-day effects by applying the statistical parameter Z'. Z' factor is a statistical estimate used to assess the quality of an assay

Figure 4.2. Schematic illustration of assay development and readouts. (A) Wild-type yeast can synthesize heme but utilizes exogenous heme poorly. Therefore, yeast cells are resistant to the toxic heme analog, GaPPIX. (B) Ectopic expression of CeHRG-4 confers uptake of GaPPIX, prohibiting yeast growth in microtiter plates. (C) A putative CeHRG-4 antagonist that blocks CeHRG-4 dependent GaPPIX uptake restores growth.

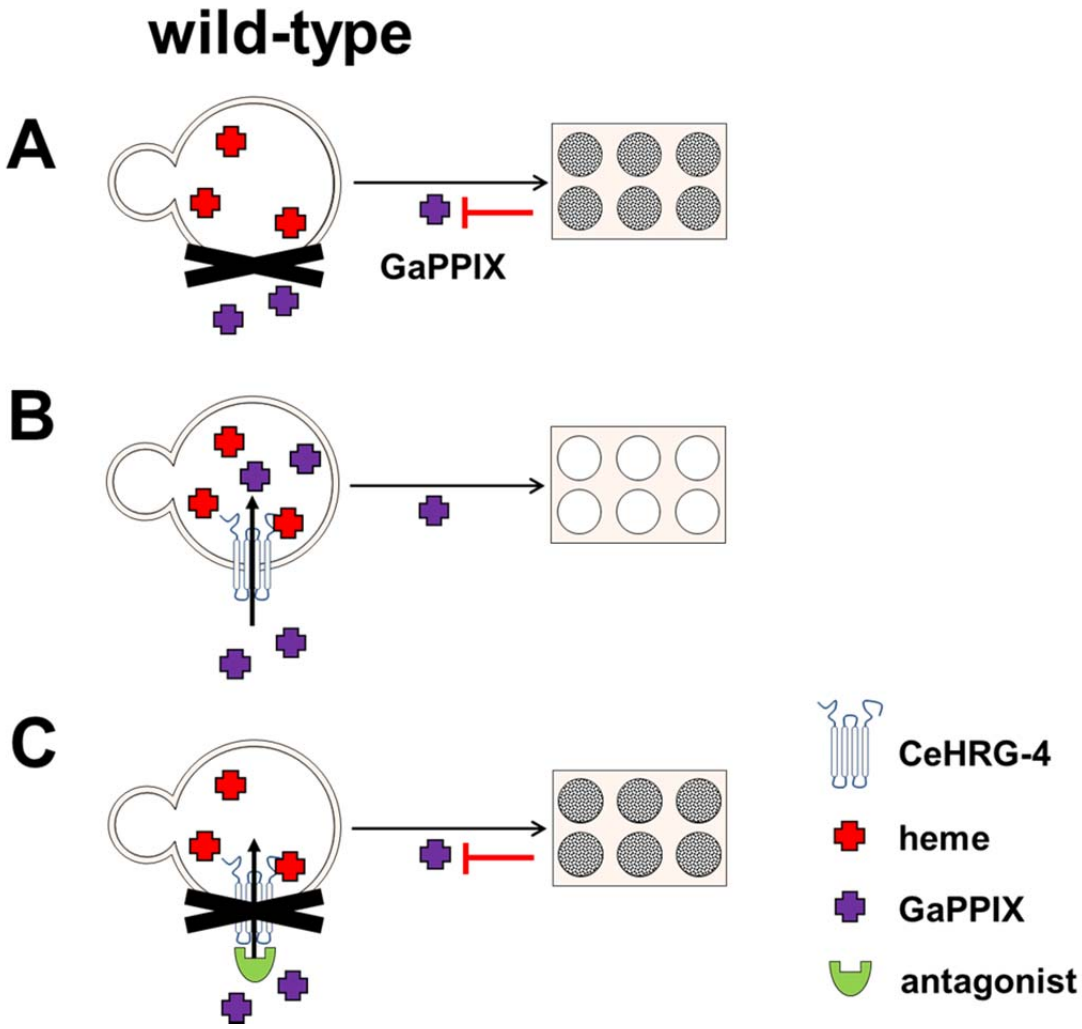
wild-type
A
GaPPIX
B
C
CeHRG-4
heme
GaPPIX
antagonist

Figure 4.3. Standard yeast growth curves of worm HRG-1 paralogs. Yeast cells expressing CeHRG-4, CeHRG-414, CeHRG-5 or CeHRG-6 were grown to stationary phase. Yeast were plated at OD_{600} = 0.05 in growth medium (70 µl/well; 384 wells/plate) containing increasing concentrations of GaPPIX. The assay plates were then incubated without shaking in a humidity container at 30ºC. OD_{600} values were measured over 48 hr. All samples contained 1% DMSO, except "-DMSO", to assess DMSO tolerance.

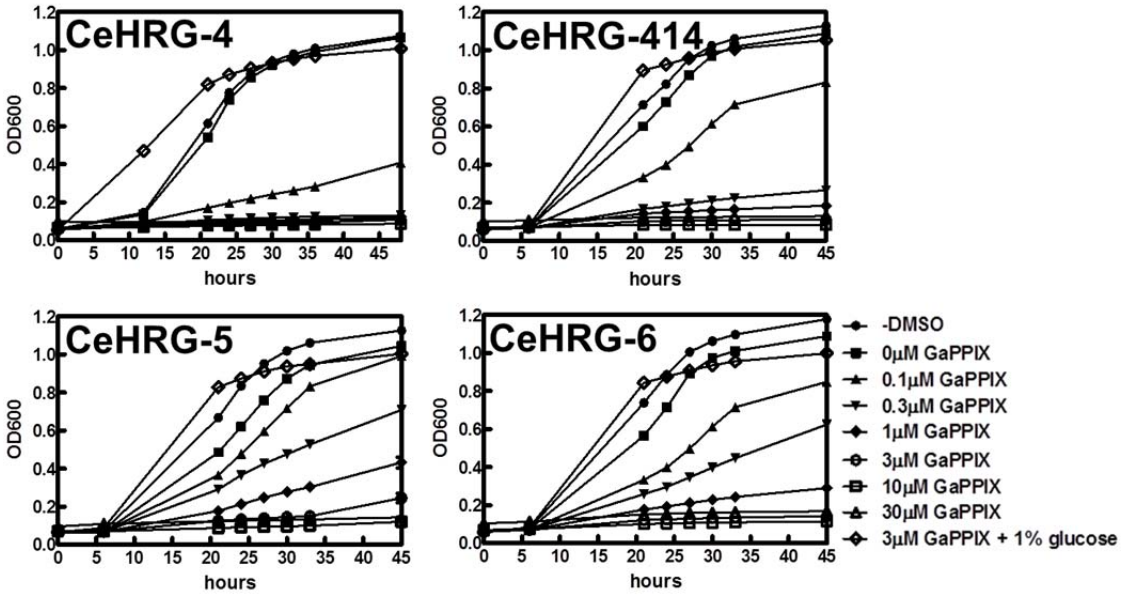
CeHRG-4
CeHRG-414
CeHRG-5
CeHRG-6
OD600
hours
-DMSO
0μM GaPPIX
0.1μM GaPPIX
0.3μM GaPPIX
1μM GaPPIX
3μM GaPPIX
10μM GaPPIX
30μM GaPPIX
3μM GaPPIX + 1% glucose

and suitability for a high-throughput setting. An assay that has a Z' factor between 0.5 and 1.0 is considered as an excellent assay for use in a full-scale, high-throughput screen. Following the procedure depicted in Fig. 4.5, three independent trial experiments were performed in triplicate on different days. All of the assay plates had a Z' factor of > 0.8 across individual plates, between plates, and between experiments (Table 4.1). A mock experiment of 30 total plates was also performed which showed an average Z' value of 0.815 (Table 4.2). These results confirmed that our assay is now suitable to be advanced into HTS.

High-throughput screen to identify antagonists of parasitic HRG-1-related proteins

The free-living nematode C. elegans and related parasitic nematodes do not synthesize heme [15]. Until recently, it was thought that all organisms synthesized heme with little variation via a well-defined pathway. We found, however, that *C. elegans* lacks the heme biosynthetic pathway enzymes [15]. It depends entirely upon diet for its heme and incorporates the ingested heme *in toto* into numerous hemoproteins involved in key biological reactions. Worms are growth-arrested in the presence of inadequate heme, but high levels of heme are toxic. Thus, these organisms must carefully control intracellular heme levels to survive. In fact, an analysis of publicly available helminths sequence databases revealed that obvious orthologs to heme biosynthesis pathway enzymes are absent [15]. A biochemical analysis of five nematodes with different host specificities did not detect any enzyme

activity for the heme synthesis pathway [15]. These measurements support the idea that *C. elegans* and parasitic nematodes of animals and, possibly, plants may have similar heme transport and assimilation pathways since none of them make heme but all contain hemoproteins.

As observed for parasitic helminths, Trypanosomatids such as *Leishmania* acquire their heme from the environment/host. In collaboration with Dr. Norma Andrews' laboratory on the UMD campus, we identified and cloned *Leishmania* LHR-1, the homolog of CeHRG-4. *L. amazonensis* promastigotes cultured in a heme deficient growth medium resulted in the upregulation of LHR-1 mRNA expression [120]. As was demonstrated with CeHRG-4, LHR-1:GFP was also found to localize to the plasma membrane and HA epitope tagged LHR-1 fully rescued the growth defect phenotype of the yeast *Δhem1* heme-defective mutant [120]. These results confirm that LHR-1 and CeHRG-4 are homologous heme transporters.

The major advantages of *Leishmania* over helminths are (a) single celled protozoa versus a multi-cellular nematode, (b) fully sequenced and annotated genome, (c) ease of growth in *ex vivo* cell culture or *in vivo* in mice, (d) genetically tractable to overexpress or knockout genes, and (e) no current drugs available except antimonials which are highly toxic to humans. The *Leishmania* LHR-1 is therefore a prototypical parasite heme transporter for a HTS to identify antagonists because of ease of follow-up studies in the parasite.

Figure 4.4. Evaluation of positive controls. CeHRG-4 yeast incubated with 0.3 μM (A) or 1μM GaPPIX (B) and increasing concentrations of heme or 0.4% glucose.

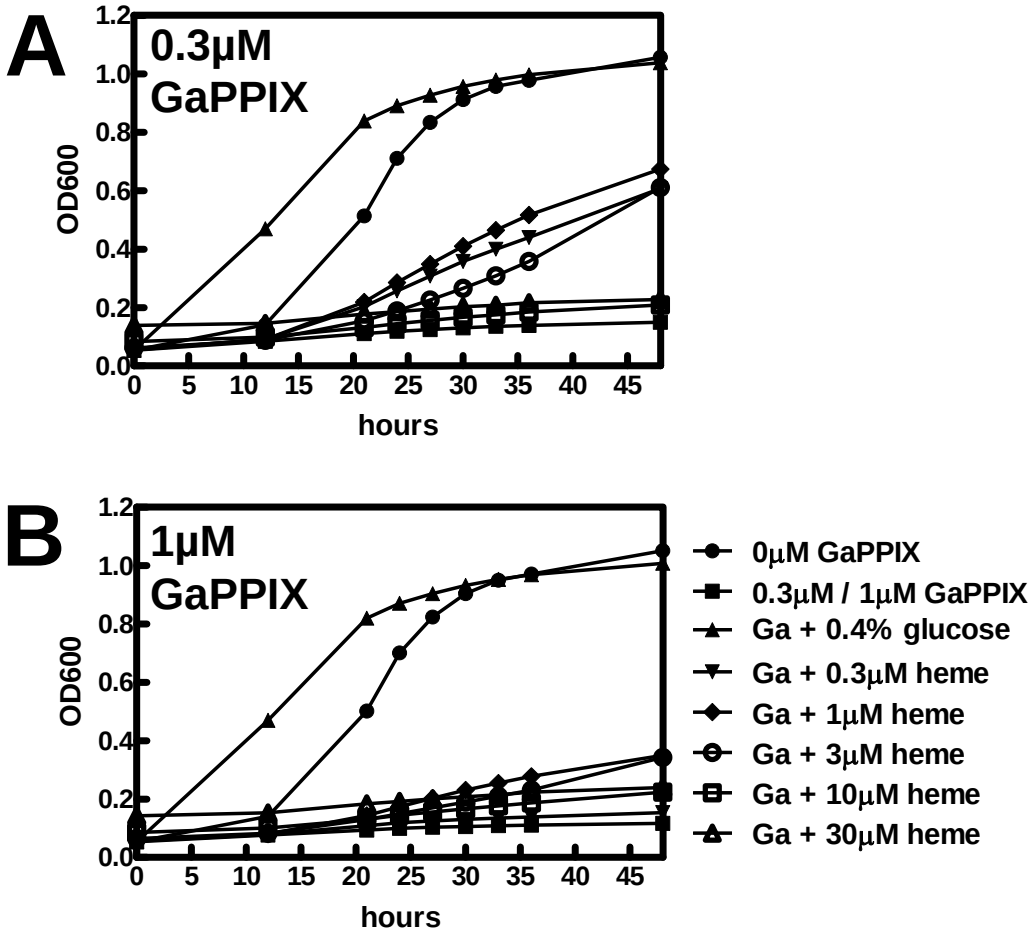
A
0.3μM
GaPPIX
OD600
hours
B
1μM
GaPPIX
OD600
hours
0μM GaPPIX
0.3μM / 1μM GaPPIX
Ga + 0.4% glucose
Ga + 0.3μM heme
Ga + 1μM heme
Ga + 3μM heme
Ga + 10μM heme
Ga + 30μM heme

Table 4.1 Plate effect statistics

		Z' score		
Day	**Plate**	**By plate**	**By day**	**Total**
	#1-1	0.895		
Day 1	#1-2	0.816	0.832	
	#1-3	0.819		
	#2-1	0.875		
Day2	#2-2	0.881	0.877	0.827
	#2-3	0.874		
	#3-1	0.892		
Day3	#3-2	0.905	0.878	
	#3-3	0.866		

Table 4.2 Mock experiment statistics

Plate#	Z' score	Plate#	Z' score	Plate#	Z' score
1	0.821	11	0.801	21	0.784
2	0.801	12	0.833	22	0.840
3	0.806	13	0.849	23	0.812
4	0.825	14	0.821	24	0.809
5	0.834	15	0.825	25	0.823
6	0.874	16	0.734	26	0.842
7	0.795	17	0.792	27	0.825
8	0.829	18	0.749	28	0.812
9	0.844	19	0.794	29	0.848
10	0.845	20	0.751	30	0.846

Figure 4.5. Outline of HTS assay procedure. Yeast integration lines were streaked on 2% w/v raffinose SC –His plate from -80°C glycerol stocks, and incubated at 30°C for 3 days until colonies with pink color formed. The day before adding the compounds, 10 to 20μL of yeast cells were collected from the plate and inoculated in 50mL 2% w/v raffinose SC –His liquid medium at 30°C, with shaking at 250rpm for 24 to 30 hours. To prepare the assay culture, 2% w/v raffinose SC (–His, +0.4% galactose) medium supplemented with 2 to 20μM GaPPIX was loaded into 384-well plates(Nunc), 35μL/well using a Multidrop reagent dispenser (TiterTek). The plates were then loaded with 0.7μL compound/well using robotic liquid handlers (Beckman). Yeast cells were prepared by centrifuging the overnight liquid culture at 3,000g for 5min and resuspending in 2% w/v raffinose SC (–His, +0.4% galactose) of an OD_{600} = 0.1. 35μL/well of yeast culture was added to the preloaded 384-well plates using Multidrop and incubated in a humidity container at 30°C without shaking. After 33-42 hours incubation, OD_{600} was measured using Synergy 2 plate reader (BioTek).

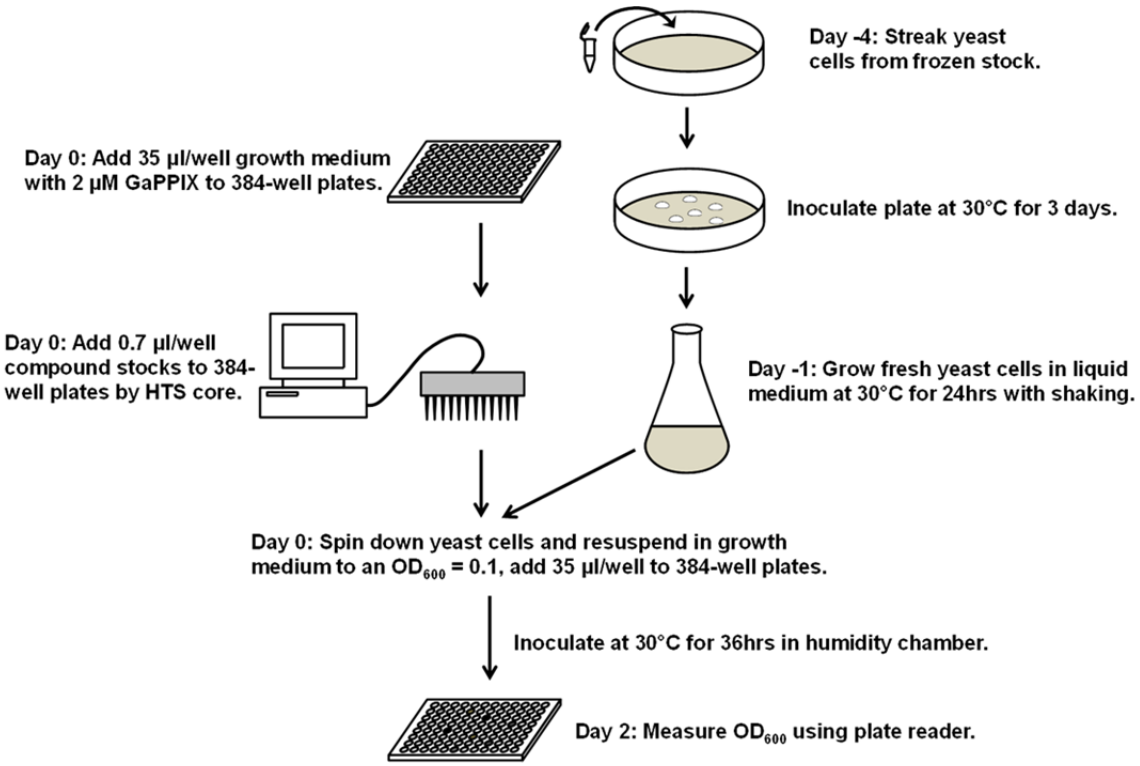
Day -4: Streak yeast cells from frozen stock.
Inoculate plate at 30°C for 3 days.
Day -1: Grow fresh yeast cells in liquid medium at 30°C for 24hrs with shaking.
Day 0: Add 35 µl/well growth medium with 2 µM GaPPIX to 384-well plates.
Day 0: Add 0.7 µl/well compound stocks to 384-well plates by HTS core.
Day 0: Spin down yeast cells and resuspend in growth medium to an OD_{600} = 0.1, add 35 µl/well to 384-well plates.
Inoculate at 30°C for 36hrs in humidity chamber.
Day 2: Measure OD_{600} using plate reader.

In addition to LHR-1, we also identified and assembled HRG-1 orthologs from an additional 34 published parasite genomes, ranging from human, companion animal or cattle parasites to plant pathogens with potential economical value (Table 4.3). Among these, HRG-1 orthologs of human (hHRG-1), three trypanosomatids *Leishmania amazonesis* (LHR-1), *Trypanosoma brucei* (TbHRG-1) and *Trypanosoma cruzi* (TcHRG-1), two filarial worms *Brugia malayi* (BmHRG-1) and *Dirofilaria immitis* (DiHRG-1), a hookworm *Ancylostoma ceylanicum* (AceHRG-1) and a plant parasite *Meloidogyne incognita* (MiHRG-1) were chosen for identifying small molecule antagonists (Fig. 4.6).

Two full primary screens were performed on LHR-1 and MiHRG-1, respectively, employing a library of 233,360 chemically distinct small molecules assembled by the UT Southwestern Medical Center's HTS Core facility from ChemBridge Corporation, Chemical Diversity Labs, ComGenex, TimTek, Prestwick, and the NIH clinical collection. The compounds in the library satisfy a relaxed set of Lipinsky's rules, with 99% having a molecular weight less than 550 (average 250-300). Compounds were assayed at 5 μM. At this concentration, 2670 primary LHR-1 hits (1.1%) and 2773 (1.2%) primary MiHRG-1 hits were identified with a Z score ≥ 3 (Fig. 4.7). The top 1,500 compounds from the two primary screens with a Z score ≥ 5 were confirmed and specified by following secondary and counter screens using all the HRG-1-related proteins listed in Fig. 4.3 and Fig. 4.6. A more stringent hit rate (~0.1%) would be achieved by decreasing compound concentration to 0.5 μM. Totally, 91 compounds were repurchased based on their activity and selectivity

Table 4.3 List of parasites containing HRG-1 orthologs from published genomes

Organism	Host	Heme-responsive Element
Caenorhabditis elegans	None	+
Oscheius tipulae	None	
Pristionchus pacificus	None	
Brugia malayi	Human	+
Wuchereria bancrofti	Human	+
Loa loa	Human	+
Dirofilaria immitis	Dog, rarely human	
Litomosoides sigmodontis	Rodents	
Onchocerca volvulus	Human	
Onchocerca ochengi	Cattle	
Ancylostoma ceylanicum	Human	+
Ancylostoma duodenale	Human	
Ancylostoma caninum	Dog	
Necator americanus	Human	
Heligmosomoides polygyrus	Woodmice	
Nippostrongylus brasiliensis	Rat	
Ascaris suum	Pig	
Schistosoma japonicum	Human	
Schistosoma mansoni	Human	+
Strongyloides ratti	Rat	
Trichuris muris	Mice	
Haemonchus contortus	Sheep / goat	+
Ostertagia ostertagi	Cattle	
Teladorsagia circumcincta	Sheep / goat	
Parastrongyloides trichosuri	Possum	
Meloidogyne incognita	Plant	
Meloidogyne hapla	Plant	+
Globodera rostochiensis	Potatoes / tomatoes	
Trichinella spiralis	Human, rat, pig	
Trichostrongylus colubriformis	Human, cattle	
Cooperia oncophora	Cattle	
Dictyocaulus viviparus	Cattle	
Oesophagostomum dentatum	Pig	
Leishmania amazonensis	Human	
Trypanosoma cruzi	Human	

Figure 4.6. Standard yeast growth curves of parasitic HRG-1 paralogs. Yeast cells expressing hHRG-1, LHR-1, AceHRG-1, BmHRG-1, DiHRG-1 or MiHRG-1 were grown to stationary phase. Yeast were plated at OD_{600} = 0.05 in growth medium (70 µl/well; 384 wells/plate) containing increasing concentrations of GaPPIX. The assay plates were then incubated without shaking in a humidity container at 30ºC. OD_{600} values were measured over 48 hr. All samples contained 1% DMSO, except "-DMSO", to assess DMSO tolerance.

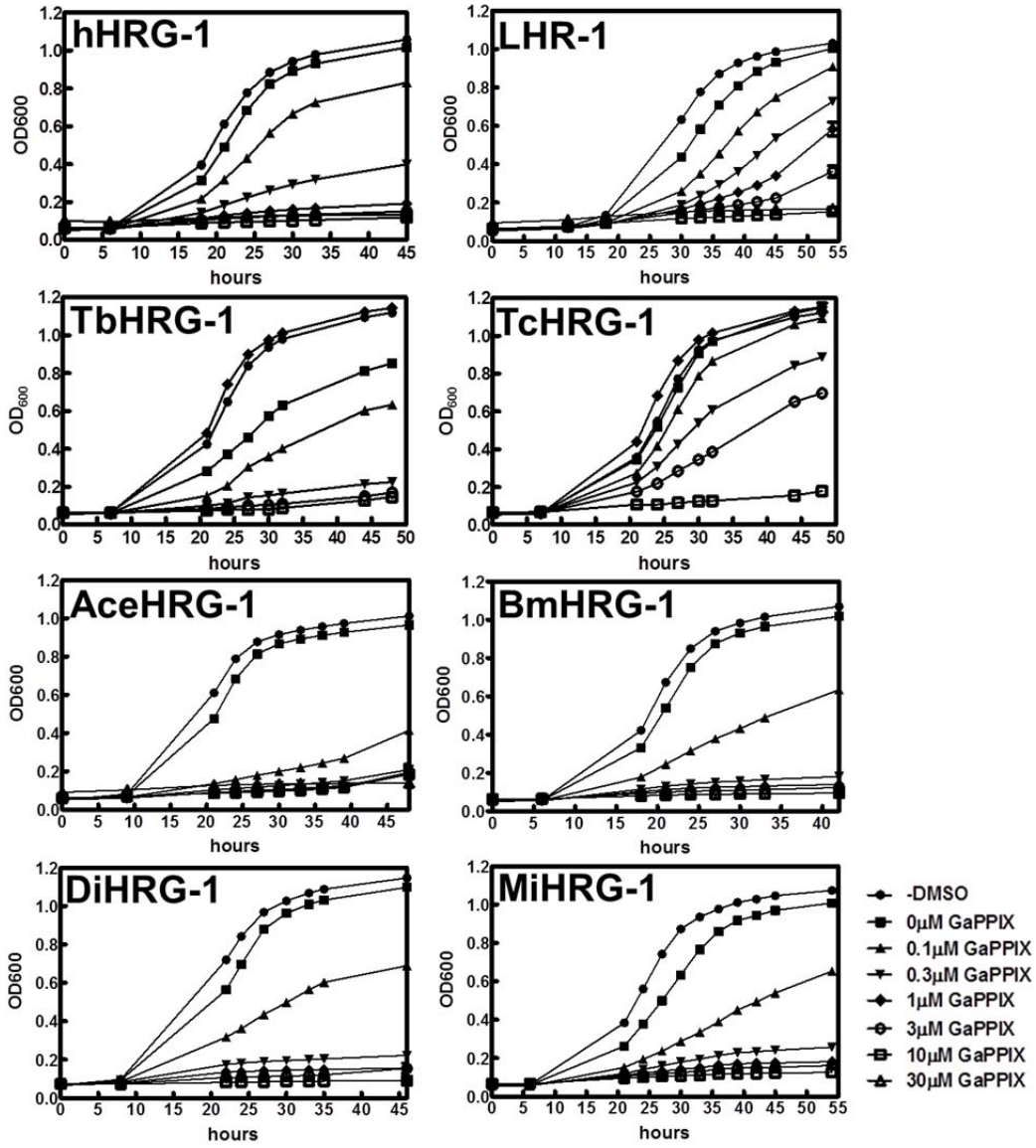
hHRG-1
LHR-1
TbHRG-1
TcHRG-1
AceHRG-1
BmHRG-1
DiHRG-1
MiHRG-1
OD600
hours
-DMSO
0μM GaPPIX
0.1μM GaPPIX
0.3μM GaPPIX
1μM GaPPIX
3μM GaPPIX
10μM GaPPIX
30μM GaPPIX

Figure 4.7. Summary of HTS screen results. (A) 233,360 compounds were assayed for rescue of LHR-1 yeast growth in the presence of 10μM GaPPIX. Each dot (black) represents the OD_{600} value of an individual well incubated with compound for 36 hr. The cutoff for a "primary hit" (Z score ≥ 3) is indicated by the orange dashed line. Negative (1% DMSO; green) and positive (0.2% glucose; red) control wells are indicated. (B) Summary of LHR-1 antagonist HTS screen.

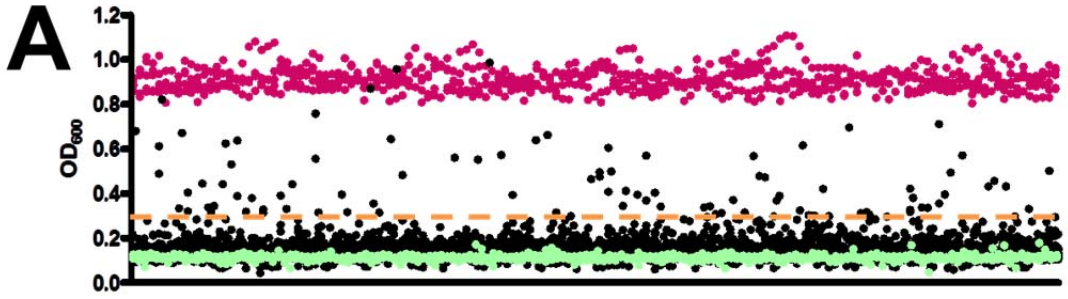
A
1.2
1.0
0.8
0.6
0.4
0.2
0.0
OD600

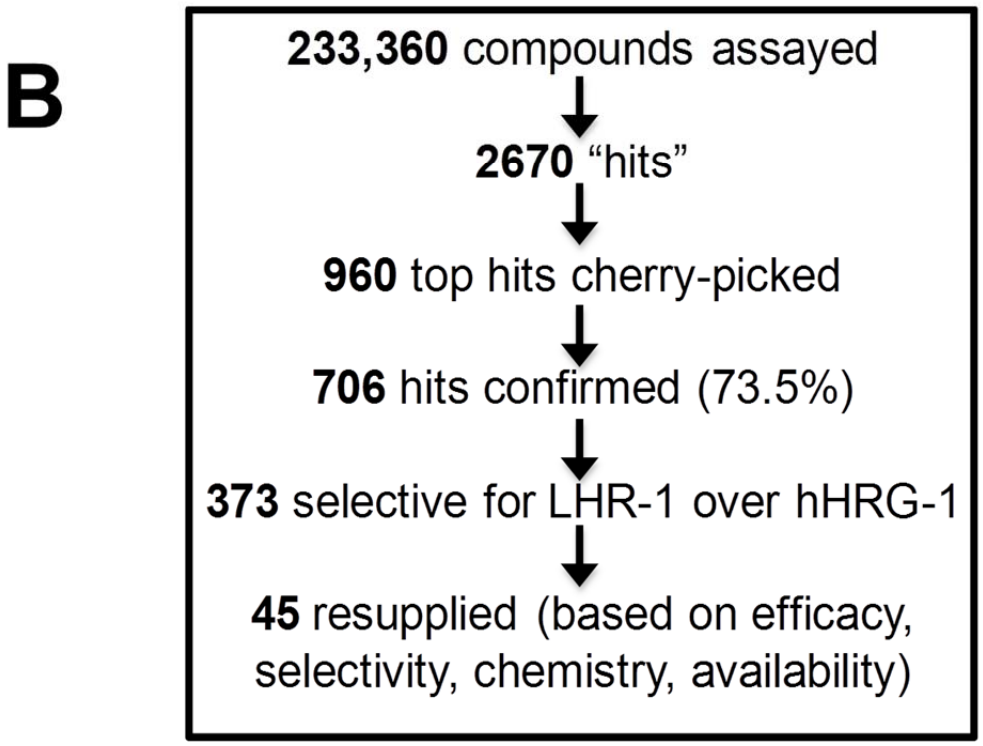
B
233,360 compounds assayed
2670 "hits"
960 top hits cherry-picked
706 hits confirmed (73.5%)
373 selective for LHR-1 over hHRG-1
45 resupplied (based on efficacy, selectivity, chemistry, availability)

against different HRG-1-related proteins, validated by LC/MS, and used to generate dose response curves (Fig. 4.8).

Validation of *C. elegans* HRG-1 paralog antagonists

Even though the original screen was conducted against LHR-1, the top compounds were rescreened using all the HRG-1-related proteins expressed in the yeast assay. To translate our results from a yeast HTS assay to an *in vivo* physiological model, we chose to evaluate the efficacy of lead antagonists against the *C. elegans* heme transporters. Two compounds that have CeHRG-4 inhibitor activity (#1 and #2) were further validated in *C. elegans*. Consistent with the initial assays, compound #1 was found to be an antagonist of both CeHRG-4 (AC_{50} = 0.69 ±0.11 μM) and hHRG-1 (AC_{50} = 1.89 ±0.23 μM), whereas #2 was remarkably selective for CeHRG-4 (AC_{50} = 0.54 ± 0.16 μM) over hHRG-1 (no activity detected) (Fig. 4.8A). Since the expression of the heme transporters are driven by the GAL1 promoter, false positive hits that mimic glucose suppression of CeHRG-4 expression may be obtained. To rule out this potential artifact, yeast integrated with HA-tagged CeHRG-4 (CeHRG-4-HA) was used to evaluate protein levels by immunoblotting. As shown in Fig. 4.8B, neither of the two compounds altered CeHRG-4-HA protein levels.

The two compounds were then subjected to verification of their activity in *C. elegans*. We first examined their activity in our previously established heme sensor strain, a transgenic worm that stably expressed a *Phrg-1::gfp* (IQ6011 strain) transcriptional fusion [58,145]. GFP is expressed specifically in the worm's intestine

at low heme but GFP expression is suppressed by heme (Fig. 4.9A). Knockdown of *hrg-4* or *hrg-1* result in derepression of GFP expression in IQ6011 even in the presence of sufficient heme, providing us the basis for evaluating the effects of pharmacological blocking of heme uptake in worms [58,145]. Growing IQ6011 at 20μM heme supplemented with DMSO showed no GFP fluorescence. By contrast, growing at 20μM heme supplemented with either 100μM compound #1 or #2 significantly turned on GFP expression (Fig. 4.9B). This result indicates that both of the two compounds can block heme uptake in *C. elegans*, thus activating a heme depletion signal from the *hrg-1* promoter. To demonstrate that this GFP upregulation is not an artifact we used a different reporter strain, *Pvha-6::gfp*. *vha-6* is an intestinally expressed, non-heme responsive gene [173]. Consistent with previous results, 100μM compound #1 or 10μM compound #2 significantly upregulated GFP in IQ6011 strain in the presence of 10μM heme but not in the *Pvha6::gfp* strain (Fig. 4.10), indicating that the upregulation of GFP in IQ6011 strains was not due to a non-specific effect of the compound on the GFP reporter.

C. elegans requires heme for growth and reproduction. Worms respond in a biphasic manner to heme levels in liquid axenic mCeHR medium [15]. The optimal concentration for worm growth is 20μM heme. We next examined whether the inhibitors block heme uptake, and therefore interfere with worm growth and reproduction. IQ6011 strain growing at 10μM heme lay broods of more than 50 progeny, which was reduced to 1~2 progeny at 6μM heme. Growth of the worms was fully arrested below 4μM heme. Adding 1% DMSO vehicle had a modest effect on worm growth and reproduction in the presence of 10μM heme. However, both

Figure 4.8. Dose responsive analysis on resupplied compounds. (A) Two primary CeHRG-4 hits were repurchased, validated by LC/MS, and assayed at multiple concentrations (0.003-30 μM) in triplicate. (B) A yeast strain expressing HA-tagged CeHRG-4 was used to evaluate compound effects on HRG-1-related protein expression. Cells were cultured with no GaPPIX (-Ga), or 1 μM GaPPIX with 30 μM compounds or 0.2% glucose (Glu) for 16 hr at 30ºC, 250 rpm.

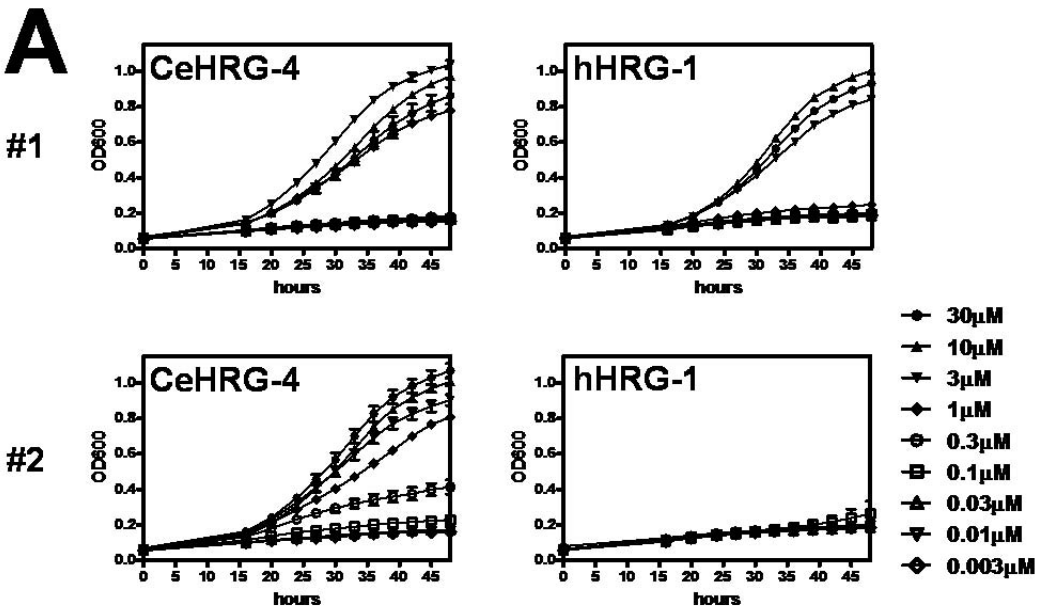
A
#1
#2
CeHRG-4
hHRG-1
OD600
hours
30μM
10μM
3μM
1μM
0.3μM
0.1μM
0.03μM
0.01μM
0.003μM

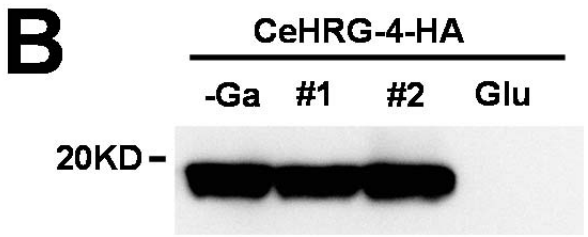
B
CeHRG-4-HA
-Ga
#1
#2
Glu
20KD

Figure 4.9. Compound hits upregulate GFP expression in heme sensor strain. Synchronized *Phrg-1::gfp* (IQ6011) worms were put in mCeHR2 medium at L1 stage, 100 worms/well in 24-well plates. Worms were grown in the presence of either (A) indicated amounts of heme, or (B) 20μM heme supplemented with 1% DMSO, 30μM GaPPIX or 100μM compounds (from 10mM DMSO stock) for 4 days.

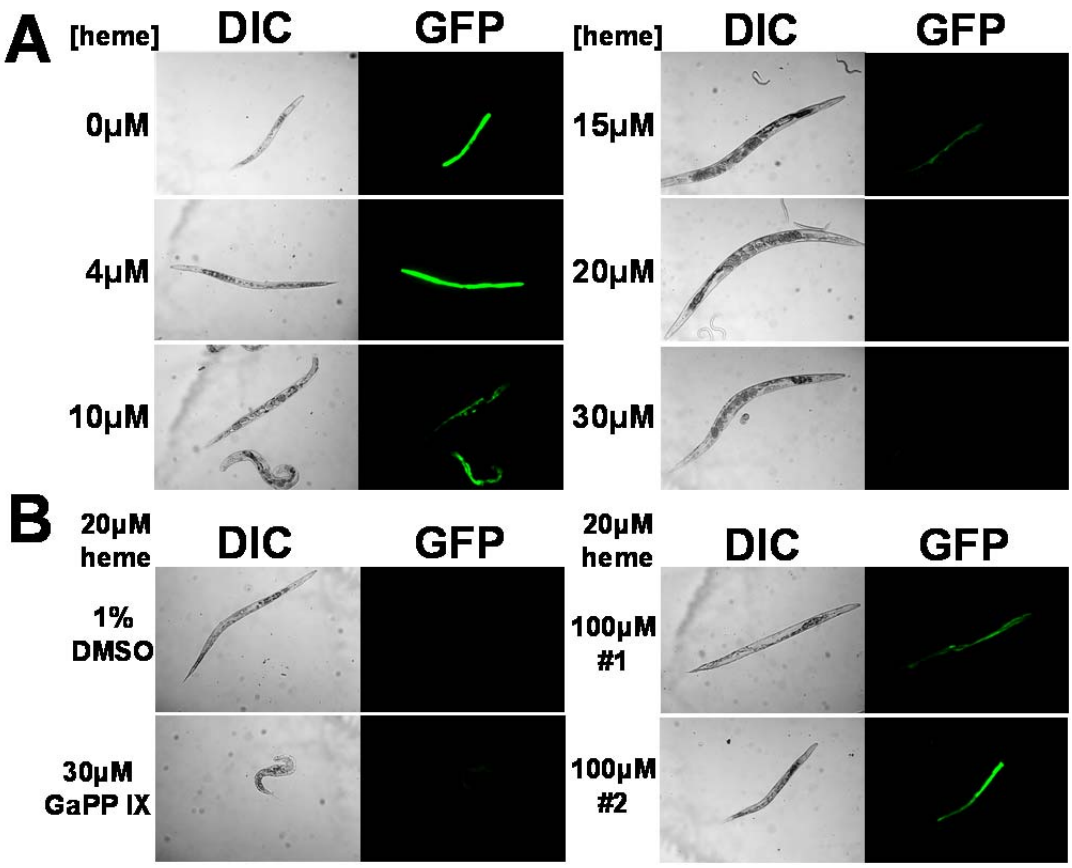
A
[heme]
DIC
GFP
0μM
4μM
10μM
[heme]
DIC
GFP
15μM
20μM
30μM
B
20μM heme
DIC
GFP
1% DMSO
30μM GaPP IX
20μM heme
DIC
GFP
100μM #1
100μM #2

Figure 4.10. Compound hits block heme uptake in a dose-responsive pattern in worms. Synchronized (A) *Phrg-1::gfp* (IQ6011) or (B) *Pvha-6::gfp* worms were put in mCeHR2 medium at L1 stage, 100 worms/well in 24-well plates. Worms were grown in the presence of 10μM, 30μM or 100μM compounds (from 10mM DMSO stock) or corresponding concentration of DMSO alone for 4 days. GFP fluorescence intensities were quantified by COPAS BioSort. The settings for GFP measurement were gain=3.0, PMT voltage=600. n=300, *** $p < 0.001$.

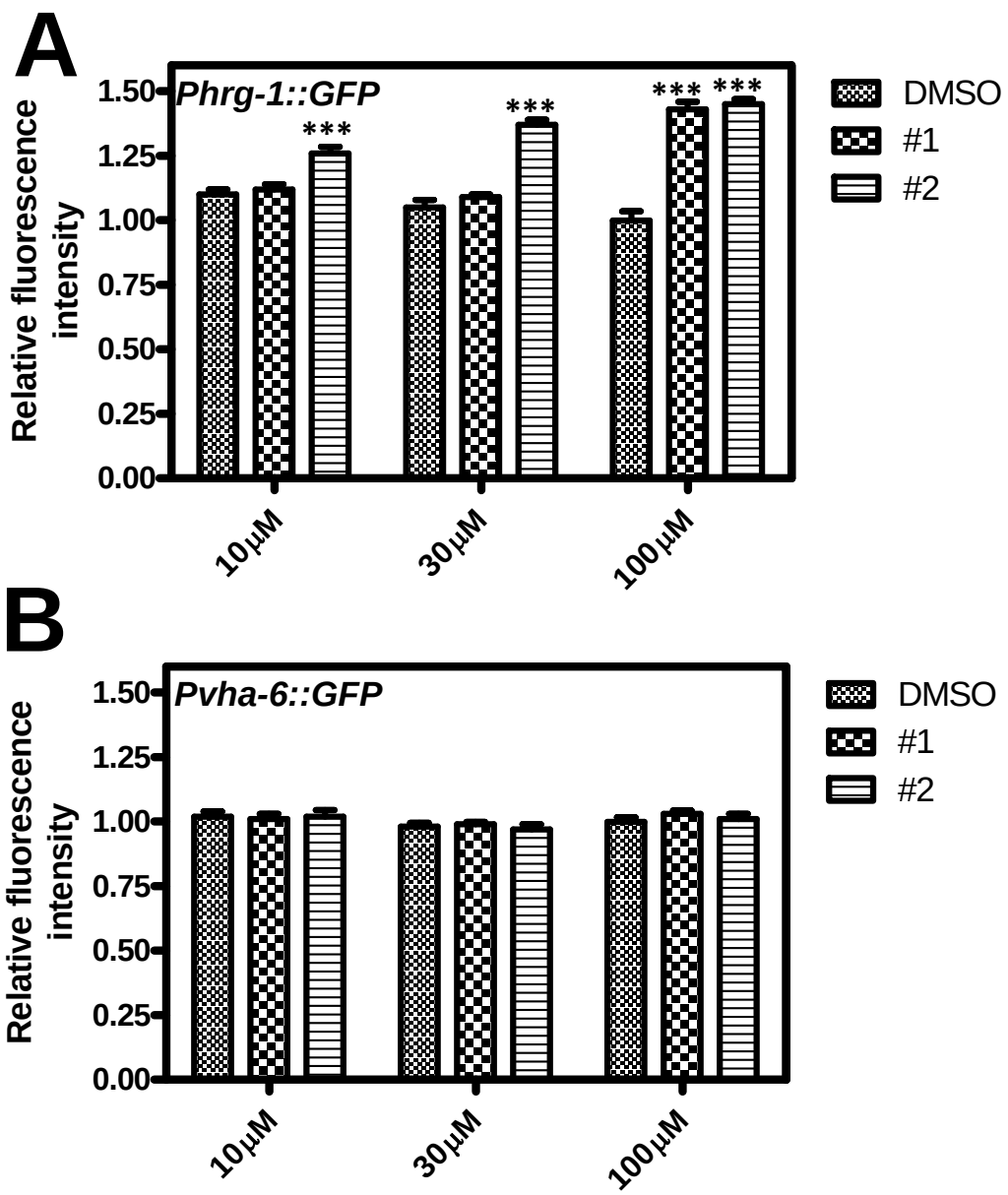
A
Phrg-1::GFP
Relative fluorescence intensity
1.50
1.25
1.00
0.75
0.50
0.25
0.00
***
***
***
***
10μM
30μM
100μM
DMSO
#1
#2
B
Pvha-6::GFP
Relative fluorescence intensity
1.50
1.25
1.00
0.75
0.50
0.25
0.00
10μM
30μM
100μM
DMSO
#1
#2

Figure 4.11. Compound hits interfere with heme dependent worm growth. 100 larvae at the L1 stage were grown in mCeHR2 medium for 9 days in a 24-well plate with each well containing an increased concentration of heme or 10μM heme with supplemented with 1% DMSO, 30μM GaPPIX or 100μM compounds (from 10mM DMSO stock). The total numbers of worms in each well were counted on day 9. Each data point represents the mean (± SEM) from experiments performed in duplicate, *** $p < 0.001$.

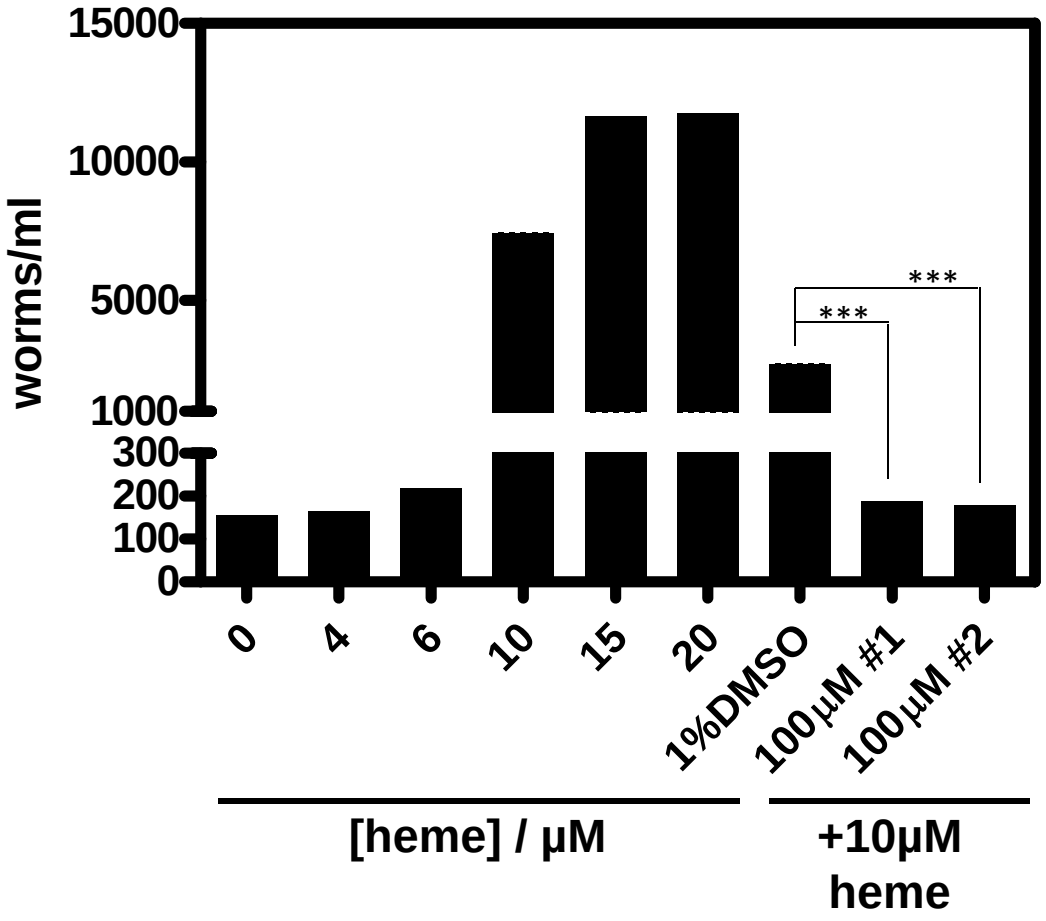
15000
10000
5000
1000
300
200
100
0
worms/ml
***
***
0
4
6
10
15
20
1%DMSO
100μM #1
100μM #2
[heme] / μM
+10μM heme

100μM compound #1 and #2 fully arrested worm growth (Fig. 4.11). This observation provides further evidence of the inhibitory activity of the compounds on *C. elegans* HRG-1 paralogs.

Discussion

Parasitic worm infections are a huge burden to public health since more than two billion people world-wide are afflicted by helminthic infections. Annual crop losses due to plant-parasitic nematodes are estimated to be around eighty billion dollars [122,123]. There is an urgent need to find new drug targets to tackle helminthic infections because drug resistance is already prevalent in these parasites [124]. We previously showed that parasitic nematodes lack the ability to make heme and rely on exogenous heme for their growth and development [15]. A recent study has demonstrated that the infectivity of hookworms, which feed on blood in the host, was significantly lower in hamsters fed a low-iron diet [125]. This observation revealed the importance of host heme and iron status in the survival of parasitic nematodes. Interestingly, protozoan parasites such as Trypanosomes, the causative agents of diseases such as sleeping sickness (*Trypanosoma brucei*), Chagas disease (*Trypanosoma cruzi*) and leishmaniasis (*Leishmania major*), also seem to lack the ability to make heme and therefore utilize exogenous heme [13,14,174].

Using the heme auxotroph *C. elegans*, we have discovered CeHRG-1 and CeHRG-4, the first eukaryotic heme importers/ transporters. We further demonstrated that HRG-1-related proteins are functionally conserved from *Leishmania* to humans,

suggesting they could potentially be used as novel drug targets against parasitic infections or heme/iron homeostasis disorders [120,152]. The assay strategy to identify HRG1-related protein antagonists exploits the observation that ectopic HRG-1-related protein expression confers uptake of heme, and heme analogs in yeast. A simple growth assay was developed in which yeast expressing HRG1-related protein are grown in the presence of the toxic heme analog GaPPIX. Antagonists that prevent heme uptake via HRG1-related proteins would be identified by their ability to suppress GaPPIX cytotoxicity as measured by yeast growth using optical absorbance. The gain-of-function phenotype (yeast viability rather death) limited the number of potential false-positive hits.

We successfully optimized conditions of the growth assay to a HTS-compatible format and validated it on a robust statistical basis. This assay was then applied to a screen of 233,360 structurally diverse small molecules, aimed at the identification of heme transport modulator compounds. Primary screening was performed on yeast expressing LHR-1 or MiHRG-1 in a 384-well plate format, followed by secondary screening of active compounds using eight HRG-1-related proteins and four *C. elegans* HRG-1 paralogs as targets. On average, ~1% of the compounds were identified as hits from primary screens, featuring a Z score of ≥ 5, none of which had previously been identified as drug candidates. Ninety-one compounds representing different groups of HRG-1-related protein antagonists were repurchased, validated by LC/MS, and used to generate dose-response curves. As a proof-of-principle, two compounds that have CeHRG-4 antagonist activity were further validated in *C. elegans*. Both compounds were able to upregulate GFP

intensity in the IQ6011 heme sensor strain. Addition of these compounds also inhibits heme dependent growth of *C. elegans* in liquid axenic medium. These results demonstrate that the HTS of small molecule libraries against HRG1-related protein in a rapid and simple 384-well plate format assay was able to identify novel heme transport modulators as anti-parasitic compounds or biological tools to study heme homeostasis.

Published reports have suggested a role for heme in the pathogenicity of various parasitic worms. Hookworm infection due to *Ancylostoma ceylanicum* is prevalent in developing countries and is associated with iron deficiency anemia. Hamsters fed a diet with reduced iron had a significant reduction in the intestinal load of worms. Hookworms, like *C. elegans*, also lack the ability to make heme; it is thus plausible that animals fed a low-iron diet have reduced worm burden due to inadequate amounts of heme for hookworm metabolism [125]. Filarial nematodes, such as *Brugia malayi* and *Dirofilaria immitis* are the causative agents of severe filariasis infections including elephantiasis. Analysis of the genome sequence of *Brugia malayi* revealed the absence of the heme biosynthesis enzymes in these parasites [126]. Therefore, it is highly likely that these parasites obtain heme from the host or from *Wolbachia*, an intracellular endosymbiotic bacterium that has a functional heme biosynthesis pathway [127]. Antibiotics that eliminate the endosymbiont have inhibitory effects on the development and fertility of the parasitic nematode and have been used to treat patients with filariasis. Recent studies on *Leishmania* and *Trypanosoma* have also reported that proliferation of these protozoa is dependent on heme [118,120]. Treatment with heme analogs SnPPIX, ZnMPIX and

PdMPIX inhibited *T. cruzi* proliferation, and this inhibition could be reverted by the presence of heme [118]. Since heme is important for the growth and development of these parasites, our small molecule antagonist screen targeting heme transporters opens new opportunities for the discovery of future candidates for anti-parasitic drug development.

Chapter 5: Conclusions and future directions

Conclusions

Our long term objectives are to identify the mechanisms for heme homeostasis in eukaryotes and develop anti-parasitic therapeutics that target the parasites' heme transport system. Utilizing the heme auxotroph *C. elegans*, we have previously identified *bona fide* heme transporters, CeHRG-1 and CeHRG-4. During the past few years, we performed extensive functional analysis using yeast and worm as model systems, to investigate the mechanism of heme transport and intracellular trafficking by HRG-1-related proteins. This work laid the groundwork for the subsequent discovery of HRG-1 homologs in parasites and for developing a high-throughput screen for antagonists against HRG-1 homologs. The major findings in this study are listed and discussed below:

1) Single knockout of either *hrg-1* or *hrg-4* showed no obvious phenotypes in *C. elegans*. Only the *Δhrg-1Δhrg-4* double mutant worms exhibited a modest growth delay at low heme, which could be fully rescued with excess heme. These results imply that worms have redundant mechanisms for heme uptake and transport. Indeed, *C. elegans* has two additional HRG-1 paralogs, CeHRG-5 and CeHRG-6, which are legitimate heme transporters as assessed in the yeast functional assays.

2) Yeast does not have a robust heme uptake system. The *hem1Δ* yeast strain, which recapitulated the heme auxotrophy of worms, was exploited to dissect the

function of HRG-1-related proteins. Ectopic expression of HRG-1-related proteins in the *hem1Δ* strain revealed heme import activity, validating the use of the yeast as a heterologous system for heme transport study.

3) CeHRG-1 and CeHRG-4 share only 27% identity and have different subcellular localizations. However, sequence analysis revealed topologically conserved residues. Functional analyses in yeast showed that CeHRG-1 requires both a specific histidine (H90) in the predicted second transmembrane domain (TMD2) and the FARKY motif in the C-terminus tail for heme transport. By contrast, the plasma membrane CeHRG-4 transports heme by utilizing a histidine in the exoplasmic (E2) loop (H108) and the FARKY motif. Optimal activity in heme limiting conditions requires a histidine in the E2 loop of CeHRG-1 (H135) and tyrosine in TMD2 of CeHRG-4 (Y63).

4) Expression of CeHRG-1 H90A mutant in the *Δhrg-1Δhrg-4* worms showed an unexpected dominant-negative phenotype only at low heme. We speculate that this result may be due to aberrant hetero-multimerization or disruption of protein-protein interactions between HRG-1 paralogs.

5) hHRG-1 is only ≈20% identical to CeHRG-1. Mutation of the synonymous histidine (H56) in TMD2 of hHRG-1, corresponding to H90 in CeHRG-1, eliminates heme transport activity, implying an evolutionary conserved heme transport mechanism. Single-nucleotide polymorphisms in *hHRG-1* are present in humans. Two such variants, P36L and W115C, show significantly reduced heme transport activity in the yeast assays.

6) FLVCR2 was recently reported as a heme importer in mammalian cells. However, FLVCR2 did not rescue heme-dependent growth of *hem1*Δ yeast strain, indicating it may be actually a heme exporter as its paralog, FLVCR1.

7) Ectopic expression in mammalian cells showed CeHRG-4 localized to the plasma membrane, whereas CeHRG-1 and hHRG-1 co-localized with endosomal and lysosomal markers. Worm and human HRG-1 have a conserved but sub-optimal tyrosine (YxxxØ in humans and YxxØ in worms) and an acidic-dileucine (DxxIL in humans and ExxxLL in worms) based sorting motifs at their C-terminal domains, which are absent in CeHRG-4. Swapping the C-terminal domains of HRG-1-related proteins resulted in an equivalent exchange in their subcellular localization. By contrast, switching the N-terminal domains or TMDs did not affect protein localization. These results reinforce the possibility that C-terminal domains of HRG-1-related proteins are required for proper intracellular trafficking.

8) The N-terminal domain chimeras of worm and human HRG-1 showed impaired heme transport activity in yeast. Swapping the N-terminal domains of CeHRG-1 and CeHRG-4 switched the protein multimerization profile. These observations indicate HRG-1-related proteins have a defined oligomerization pattern that is dependent on its respective N-terminal segment. Furthermore, multimerization may play a role in heme transport.

9) Expression of HRG-1-related proteins dramatically increase yeast sensitivity to the toxic heme analog, GaPPIX. A high-throughput screen aimed at identifying HRG-1 antagonists was developed based on the GaPPIX uptake assay.

10) A high-throughput screen employing a library of 233,360 small molecule compounds was performed to discover inhibitors of HRG-1 homologs from humans, helminths and Trypanosomatids. About 1% of the library qualified as primary antagonists with the ability to inhibit transport activity of at least one heme transporter. Ninety-one compounds representing different categories were repurchased and subjected to dose-responsive analysis in yeast.

11) Two leading compounds identified as antagonists of CeHRG-4 were validated in *in vivo* assays using *C. elegans*. Both of the compounds specifically increased GFP signal in the "heme sensor" IQ6011 strain and inhibited heme-dependent growth of worms

Significance and speculations

Trypanosomatids and helminths are unable to synthesize heme *de novo*, although they need heme to sustain their growth and reproduction. Our group previously discovered CeHRG-1 and CeHRG-4 as the first *bona fide* eukaryotic heme importers/transporters [58]. *In silico* analysis revealed topologically conserved amino acids as potential heme ligands in HRG-1-related proteins. In this dissertation, we dissected the significance of these residues in HRG-1 function as heme transporters using the *hem1*Δ yeast strain. Our results revealed HRG-1-related proteins transport heme across membranes through the coordinated actions of these topologically conserved residues in the worm and human proteins. Our results imply that the

mechanism for heme import employed by HRG-1-related proteins is ancient and predates vertebrate origins.

Our assays in *C. elegans* suggest that worms have redundant mechanisms for heme uptake and transport. We showed that in addition to CeHRG-1 and CeHRG-4, two additional HRG-1 paralogs exist in worms; CeHRG-5 and CeHRG-6 are capable of heme transport in yeast. It is unclear why expressing the CeHRG-1 H90A mutant in worms causes a dominant-negative phenotype. One possibility is that HRG-1 paralogs may oligomerize as homo- and/or hetero- multimers to transport heme in *C. elegans*. If true, the physiological consequence of this would be far-reaching for a soil nematode that is a heme auxotroph. It would provide the worm with a competitive advantage in the rhizosphere by maximizing heme uptake in different environmental and nutrient conditions. Further study on the regulation and interaction of worm HRG-1 paralogs will lead to a deeper understanding of the mechanism of HRG-1-related proteins in organismal heme homeostasis.

The trafficking studies in mammalian cell lines revealed the proper topology of HRG-1-related proteins and provide the first description for how HRG-1 trafficking may be regulated in worms and humans. Assays using HRG-1 chimera mutants demonstrate that the N-terminal and C-terminal domains of HRG-1-related proteins are important for their function and localization, respectively. The N-terminal domains may be involved in the multimerization process of HRG-1-related proteins, whereas the C-terminal domains possibly direct their intracellular trafficking through the tyrosine and di-leucine based sorting motifs.

Currently, there are no pharmacological means to aid in the study of the cellular and physiological roles of eukaryotic heme transporters. We, for the first time, developed a high-throughput screen and identified potential antagonists of HRG-1-related proteins. This HTS strategy can be used to screen inhibitors targeting heme transporters in a labor and cost effective manner. The lead compounds identified in this screen will be invaluable biological tools to study the mechanism of eukaryotic heme transport. Subsequent study in parasites will provide novel drug candidates for treatment in helminths that infect humans, livestock, and plants, as well as in humans with genetic disorders of heme and iron metabolism.

Future directions

In vivo analysis of worm HRG-1 paralogs

While detailed studies have been conducted to characterize the function of CeHRG-1 and CeHRG-4 in mediating heme homeostasis, not much is known about the role of CeHRG-5 and CeHRG-6. We postulate that, since worms rely solely on exogenous heme for their growth and development, they have additional mechanisms for heme acquisition that might include CeHRG-5 and CeHRG-6. Therefore, spatial and temporal expression patterns, along with the intracellular location need to be determined for CeHRG-5 and CeHRG-6. We have identified a *cis* element, termed HEme-Responsive Element (HERE), in the promoter region of *hrg-1*, which is responsible for its heme-dependent transcriptional regulation [145]. However, this conserved HERE element is not present in the promoter regions of other *hrg-1*

paralogs. Instead, the 3' UTR might be important for the regulation of *hrg-4*. While worms expressing *hrg-4::yfp* with *hrg-4* 3' UTR had YFP expression, there was no fluorescence in the worms expressing *hrg-4::yfp* with *unc-54* 3' UTR (unpublished observations). It has been shown before that 3' UTRs are important for the downregulation of mRNA levels [175].

By contrast, the expression levels of *hrg-5* and *hrg-6* mRNAs are not responsive to heme. Interestingly, while cloning *hrg-5*, we observed that there were discrepancies between the genomic DNA and the cDNA sequences. Further studies conducted on *hrg-5* in worms suggest that this gene might undergo editing at the RNA level (unpublished observations). Investigating the effects of heme on *hrg-5* editing and analyzing *hrg-5* genomic DNA and mRNA in the *C. elegans* ADAR mutants (ADAR encodes the enzyme responsible for RNA editing by converting adenosines to inosines) will provide a better understanding of the posttranscriptional control of *hrg-5* [176]. The *hrg-6* gene, on the other hand, shares its promoter region with *hrg-4* on an opposite orientation. A graduate student in the lab, Haifa Bensaidan, has been conducting studies to determine whether *hrg-6* is regulated via *hrg-4* expression and promoter competition (unpublished observations).

These findings reveal the possibility of a complex regulatory circuit involving the regulation of *hrg-1* paralogs in *C. elegans*. The differences in regulation of individual *hrg-1* genes could provide molecular insights into their functional aspects and individual contribution to heme homeostasis within the intact animal.

In vivo analysis of human HRG-1 protein

As mentioned above, we have identified topologically conserved residues in the worm and human HRG-1 proteins despite only ≈20% amino acid identity. Although it is expected that worms need heme transporters, why do humans need HRG-1 when vertebrates make their own heme? It has been shown that some of the heme released within the macrophages after phagocytosis of senescent RBCs can be exported by FLVCR1 [63]. Carine White, a post-doctoral fellow in the Hamza lab has investigated the expression, regulation, intracellular trafficking, and activity of hHRG-1 in macrophages during erythrophagocytosis (EP). Her data reveal that the expression of *hHRG-1* is upregulated during EP and the protein localizes to the phagolysosomal membranes which surround the engulfed RBCs. Depletion of *Hrg-1* by siRNA in mouse bone marrow macrophages results in significant reduction of heme transport from the phagolysosomal compartment into the cytoplasm. In addition, the hHRG-1 P36L variant has impaired heme transport activity as determined by experiments in zebrafish and macrophages confirming our results in yeast (unpublished observations). Further studies to determine whether genetic lesions in *hHRG-1* cause unexplained anemia or iron accumulation in the reticuloendothelial system of humans are underway and could provide functional insights into the role of hHRG-1 in heme transport in mammals.

Structure-function analysis of HRG-1 proteins

The domain-swapping experiments revealed that the C-terminal domains of HRG-1-related proteins are important for their localization. Specifically, the tyrosine and di-leucine based sorting motifs may direct the localization of worm and human

HRG-1 to endo-lysosomal compartments. Interestingly, hHRG-1 has an suboptimal tyrosine based (YxxxØ) and di-leucine based (DxxIL) sorting motifs. This provides a possible explanation to the observation that, instead of basolateral localization, hHRG-1 was detected in vesicles beneath the apical plasma membrane in polarized MDCK II cells. It is plausible that the two imperfect motifs might not be strong enough to direct basolateral membrane trafficking in polarized cells. However, in non-polarized cells such as the macrophage, these motifs permit hHRG-1 to be retrieved from the plasma membrane via the DxxIL motif and localize to the endo-lysosomal compartments directed by the YxxxØ motif. Point mutations of these sorting motifs have been generated to either abolish them altogether or to make them into a strong canonical motif to explore and the trafficking of hHRG-1 in both polarized and non-polarized cells.

HRG-1-related proteins migrate as multimers on SDS-PAGE gels. Preliminary crystallography studies performed by our collaborator, Dr. Daniel Rosenbaum at UTSW, reveal that HRG-1 proteins from six different species form similar, large multimeric complexes equivalent to about 10 protomers (unpublished observations). We showed that the N-terminal domains are important for the function of HRG-1-related proteins, possibly by affecting the multimeric state. It will be interesting to analyze the crystal structures of these N-terminal mutant proteins. Furthermore, fluorescence resonance energy transfer (FRET) techniques could be applied to assess whether HRG-1-related proteins physically interact with each other to form hetero-multimers, each dictated by the corresponding N-terminus.

Identification of interacting partners

Heme uptake and transport in bacteria have been shown to involve complex molecular networks. Hence, we speculate that the HRG-1-related proteins might also be a part of an elaborate network of molecules regulating heme uptake, transport and storage. The RNAi screen of trafficking factors in the strain IQ6111 has identified a number of regulators of secretion and endocytosis that altered CeHRG-1 stability or localization in worms. Celine Vanhee, a post-doctoral fellow, is currently working on identifying interacting proteins that coimmunoprecipitate with HRG-1 in worms and mammalian cells using multidimensional protein identification technology (MudPIT). Furthermore, transcriptional profiling experiments of the *hrg-1* and *hrg-4* deletion worms grown under different heme concentrations might identify genes that are dysregulated due to disruption in heme homeostasis.

Discover potent and selective HRG-1 antagonists

We have developed and executed a high-throughput screen of 233,360 compounds for HRG-1 antagonists in a heterologous assay in yeast, and validated several leads from this screen in worms. The lead compounds will be further analyzed in our functional downstream assays. We will assess the efficacy, selectivity, and chemical liabilities (metabolism, cell permeability, toxicity) of these compounds in yeast, worms, mammalian cells and zebrafish, to ultimately develop the compounds not only as pharmacological tools but also as therapeutic agents.

Appendices

Appendix I. Yeast strains used in this study

Strain name	Genetic background	Relevant genotype	Source
DY1457	W303	W303 *MAT_ ura3-52 leu2-3,112 trp1-1 his3-11 ade6 can1-100*	
	DY1457	*hem1*::*LEU2 trp1-1 his3-11 ura3-52 can1-100*	
YPH499		*MAT*a *ura3-52 lys2-801*(amber) *ade2-101*(ocher) *trp1-63 his3-200 leu2-1*	
OPY102	YPH499	*hem1*Δ::KanMX *fre1*::*LEU2 fre2*::*HIS3*	
	YPH499	*hem1*Δ::KanMX *fre1*::*LEU2 fre2*::*HIS3 trp1-63*::*TRP1* pMET3-FRE1	This study
CeHRG-4	DY1457	*his3-11*::*HIS3* pGAL1-CeHRG-4	This study
CeHRG-4-HA	DY1457	*his3-11*::*HIS3* pGAL1-CeHRG-4-HA	This study
yhHRG-1	DY1457	*his3-11*::*HIS3* pGAL1-yhHRG-1	This study
CeHRG-414	DY1457	*his3-11*::*HIS3* pGAL1-CeHRG-414	This study
CeHRG-5	DY1457	*his3-11*::*HIS3* pGAL1-CeHRG-5	This study
CeHRG-6	DY1457	*his3-11*::*HIS3* pGAL1-CeHRG-6	This study
yLHR-1	DY1457	*his3-11*::*HIS3* pGAL1-yLHR-1	This study
yTbHRG-1	DY1457	*his3-11*::*HIS3* pGAL1-yTbHRG-1	This study
yTcHRG-1	DY1457	*his3-11*::*HIS3* pGAL1-yTcHRG-1	This study
yAceHRG-1	DY1457	*his3-11*::*HIS3* pGAL1-yAceHRG-1	This study
yBmHRG-1	DY1457	*his3-11*::*HIS3* pGAL1-yBmHRG-1	This study
yDiHRG-1	DY1457	*his3-11*::*HIS3* pGAL1-yDiHRG-1	This study
yMiHRG-1	DY1457	*his3-11*::*HIS3* pGAL1-yMiHRG-1	This study

Appendix II. Oligonucleotides used in this study

Name	Sequence (5' to 3')
CeHRG-4H14A	CTGTCAACTGATTTGTGCTATAAACGTTCGAATTGG
CeHRG-4H41A	ACATATGCAATCAAATTTGCTAATTGGTCAGCCACA
CeHRG-4Y61A	GCGTGTGAAACATTGGCTTTGTATTGGGCTTTG
CeHRG-4Y63A	GTGAAACATTGTATTTGGCTTGGGCTTTGAAGAAAAAT
CeHRG-4Y61A/Y63A	GCGTGTGAAACATTGGCTTTGGCTTGGGCTTTGAAGAAAAA
CeHRG-4C97A	CGGACTTCTCGGCGCCCTTGTTTGCTACATTAT
CeHRG-4CLV	GTCTTCTCGGACTTCTCGGCGCCGCTGCTTGCTACATTATTGCAGG
CeHRG-4H108A	TATTGCAGGAATCACTGCTCAGGGTGCAGGAT
CeHRG-4FARKY	ATGGACTTGGCAAAATGCATTCGCTGCCGCAGCAGCCCTCAACAA AATTGGAACAGCTT
CeHRG-1H40A	GCTGTACCTGGTTCGCCAGTCTGAAAGTTCAAATC
CeHRG-1Y67A	GTGTTCGCAATTCAGGCCCAAAATTGGATCGCC
CeHRG-1H88A	GCAACTCTGGTTCTCGCTCTTCACCTGGCCTA
CeHRG-1H90A	CTGGTTCTCCATCTTGCCCTGGCCTATAAGAAAAC
CeHRG-1H88A/H90A	GCAACTCTGGTTCTCGCTCTTGCCCTGGCCTATAAGAAAAC
CeHRG-1C127A	CATCGCAATGGTGTTCGCCCTGGTGGTTGCTGG
CeHRG-1CLV	TTCATTCATCGCAATGGTGTTCGCCGCGGCGGTTGCTGGAATTGAG CATCAG
CeHRG-1H135A	GTTGCTGGAATTGAGGCTCAGACGTTGGATAAG
CeHRG-1FARKY	AATGGAGTGCATTAACCTGGAGAGCTGCCGCAGCAGCCCGAGCAT TCTGTGAAGAGTCT
yhHRG-1H56A	GTGGGTTTTGGTTACTGCTGTTATGTACATGCAAG
CeHRG-1_del_f	GGCACAAGGTCCAATAGTTA
CeHRG-1_del_b	AGTCGAGCCATATGGTGCAA
CeHRG-4_del_f	CAATCAAATTTCATAATTGGTCAGC
CeHRG-4_del_b	TTAACTTTTAATGACTTCAACATCGTC

Appendix III. Genotyping of HRG-1-related deletion worms.

(A) Left: PCR analysis of genomic DNA obtained from wild-type N2 worms (lanes 1 and 3) and homozygous mutants. *hrg-1* specific primers were used in lanes 1 and 2; *hrg-4* primers were used for lanes 3 and 4. Right: PCR screening of cDNA synthesized from total RNA isolated from wild-type N2 worms and homozygous mutants. The *hrg-1* primers were used for lanes 1 and 2; *hrg-4* primers were used for lanes 3 and 4. (B) DNA sequence for *Δhrg-4* (tm2994) along with predicted amino acid sequence of the RT-PCR product. The boxed region indicates the new sequences that are added.

(Abbhirami Rajagopal and Xiaojing Yuan conducted the experiment.)

(Adapted from Yuan, X., et al., [152])

A

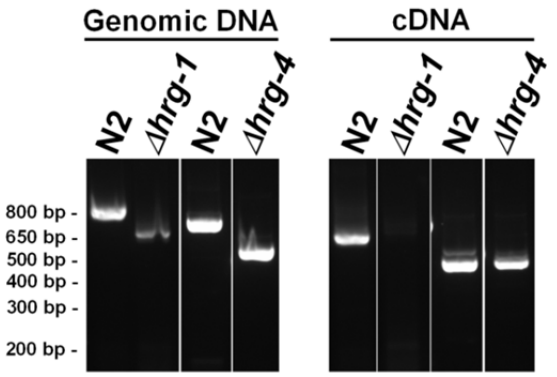

B

```
M  T  A  E  N  R  G  F  C  Q  L  I  C  H  I  N  V
ATGACTGCTGAAAATCGAGGATTCTGTCAACTGATTTGTCATATAAACGTC

R  I  G  W  T  I  F  G  I  V  F  G  I  S  A  I  L
GAATTGGATGGACAATATTTGGAATTGTTTTTGGAATATCTGCAATTTTTA

T  Y  A  I  K  F  H  N  W  S  A  T  A  T  T  A  I
ACATATGCAATCAAATTTCATAATTGGTCAGCCACAGCAACAACTGCTATT

A  T  L  F  A  C  E  T  L  Y  L  Y  W  A  L  K  K
GCTACACTTTTTGCGTGTGAAACATTGTATTTGTATTGGGCTTTGAAGAAA

N  T  I  V  N  W  K  S  S  T  F  Q  L  M  I  W  P
AATACAATTGTTAACTGGAAGAGTAGTACTTTTCAGTTGATGATATGGCCA

S  E  Y  S  N  S  *  *  I  T  C  I  N  *  *  S  R
AGTGAGTACTCTAATAGTTGATAAATTACATGCATCAATTGATAATCAAGA

F  C  V  H  N  L  N  S  N  *  L  Q  F  G  F  R  *
TTTTGCGTACACAATCTGAATTCTAATTGATTGCAATTTGGCTTAAGATGA

F  F  N  N  N  C  R  M  G  H  R  L  L  Y  A  I  F
TTTTTTAATAACAACTGTAGAATGGGACATAGATTGCTTTATGCAATTTTT

F  *  M  E  R  I  F  G  L  L  D  H  G  V  L  *  S
TTTTGAATGGAGAGAATCTTTGGTTTACTGGATCATGGAGTCTTGTGATCA

L  N  G  L  G  K  M  H  S  L  P  E  N  T  S  T  K
CTAAATGGACTTGGCAAAATGCATTCTTTGCCAGAAAATACCTCAACAAAA

L  E  Q  L  P  K  M  E  T  L  M  M  T  M  L  K  S
TTGGAACAGCTTCCGAAGATGGAGACATTGATGATGACGATGTTGAAGTCA

L  K  V
TTAAAAGTT AA
```

Appendix IV. Summary of HRG-1-related proteins intracellular localization.

Gene	Localization in HEK293 cells	Localization in MDCKII cells
CeHRG-1	Endosomal / lysosomal	Vesicles underneath the apical surface
CeHRG-4	Plasma membrane	Apical surface
hHRG-1	Endosomal / lysosomal	Vesicles underneath the apical surface
CeHRG-114	Plasma membrane	Apical surface
CeHRG-441	Endosomal / lysosomal	Vesicles underneath the apical surface
CeHRG-144	Plasma membrane	Apical surface
CeHRG-411	Endosomal / lysosomal	Vesicles underneath the apical surface
CeHRG-141	Endosomal / lysosomal	Vesicles underneath the apical surface
CeHRG-414	Plasma membrane	Apical surface
CeHRG-1ΔN	Endosomal / lysosomal	Vesicles underneath the apical surface
CeHRG-4ΔN	Plasma membrane	Apical surface
hHRG-11-Ce4	Plasma membrane	Apical surface
CeHRG-44-h1	Endosomal / lysosomal	Vesicles underneath the apical surface

(Caitlin Hall conducted the experiment.)

Bibliography

[1] M. Roche, M. Layrisse, The nature and causes of "hookworm anemia", Am J Trop Med Hyg 15 (1966) 1029-1102.

[2] R. Bungiro, M. Cappello, Hookworm infection: new developments and prospects for control, Curr Opin Infect Dis 17 (2004) 421-426.

[3] C. Menendez, E. Kahigwa, R. Hirt, P. Vounatsou, J.J. Aponte, F. Font, C.J. Acosta, D.M. Schellenberg, C.M. Galindo, J. Kimario, H. Urassa, B. Brabin, T.A. Smith, A.Y. Kitua, M. Tanner, P.L. Alonso, Randomised placebo-controlled trial of iron supplementation and malaria chemoprophylaxis for prevention of severe anaemia and malaria in Tanzanian infants, Lancet 350 (1997) 844-850.

[4] E.R. Monsen, L. Hallberg, M. Layrisse, D.M. Hegsted, J.D. Cook, W. Mertz, C.A. Finch, Estimation of available dietary iron, Am J Clin Nutr 31 (1978) 134-141.

[5] M.E. Conrad, J.N. Umbreit, Iron absorption and transport-an update, Am J Hematol 64 (2000) 287-298.

[6] C.E. Carpenter, A.W. Mahoney, Contributions of heme and nonheme iron to human nutrition, Crit Rev Food Sci Nutr 31 (1992) 333-367.

[7] A.S. Tsiftsoglou, A.I. Tsamadou, L.C. Papadopoulou, Heme as key regulator of major mammalian cellular functions: molecular, cellular, and pharmacological aspects, Pharmacol Ther 111 (2006) 327-345.

[8] O. Nakajima, S. Takahashi, H. Harigae, K. Furuyama, N. Hayashi, S. Sassa, M. Yamamoto, Heme deficiency in erythroid lineage causes differentiation arrest and cytoplasmic iron overload, EMBO J 18 (1999) 6282-6289.

[9] K. Ogawa, J. Sun, S. Taketani, O. Nakajima, C. Nishitani, S. Sassa, N. Hayashi, M. Yamamoto, S. Shibahara, H. Fujita, K. Igarashi, Heme mediates derepression of Maf recognition element through direct binding to transcription repressor Bach1, EMBO J 20 (2001) 2835-2843.

[10] P. Ponka, Cell biology of heme, Am J Med Sci 318 (1999) 241-256.

[11] L. Yin, N. Wu, J.C. Curtin, M. Qatanani, N.R. Szwergold, R.A. Reid, G.M. Waitt, D.J. Parks, K.H. Pearce, G.B. Wisely, M.A. Lazar, Rev-erbalpha, a heme sensor that coordinates metabolic and circadian pathways, Science 318 (2007) 1786-1789.

[12] M. Faller, M. Matsunaga, S. Yin, J.A. Loo, F. Guo, Heme is involved in microRNA processing, Nat Struct Mol Biol 14 (2007) 23-29.

[13] K.P. Chang, C.S. Chang, S. Sassa, Heme biosynthesis in bacterium-protozoon symbioses: enzymic defects in host hemoflagellates and complemental role of their intracellular symbiotes, Proc Natl Acad Sci U S A 72 (1975) 2979-2983.

[14] S. Dutta, K. Furuyama, S. Sassa, K.P. Chang, Leishmania spp.: delta-aminolevulinate-inducible neogenesis of porphyria by genetic complementation of incomplete heme biosynthesis pathway, Exp Parasitol 118 (2008) 629-636.

[15] A.U. Rao, L.K. Carta, E. Lesuisse, I. Hamza, Lack of heme synthesis in a free-living eukaryote, Proc Natl Acad Sci U S A 102 (2005) 4270-4275.

[16] I.J. Schultz, C. Chen, B.H. Paw, I. Hamza, Iron and porphyrin trafficking in heme biogenesis, J Biol Chem 285 (2010) 26753-26759.
[17] A. Iolascon, L. De Falco, C. Beaumont, Molecular basis of inherited microcytic anemia due to defects in iron acquisition or heme synthesis, Haematologica 94 (2009) 395-408.
[18] T.C. Cox, M.J. Bawden, A. Martin, B.K. May, Human erythroid 5-aminolevulinate synthase: promoter analysis and identification of an iron-responsive element in the mRNA, EMBO J 10 (1991) 1891-1902.
[19] G.R. Sutherland, E. Baker, D.F. Callen, V.J. Hyland, B.K. May, M.J. Bawden, H.M. Healy, I.A. Borthwick, 5-Aminolevulinate synthase is at 3p21 and thus not the primary defect in X-linked sideroblastic anemia, Am J Hum Genet 43 (1988) 331-335.
[20] R.D. Riddle, M. Yamamoto, J.D. Engel, Expression of delta-aminolevulinate synthase in avian cells: separate genes encode erythroid-specific and nonspecific isozymes, Proc Natl Acad Sci U S A 86 (1989) 792-796.
[21] B.K. May, C.R. Bhasker, M.J. Bawden, T.C. Cox, Molecular regulation of 5-aminolevulinate synthase. Diseases related to heme biosynthesis, Mol Biol Med 7 (1990) 405-421.
[22] D.F. Bishop, A.S. Henderson, K.H. Astrin, Human delta-aminolevulinate synthase: assignment of the housekeeping gene to 3p21 and the erythroid-specific gene to the X chromosome, Genomics 7 (1990) 207-214.
[23] D.F. Bishop, V. Tchaikovskii, A.V. Hoffbrand, M.E. Fraser, S. Margolis, X-linked sideroblastic anemia due to carboxyl-terminal ALAS2 mutations that cause loss of binding to the beta-subunit of succinyl-CoA synthetase (SUCLA2), J Biol Chem 287 (2012) 28943-28955.
[24] D.L. Guernsey, H. Jiang, D.R. Campagna, S.C. Evans, M. Ferguson, M.D. Kellogg, M. Lachance, M. Matsuoka, M. Nightingale, A. Rideout, L. Saint-Amant, P.J. Schmidt, A. Orr, S.S. Bottomley, M.D. Fleming, M. Ludman, S. Dyack, C.V. Fernandez, M.E. Samuels, Mutations in mitochondrial carrier family gene SLC25A38 cause nonsyndromic autosomal recessive congenital sideroblastic anemia, Nat Genet 41 (2009) 651-653.
[25] J. To-Figueras, S. Ducamp, J. Clayton, C. Badenas, C. Delaby, C. Ged, S. Lyoumi, L. Gouya, H. de Verneuil, C. Beaumont, G.C. Ferreira, J.C. Deybach, C. Herrero, H. Puy, ALAS2 acts as a modifier gene in patients with congenital erythropoietic porphyria, Blood 118 (2011) 1443-1451.
[26] P.C. Krishnamurthy, G. Du, Y. Fukuda, D. Sun, J. Sampath, K.E. Mercer, J. Wang, B. Sosa-Pineda, K.G. Murti, J.D. Schuetz, Identification of a mammalian mitochondrial porphyrin transporter, Nature 443 (2006) 586-589.
[27] J. Lynch, Y. Fukuda, P. Krishnamurthy, G. Du, J.D. Schuetz, Cell survival under stress is enhanced by a mitochondrial ATP-binding cassette transporter that regulates hemoproteins, Cancer Res 69 (2009) 5560-5567.
[28] L. Wang, F. He, J. Bu, Y. Zhen, X. Liu, W. Du, J. Dong, J.D. Cooney, S.K. Dubey, Y. Shi, B. Gong, J. Li, P.F. McBride, Y. Jia, F. Lu, K.A. Soltis, Y. Lin, P. Namburi, C. Liang, P. Sundaresan, B.H. Paw, W. Li, D.Y. Li, J.D. Phillips, Z. Yang, ABCB6 mutations cause ocular coloboma, Am J Hum Genet 90 (2012) 40-48.

[29] V. Helias, C. Saison, B.A. Ballif, T. Peyrard, J. Takahashi, H. Takahashi, M. Tanaka, J.C. Deybach, H. Puy, M. Le Gall, C. Sureau, B.N. Pham, P.Y. Le Pennec, Y. Tani, J.P. Cartron, L. Arnaud, ABCB6 is dispensable for erythropoiesis and specifies the new blood group system Langereis, Nat Genet 44 (2012) 170-173.
[30] K. Kiss, A. Brozik, N. Kucsma, A. Toth, M. Gera, L. Berry, A. Vallentin, H. Vial, M. Vidal, G. Szakacs, Shifting the paradigm: the putative mitochondrial protein ABCB6 resides in the lysosomes of cells and in the plasma membrane of erythrocytes, PLoS One 7 (2012) e37378.
[31] M.H. Barros, A. Tzagoloff, Regulation of the heme A biosynthetic pathway in Saccharomyces cerevisiae, FEBS Lett 516 (2002) 119-123.
[32] C.T. Moraes, F. Diaz, A. Barrientos, Defects in the biosynthesis of mitochondrial heme c and heme a in yeast and mammals, Biochim Biophys Acta 1659 (2004) 153-159.
[33] M.W. Hentze, M.U. Muckenthaler, B. Galy, C. Camaschella, Two to tango: regulation of Mammalian iron metabolism, Cell 142 (2010) 24-38.
[34] G.C. Shaw, J.J. Cope, L. Li, K. Corson, C. Hersey, G.E. Ackermann, B. Gwynn, A.J. Lambert, R.A. Wingert, D. Traver, N.S. Trede, B.A. Barut, Y. Zhou, E. Minet, A. Donovan, A. Brownlie, R. Balzan, M.J. Weiss, L.L. Peters, J. Kaplan, L.I. Zon, B.H. Paw, Mitoferrin is essential for erythroid iron assimilation, Nature 440 (2006) 96-100.
[35] J.D. Amigo, M. Yu, M.B. Troadec, B. Gwynn, J.D. Cooney, A.J. Lambert, N.C. Chi, M.J. Weiss, L.L. Peters, J. Kaplan, A.B. Cantor, B.H. Paw, Identification of distal cis-regulatory elements at mouse mitoferrin loci using zebrafish transgenesis, Mol Cell Biol 31 (2011) 1344-1356.
[36] P.N. Paradkar, K.B. Zumbrennen, B.H. Paw, D.M. Ward, J. Kaplan, Regulation of mitochondrial iron import through differential turnover of mitoferrin 1 and mitoferrin 2, Mol Cell Biol 29 (2009) 1007-1016.
[37] G. Srivastava, I.A. Borthwick, D.J. Maguire, C.J. Elferink, M.J. Bawden, J.F. Mercer, B.K. May, Regulation of 5-aminolevulinate synthase mRNA in different rat tissues, J Biol Chem 263 (1988) 5202-5209.
[38] A.G. Roberts, G.H. Elder, Alternative splicing and tissue-specific transcription of human and rodent ubiquitous 5-aminolevulinate synthase (ALAS1) genes, Biochim Biophys Acta 1518 (2001) 95-105.
[39] J.T. Lathrop, M.P. Timko, Regulation by heme of mitochondrial protein transport through a conserved amino acid motif, Science 259 (1993) 522-525.
[40] T.R. Bishop, M.W. Miller, J. Beall, L.I. Zon, P. Dierks, Genetic regulation of delta-aminolevulinate dehydratase during erythropoiesis, Nucleic Acids Res 24 (1996) 2511-2518.
[41] V. Mignotte, J.F. Eleouet, N. Raich, P.H. Romeo, Cis- and trans-acting elements involved in the regulation of the erythroid promoter of the human porphobilinogen deaminase gene, Proc Natl Acad Sci U S A 86 (1989) 6548-6552.
[42] S. Chretien, A. Dubart, D. Beaupain, N. Raich, B. Grandchamp, J. Rosa, M. Goossens, P.H. Romeo, Alternative transcription and splicing of the human

porphobilinogen deaminase gene result either in tissue-specific or in housekeeping expression, Proc Natl Acad Sci U S A 85 (1988) 6-10.
[43] G.I. Aizencang, D.F. Bishop, D. Forrest, K.H. Astrin, R.J. Desnick, Uroporphyrinogen III synthase. An alternative promoter controls erythroid-specific expression in the murine gene, J Biol Chem 275 (2000) 2295-2304.
[44] P.H. Romeo, N. Raich, A. Dubart, D. Beaupain, M. Pryor, J. Kushner, M. Cohen-Solal, M. Goossens, Molecular cloning and nucleotide sequence of a complete human uroporphyrinogen decarboxylase cDNA, J Biol Chem 261 (1986) 9825-9831.
[45] S. Takahashi, S. Taketani, J.E. Akasaka, A. Kobayashi, N. Hayashi, M. Yamamoto, T. Nagai, Differential regulation of coproporphyrinogen oxidase gene between erythroid and nonerythroid cells, Blood 92 (1998) 3436-3444.
[46] S. Takahashi, K. Furuyama, A. Kobayashi, S. Taketani, H. Harigae, M. Yamamoto, K. Igarashi, T. Sasaki, N. Hayashi, Cloning of a coproporphyrinogen oxidase promoter regulatory element binding protein, Biochem Biophys Res Commun 273 (2000) 596-602.
[47] K.M. de Vooght, R. van Wijk, W.W. van Solinge, GATA-1 binding sites in exon 1 direct erythroid-specific transcription of PPOX, Gene 409 (2008) 83-91.
[48] A. Tugores, S.T. Magness, D.A. Brenner, A single promoter directs both housekeeping and erythroid preferential expression of the human ferrochelatase gene, J Biol Chem 269 (1994) 30789-30797.
[49] E. Di Pierro, M.D. Cappellini, R. Mazzucchelli, V. Moriondo, D. Mologni, B. Zanone Poma, A. Riva, A point mutation affecting an SP1 binding site in the promoter of the ferrochelatase gene impairs gene transcription and causes erythropoietic protoporphyria, Exp Hematol 33 (2005) 584-591.
[50] S.T. Magness, A. Tugores, D.A. Brenner, Analysis of ferrochelatase expression during hematopoietic development of embryonic stem cells, Blood 95 (2000) 3568-3577.
[51] S. Taketani, Y. Adachi, Y. Nakahashi, Regulation of the expression of human ferrochelatase by intracellular iron levels, Eur J Biochem 267 (2000) 4685-4692.
[52] Y.L. Liu, S.O. Ang, D.A. Weigent, J.T. Prchal, J.R. Bloomer, Regulation of ferrochelatase gene expression by hypoxia, Life Sci 75 (2004) 2035-2043.
[53] S. Severance, I. Hamza, Trafficking of heme and porphyrins in metazoa, Chem Rev 109 (2009) 4596-4616.
[54] M. Shayeghi, G.O. Latunde-Dada, J.S. Oakhill, A.H. Laftah, K. Takeuchi, N. Halliday, Y. Khan, A. Warley, F.E. McCann, R.C. Hider, D.M. Frazer, G.J. Anderson, C.D. Vulpe, R.J. Simpson, A.T. McKie, Identification of an intestinal heme transporter, Cell 122 (2005) 789-801.
[55] A. Qiu, M. Jansen, A. Sakaris, S.H. Min, S. Chattopadhyay, E. Tsai, C. Sandoval, R. Zhao, M.H. Akabas, I.D. Goldman, Identification of an intestinal folate transporter and the molecular basis for hereditary folate malabsorption, Cell 127 (2006) 917-928.
[56] K.V. Salojin, R.M. Cabrera, W. Sun, W.C. Chang, C. Lin, L. Duncan, K.A. Platt, R. Read, P. Vogel, Q. Liu, R.H. Finnell, T. Oravecz, A mouse model of

hereditary folate malabsorption: deletion of the PCFT gene leads to systemic folate deficiency, Blood 117 (2011) 4895-4904.
[57] O. Dary, Nutritional interpretation of folic acid interventions, Nutr Rev 67 (2009) 235-244.
[58] A. Rajagopal, A.U. Rao, J. Amigo, M. Tian, S.K. Upadhyay, C. Hall, S. Uhm, M.K. Mathew, M.D. Fleming, B.H. Paw, M. Krause, I. Hamza, Haem homeostasis is regulated by the conserved and concerted functions of HRG-1 proteins, Nature 453 (2008) 1127-1131.
[59] I. Yanatori, M. Tabuchi, Y. Kawai, Y. Yasui, R. Akagi, F. Kishi, Heme and non-heme iron transporters in non-polarized and polarized cells, BMC Cell Biol 11 (2010) 39.
[60] K.M. O'Callaghan, V. Ayllon, J. O'Keeffe, Y. Wang, O.T. Cox, G. Loughran, M. Forgac, R. O'Connor, Heme-binding protein HRG-1 is induced by insulin-like growth factor I and associates with the vacuolar H+-ATPase to control endosomal pH and receptor trafficking, J Biol Chem 285 (2010) 381-391.
[61] S. Severance, A. Rajagopal, A.U. Rao, G.C. Cerqueira, M. Mitreva, N.M. El-Sayed, M. Krause, I. Hamza, Genome-wide analysis reveals novel genes essential for heme homeostasis in Caenorhabditis elegans, PLoS Genet 6 (2010) e1001044.
[62] J.G. Quigley, Z. Yang, M.T. Worthington, J.D. Phillips, K.M. Sabo, D.E. Sabath, C.L. Berg, S. Sassa, B.L. Wood, J.L. Abkowitz, Identification of a human heme exporter that is essential for erythropoiesis, Cell 118 (2004) 757-766.
[63] S.B. Keel, R.T. Doty, Z. Yang, J.G. Quigley, J. Chen, S. Knoblaugh, P.D. Kingsley, I. De Domenico, M.B. Vaughn, J. Kaplan, J. Palis, J.L. Abkowitz, A heme export protein is required for red blood cell differentiation and iron homeostasis, Science 319 (2008) 825-828.
[64] A.M. Rajadhyaksha, O. Elemento, E.G. Puffenberger, K.C. Schierberl, J.Z. Xiang, M.L. Putorti, J. Berciano, C. Poulin, B. Brais, M. Michaelides, R.G. Weleber, J.J. Higgins, Mutations in FLVCR1 cause posterior column ataxia and retinitis pigmentosa, Am J Hum Genet 87 (2010) 643-654.
[65] S.P. Duffy, J. Shing, P. Saraon, L.C. Berger, M.V. Eiden, A. Wilde, C.S. Tailor, The Fowler syndrome-associated protein FLVCR2 is an importer of heme, Mol Cell Biol 30 (2010) 5318-5324.
[66] E. Lalonde, S. Albrecht, K.C. Ha, K. Jacob, N. Bolduc, C. Polychronakos, P. Dechelotte, J. Majewski, N. Jabado, Unexpected allelic heterogeneity and spectrum of mutations in Fowler syndrome revealed by next-generation exome sequencing, Hum Mutat 31 (2010) 918-923.
[67] E. Meyer, C. Ricketts, N.V. Morgan, M.R. Morris, S. Pasha, L.J. Tee, F. Rahman, A. Bazin, B. Bessieres, P. Dechelotte, M.T. Yacoubi, M. Al-Adnani, T. Marton, D. Tannahill, R.C. Trembath, C. Fallet-Bianco, P. Cox, D. Williams, E.R. Maher, Mutations in FLVCR2 are associated with proliferative vasculopathy and hydranencephaly-hydrocephaly syndrome (Fowler syndrome), Am J Hum Genet 86 (2010) 471-478.
[68] E. Desuzinges-Mandon, O. Arnaud, L. Martinez, F. Huche, A. Di Pietro, P. Falson, ABCG2 transports and transfers heme to albumin through its large extracellular loop, J Biol Chem 285 (2010) 33123-33133.

[69] P. Krishnamurthy, D.D. Ross, T. Nakanishi, K. Bailey-Dell, S. Zhou, K.E. Mercer, B. Sarkadi, B.P. Sorrentino, J.D. Schuetz, The stem cell marker Bcrp/ABCG2 enhances hypoxic cell survival through interactions with heme, J Biol Chem 279 (2004) 24218-24225.
[70] H.L. Bonkovsky, J.F. Healey, A.N. Lourie, G.G. Gerron, Intravenous heme-albumin in acute intermittent porphyria: evidence for repletion of hepatic hemoproteins and regulatory heme pools, Am J Gastroenterol 86 (1991) 1050-1056.
[71] H. Puy, L. Gouya, J.C. Deybach, Porphyrias, Lancet 375 (2010) 924-937.
[72] E. Tolosano, S. Fagoonee, E. Hirsch, F.G. Berger, H. Baumann, L. Silengo, F. Altruda, Enhanced splenomegaly and severe liver inflammation in haptoglobin/hemopexin double-null mice after acute hemolysis, Blood 100 (2002) 4201-4208.
[73] C. Chen, T.K. Samuel, J. Sinclair, H.A. Dailey, I. Hamza, An intercellular heme-trafficking protein delivers maternal heme to the embryo during development in C. elegans, Cell 145 (2011) 720-731.
[74] K.D. Poss, S. Tonegawa, Heme oxygenase 1 is required for mammalian iron reutilization, Proc Natl Acad Sci U S A 94 (1997) 10919-10924.
[75] Y.A. Cao, S. Kusy, R. Luong, R.J. Wong, D.K. Stevenson, C.H. Contag, Heme oxygenase-1 deletion affects stress erythropoiesis, PLoS One 6 (2011) e20634.
[76] Z. Zhang, F. Zhang, P. An, X. Guo, Y. Shen, Y. Tao, Q. Wu, Y. Zhang, Y. Yu, B. Ning, G. Nie, M.D. Knutson, G.J. Anderson, F. Wang, Ferroportin1 deficiency in mouse macrophages impairs iron homeostasis and inflammatory responses, Blood 118 (2011) 1912-1922.
[77] J.E. Levy, O. Jin, Y. Fujiwara, F. Kuo, N.C. Andrews, Transferrin receptor is necessary for development of erythrocytes and the nervous system, Nat Genet 21 (1999) 396-399.
[78] C. Delaby, C. Rondeau, C. Pouzet, A. Willemetz, N. Pilard, M. Desjardins, F. Canonne-Hergaux, Subcellular localization of iron and heme metabolism related proteins at early stages of erythrophagocytosis, PLoS One 7 (2012) e42199.
[79] B.G. Yun, J.A. Matts, R.L. Matts, Interdomain interactions regulate the activation of the heme-regulated eIF 2 alpha kinase, Biochim Biophys Acta 1725 (2005) 174-181.
[80] T. Oyake, K. Itoh, H. Motohashi, N. Hayashi, H. Hoshino, M. Nishizawa, M. Yamamoto, K. Igarashi, Bach proteins belong to a novel family of BTB-basic leucine zipper transcription factors that interact with MafK and regulate transcription through the NF-E2 site, Mol Cell Biol 16 (1996) 6083-6095.
[81] T. Tahara, J. Sun, K. Igarashi, S. Taketani, Heme-dependent up-regulation of the alpha-globin gene expression by transcriptional repressor Bach1 in erythroid cells, Biochem Biophys Res Commun 324 (2004) 77-85.
[82] T. Tahara, J. Sun, K. Nakanishi, M. Yamamoto, H. Mori, T. Saito, H. Fujita, K. Igarashi, S. Taketani, Heme positively regulates the expression of beta-globin at the locus control region via the transcriptional factor Bach1 in erythroid cells, J Biol Chem 279 (2004) 5480-5487.

[83] H. Suzuki, S. Tashiro, S. Hira, J. Sun, C. Yamazaki, Y. Zenke, M. Ikeda-Saito, M. Yoshida, K. Igarashi, Heme regulates gene expression by triggering Crm1-dependent nuclear export of Bach1, EMBO J 23 (2004) 2544-2553.
[84] J. Sun, H. Hoshino, K. Takaku, O. Nakajima, A. Muto, H. Suzuki, S. Tashiro, S. Takahashi, S. Shibahara, J. Alam, M.M. Taketo, M. Yamamoto, K. Igarashi, Hemoprotein Bach1 regulates enhancer availability of heme oxygenase-1 gene, EMBO J 21 (2002) 5216-5224.
[85] H.J. Warnatz, D. Schmidt, T. Manke, I. Piccini, M. Sultan, T. Borodina, D. Balzereit, W. Wruck, A. Soldatov, M. Vingron, H. Lehrach, M.L. Yaspo, The BTB and CNC homology 1 (BACH1) target genes are involved in the oxidative stress response and in control of the cell cycle, J Biol Chem 286 (2011) 23521-23532.
[86] I. Barr, A.T. Smith, Y. Chen, R. Senturia, J.N. Burstyn, F. Guo, Ferric, not ferrous, heme activates RNA-binding protein DGCR8 for primary microRNA processing, Proc Natl Acad Sci U S A 109 (2012) 1919-1924.
[87] L.C. Dore, J.D. Amigo, C.O. Dos Santos, Z. Zhang, X. Gai, J.W. Tobias, D. Yu, A.M. Klein, C. Dorman, W. Wu, R.C. Hardison, B.H. Paw, M.J. Weiss, A GATA-1-regulated microRNA locus essential for erythropoiesis, Proc Natl Acad Sci U S A 105 (2008) 3333-3338.
[88] N. Felli, L. Fontana, E. Pelosi, R. Botta, D. Bonci, F. Facchiano, F. Liuzzi, V. Lulli, O. Morsilli, S. Santoro, M. Valtieri, G.A. Calin, C.G. Liu, A. Sorrentino, C.M. Croce, C. Peschle, MicroRNAs 221 and 222 inhibit normal erythropoiesis and erythroleukemic cell growth via kit receptor down-modulation, Proc Natl Acad Sci U S A 102 (2005) 18081-18086.
[89] J. Lu, S. Guo, B.L. Ebert, H. Zhang, X. Peng, J. Bosco, J. Pretz, R. Schlanger, J.Y. Wang, R.H. Mak, D.M. Dombkowski, F.I. Preffer, D.T. Scadden, T.R. Golub, MicroRNA-mediated control of cell fate in megakaryocyte-erythrocyte progenitors, Dev Cell 14 (2008) 843-853.
[90] H. Zhao, A. Kalota, S. Jin, A.M. Gewirtz, The c-myb proto-oncogene and microRNA-15a comprise an active autoregulatory feedback loop in human hematopoietic cells, Blood 113 (2009) 505-516.
[91] J.J. Chen, I.M. London, Regulation of protein synthesis by heme-regulated eIF-2 alpha kinase, Trends Biochem Sci 20 (1995) 105-108.
[92] R.N. Suragani, R.S. Zachariah, J.G. Velazquez, S. Liu, C.W. Sun, T.M. Townes, J.J. Chen, Heme-regulated eIF2alpha kinase activated Atf4 signaling pathway in oxidative stress and erythropoiesis, Blood 119 (2012) 5276-5284.
[93] J. Igarashi, M. Murase, A. Iizuka, F. Pichierri, M. Martinkova, T. Shimizu, Elucidation of the heme binding site of heme-regulated eukaryotic initiation factor 2alpha kinase and the role of the regulatory motif in heme sensing by spectroscopic and catalytic studies of mutant proteins, J Biol Chem 283 (2008) 18782-18791.
[94] C. Wandersman, I. Stojiljkovic, Bacterial heme sources: the role of heme, hemoprotein receptors and hemophores, Curr Opin Microbiol 3 (2000) 215-220.
[95] I. Stojiljkovic, D. Perkins-Balding, Processing of heme and heme-containing proteins by bacteria, DNA Cell Biol 21 (2002) 281-295.

[96] I. Stojiljkovic, K. Hantke, Transport of haemin across the cytoplasmic membrane through a haemin-specific periplasmic binding-protein-dependent transport system in Yersinia enterocolitica, Mol Microbiol 13 (1994) 719-732.
[97] C. Wandersman, Protein and peptide secretion by ABC exporters, Res Microbiol 149 (1998) 163-170.
[98] S. Letoffe, K. Omori, C. Wandersman, Functional characterization of the HasA(PF) hemophore and its truncated and chimeric variants: determination of a region involved in binding to the hemophore receptor, J Bacteriol 182 (2000) 4401-4405.
[99] S. Letoffe, V. Redeker, C. Wandersman, Isolation and characterization of an extracellular haem-binding protein from Pseudomonas aeruginosa that shares function and sequence similarities with the Serratia marcescens HasA haemophore, Mol Microbiol 28 (1998) 1223-1234.
[100] C. Caillet-Saguy, M. Piccioli, P. Turano, G. Lukat-Rodgers, N. Wolff, K.R. Rodgers, N. Izadi-Pruneyre, M. Delepierre, A. Lecroisey, Role of the iron axial ligands of heme carrier HasA in heme uptake and release, J Biol Chem 287 (2012) 26932-26943.
[101] S. Letoffe, F. Nato, M.E. Goldberg, C. Wandersman, Interactions of HasA, a bacterial haemophore, with haemoglobin and with its outer membrane receptor HasR, Mol Microbiol 33 (1999) 546-555.
[102] A.A. DeCarlo, M. Paramaesvaran, P.L. Yun, C. Collyer, N. Hunter, Porphyrin-mediated binding to hemoglobin by the HA2 domain of cysteine proteinases (gingipains) and hemagglutinins from the periodontal pathogen Porphyromonas gingivalis, J Bacteriol 181 (1999) 3784-3791.
[103] B.R. Otto, S.J. van Dooren, J.H. Nuijens, J. Luirink, B. Oudega, Characterization of a hemoglobin protease secreted by the pathogenic Escherichia coli strain EB1, J Exp Med 188 (1998) 1091-1103.
[104] C.A. Genco, D.W. Dixon, Emerging strategies in microbial haem capture, Mol Microbiol 39 (2001) 1-11.
[105] T. Olczak, W. Simpson, X. Liu, C.A. Genco, Iron and heme utilization in Porphyromonas gingivalis, FEMS Microbiol Rev 29 (2005) 119-144.
[106] E.P. Skaar, M. Humayun, T. Bae, K.L. DeBord, O. Schneewind, Iron-source preference of Staphylococcus aureus infections, Science 305 (2004) 1626-1628.
[107] T.J. Brickman, C.K. Vanderpool, S.K. Armstrong, Heme transport contributes to in vivo fitness of Bordetella pertussis during primary infection in mice, Infect Immun 74 (2006) 1741-1744.
[108] Z. Weissman, D. Kornitzer, A family of Candida cell surface haem-binding proteins involved in haemin and haemoglobin-iron utilization, Mol Microbiol 53 (2004) 1209-1220.
[109] F. Navarro-Garcia, M. Sanchez, C. Nombela, J. Pla, Virulence genes in the pathogenic yeast Candida albicans, FEMS Microbiol Rev 25 (2001) 245-268.
[110] M.L. Pendrak, M.P. Chao, S.S. Yan, D.D. Roberts, Heme oxygenase in Candida albicans is regulated by hemoglobin and is necessary for metabolism of exogenous heme and hemoglobin to alpha-biliverdin, J Biol Chem 279 (2004) 3426-3433.

[111] R. Santos, N. Buisson, S. Knight, A. Dancis, J.M. Camadro, E. Lesuisse, Haemin uptake and use as an iron source by Candida albicans: role of CaHMX1-encoded haem oxygenase, Microbiology 149 (2003) 579-588.
[112] D.H. Navarathna, D.D. Roberts, Candida albicans heme oxygenase and its product CO contribute to pathogenesis of candidemia and alter systemic chemokine and cytokine expression, Free Radic Biol Med 49 (2010) 1561-1573.
[113] M.P. Barrett, R.J. Burchmore, A. Stich, J.O. Lazzari, A.C. Frasch, J.J. Cazzulo, S. Krishna, The trypanosomiases, Lancet 362 (2003) 1469-1480.
[114] L. Koreny, J. Lukes, M. Obornik, Evolution of the haem synthetic pathway in kinetoplastid flagellates: an essential pathway that is not essential after all?, Int J Parasitol 40 (2010) 149-156.
[115] J.F. Sah, H. Ito, B.K. Kolli, D.A. Peterson, S. Sassa, K.P. Chang, Genetic rescue of Leishmania deficiency in porphyrin biosynthesis creates mutants suitable for analysis of cellular events in uroporphyria and for photodynamic therapy, J Biol Chem 277 (2002) 14902-14909.
[116] O.E. Akilov, S. Kosaka, K. O'Riordan, T. Hasan, Parasiticidal effect of delta-aminolevulinic acid-based photodynamic therapy for cutaneous leishmaniasis is indirect and mediated through the killing of the host cells, Exp Dermatol 16 (2007) 651-660.
[117] K.P. Chang, W. Trager, Nutritional significance of symbiotic bacteria in two species of hemoflagellates, Science 183 (1974) 531-532.
[118] M.P. Cupello, C.F. Souza, C. Buchensky, J.B. Soares, G.A. Laranja, M.G. Coelho, J.A. Cricco, M.C. Paes, The heme uptake process in Trypanosoma cruzi epimastigotes is inhibited by heme analogues and by inhibitors of ABC transporters, Acta Trop 120 (2011) 211-218.
[119] B. Vanhollebeke, G. De Muylder, M.J. Nielsen, A. Pays, P. Tebabi, M. Dieu, M. Raes, S.K. Moestrup, E. Pays, A haptoglobin-hemoglobin receptor conveys innate immunity to Trypanosoma brucei in humans, Science 320 (2008) 677-681.
[120] C. Huynh, X. Yuan, D.C. Miguel, R.L. Renberg, O. Protchenko, C.C. Philpott, I. Hamza, N.W. Andrews, Heme uptake by Leishmania amazonensis is mediated by the transmembrane protein LHR1, PLoS Pathog 8 (2012) e1002795.
[121] J. Campos-Salinas, M. Cabello-Donayre, R. Garcia-Hernandez, I. Perez-Victoria, S. Castanys, F. Gamarro, J.M. Perez-Victoria, A new ATP-binding cassette protein is involved in intracellular haem trafficking in Leishmania, Mol Microbiol 79 (2011) 1430-1444.
[122] D.J. Chitwood, Research on plant-parasitic nematode biology conducted by the United States Department of Agriculture-Agricultural Research Service, Pest Manag Sci 59 (2003) 748-753.
[123] D.G. Colley, P.T. LoVerde, L. Savioli, Infectious disease. Medical helminthology in the 21st century, Science 293 (2001) 1437-1438.
[124] J.S. Gilleard, Understanding anthelmintic resistance: the need for genomics and genetics, Int J Parasitol 36 (2006) 1227-1239.

[125] M.R. Held, R.D. Bungiro, L.M. Harrison, I. Hamza, M. Cappello, Dietary iron content mediates hookworm pathogenesis in vivo, Infect Immun 74 (2006) 289-295.
[126] E. Ghedin, S. Wang, J.M. Foster, B.E. Slatko, First sequenced genome of a parasitic nematode, Trends Parasitol 20 (2004) 151-153.
[127] J. Foster, M. Ganatra, I. Kamal, J. Ware, K. Makarova, N. Ivanova, A. Bhattacharyya, V. Kapatral, S. Kumar, J. Posfai, T. Vincze, J. Ingram, L. Moran, A. Lapidus, M. Omelchenko, N. Kyrpides, E. Ghedin, S. Wang, E. Goltsman, V. Joukov, O. Ostrovskaya, K. Tsukerman, M. Mazur, D. Comb, E. Koonin, B. Slatko, The Wolbachia genome of Brugia malayi: endosymbiont evolution within a human pathogenic nematode, PLoS Biol 3 (2005) e121.
[128] B. Wu, J. Novelli, J. Foster, R. Vaisvila, L. Conway, J. Ingram, M. Ganatra, A.U. Rao, I. Hamza, B. Slatko, The heme biosynthetic pathway of the obligate Wolbachia endosymbiont of Brugia malayi as a potential anti-filarial drug target, PLoS Negl Trop Dis 3 (2009) e475.
[129] R.J. Crisp, A. Pollington, C. Galea, S. Jaron, Y. Yamaguchi-Iwai, J. Kaplan, Inhibition of heme biosynthesis prevents transcription of iron uptake genes in yeast, J Biol Chem 278 (2003) 45499-45506.
[130] O. Protchenko, M. Shakoury-Elizeh, P. Keane, J. Storey, R. Androphy, C.C. Philpott, Role of PUG1 in inducible porphyrin and heme transport in Saccharomyces cerevisiae, Eukaryot Cell 7 (2008) 859-871.
[131] F. Sherman, Getting started with yeast, Methods Enzymol 194 (1991) 3-21.
[132] H. Ito, Y. Fukuda, K. Murata, A. Kimura, Transformation of intact yeast cells treated with alkali cations, J Bacteriol 153 (1983) 163-168.
[133] A. Dancis, R.D. Klausner, A.G. Hinnebusch, J.G. Barriocanal, Genetic evidence that ferric reductase is required for iron uptake in Saccharomyces cerevisiae, Mol Cell Biol 10 (1990) 2294-2301.
[134] A. Adams, D.E. Gottschling, C.A. Kaiser, T. Stearns, in Methods in yeast genetics. eds Adams A, et al (Cold Spring Harbor Press, Cold Spring Harbor), (2000) pp123-125, 133-135.
[135] G. Basu, D. Daniel, A. Rajagopal, N. Neelakantan, G.T. John, A model for human leukocyte antigen-matched donor-swap transplantation in India, Transplantation 85 (2008) 687-692.
[136] O. Protchenko, R. Rodriguez-Suarez, R. Androphy, H. Bussey, C.C. Philpott, A screen for genes of heme uptake identifies the FLC family required for import of FAD into the endoplasmic reticulum, J Biol Chem 281 (2006) 21445-21457.
[137] E. Georgatsou, D. Alexandraki, Two distinctly regulated genes are required for ferric reduction, the first step of iron uptake in Saccharomyces cerevisiae, Mol Cell Biol 14 (1994) 3065-3073.
[138] J.M. Li, H. Umanoff, R. Proenca, C.S. Russell, S.D. Cosloy, Cloning of the Escherichia coli K-12 hemB gene, J Bacteriol 170 (1988) 1021-1025.
[139] Sudha, A.V. Gopala Rao, A.R. Usha Devi, A.K. Rajagopal, Positive-operator-valued-measure view of the ensemble approach to polarization optics, J Opt Soc Am A Opt Image Sci Vis 25 (2008) 874-880.

[140] A.R. West, P.S. Oates, Mechanisms of heme iron absorption: Current questions and controversies, World J Gastroenterol 14 (2008) 4101-4110.
[141] M.D. Maines, The heme oxygenase system: update 2005, Antioxid Redox Signal 7 (2005) 1761-1766.
[142] G. Layer, J. Reichelt, D. Jahn, D.W. Heinz, Structure and function of enzymes in heme biosynthesis, Protein Sci 19 (2010) 1137-1161.
[143] Y. Tong, M. Guo, Bacterial heme-transport proteins and their heme-coordination modes, Arch Biochem Biophys 481 (2009) 1-15.
[144] A. Wilks, K.A. Burkhard, Heme and virulence: how bacterial pathogens regulate, transport and utilize heme, Nat Prod Rep 24 (2007) 511-522.
[145] J. Sinclair, I. Hamza, A novel heme-responsive element mediates transcriptional regulation in Caenorhabditis elegans, J Biol Chem 285 (2010) 39536-39543.
[146] L. Guarente, T. Mason, Heme regulates transcription of the CYC1 gene of S. cerevisiae via an upstream activation site, Cell 32 (1983) 1279-1286.
[147] T. Hon, A. Dodd, R. Dirmeier, N. Gorman, P.R. Sinclair, L. Zhang, R.O. Poyton, A mechanism of oxygen sensing in yeast. Multiple oxygen-responsive steps in the heme biosynthetic pathway affect Hap1 activity, J Biol Chem 278 (2003) 50771-50780.
[148] D.C. Goodwin, S.W. Rowlinson, L.J. Marnett, Substitution of tyrosine for the proximal histidine ligand to the heme of prostaglandin endoperoxide synthase 2: implications for the mechanism of cyclooxygenase activation and catalysis, Biochemistry 39 (2000) 5422-5432.
[149] Y. Liu, P. Moenne-Loccoz, D.P. Hildebrand, A. Wilks, T.M. Loehr, A.G. Mauk, P.R. Ortiz de Montellano, Replacement of the proximal histidine iron ligand by a cysteine or tyrosine converts heme oxygenase to an oxidase, Biochemistry 38 (1999) 3733-3743.
[150] I.E. Zohn, I. De Domenico, A. Pollock, D.M. Ward, J.F. Goodman, X. Liang, A.J. Sanchez, L. Niswander, J. Kaplan, The flatiron mutation in mouse ferroportin acts as a dominant negative to cause ferroportin disease, Blood 109 (2007) 4174-4180.
[151] J.S. Bonifacino, L.M. Traub, Signals for sorting of transmembrane proteins to endosomes and lysosomes, Annu Rev Biochem 72 (2003) 395-447.
[152] X. Yuan, O. Protchenko, C.C. Philpott, I. Hamza, Topologically conserved residues direct heme transport in HRG-1-related proteins, J Biol Chem 287 (2012) 4914-4924.
[153] E.R. Frawley, R.G. Kranz, CcsBA is a cytochrome c synthetase that also functions in heme transport, Proc Natl Acad Sci U S A 106 (2009) 10201-10206.
[154] C.J. De Feo, S.G. Aller, G.S. Siluvai, N.J. Blackburn, V.M. Unger, Three-dimensional structure of the human copper transporter hCTR1, Proc Natl Acad Sci U S A 106 (2009) 4237-4242.
[155] S.S. Merchant, His protects heme as it crosses the membrane, Proc Natl Acad Sci U S A 106 (2009) 10069-10070.
[156] G. Diallinas, Biochemistry. An almost-complete movie, Science 322 (2008) 1644-1645.

[157] S.K. Singh, C.L. Piscitelli, A. Yamashita, E. Gouaux, A competitive inhibitor traps LeuT in an open-to-out conformation, Science 322 (2008) 1655-1661.
[158] F. Raguzzi, E. Lesuisse, R.R. Crichton, Iron storage in Saccharomyces cerevisiae, FEBS Lett 231 (1988) 253-258.
[159] H.P. Bode, M. Dumschat, S. Garotti, G.F. Fuhrmann, Iron sequestration by the yeast vacuole. A study with vacuolar mutants of Saccharomyces cerevisiae, Eur J Biochem 228 (1995) 337-342.
[160] J.C. Grigg, G. Ukpabi, C.F. Gaudin, M.E. Murphy, Structural biology of heme binding in the Staphylococcus aureus Isd system, J Inorg Biochem 104 (2010) 341-348.
[161] V.A. Villareal, T. Spirig, S.A. Robson, M. Liu, B. Lei, R.T. Clubb, Transient weak protein-protein complexes transfer heme across the cell wall of Staphylococcus aureus, J Am Chem Soc 133 (2011) 14176-14179.
[162] S. Cescau, H. Cwerman, S. Letoffe, P. Delepelaire, C. Wandersman, F. Biville, Heme acquisition by hemophores, Biometals 20 (2007) 603-613.
[163] J. Yadav, S. Muend, Y. Zhang, R. Rao, A phenomics approach in yeast links proton and calcium pump function in the Golgi, Mol Biol Cell 18 (2007) 1480-1489.
[164] J.K. Brown, C. Fung, C.S. Tailor, Comprehensive mapping of receptor-functioning domains in feline leukemia virus subgroup C receptor FLVCR1, J Virol 80 (2006) 1742-1751.
[165] L. Lipovich, A.L. Hughes, M.C. King, J.L. Abkowitz, J.G. Quigley, Genomic structure and evolutionary context of the human feline leukemia virus subgroup C receptor (hFLVCR) gene: evidence for block duplications and de novo gene formation within duplicons of the hFLVCR locus, Gene 286 (2002) 203-213.
[166] Z. Yang, J.D. Philips, R.T. Doty, P. Giraudi, J.D. Ostrow, C. Tiribelli, A. Smith, J.L. Abkowitz, Kinetics and specificity of feline leukemia virus subgroup C receptor (FLVCR) export function and its dependence on hemopexin, J Biol Chem 285 (2010) 28874-28882.
[167] A. Chandy, A.S. Thakur, M.P. Singh, A. Manigauha, A review of neglected tropical diseases: filariasis, Asian Pac J Trop Med 4 (2011) 581-586.
[168] P.J. Hotez, P.J. Brindley, J.M. Bethony, C.H. King, E.J. Pearce, J. Jacobson, Helminth infections: the great neglected tropical diseases, J Clin Invest 118 (2008) 1311-1321.
[169] J. Kristjansson, S. Gudmundsson, [Neglected tropical diseases - review], Laeknabladid 97 (2011) 693-697.
[170] F.F. Norman, A. Perez de Ayala, J.A. Perez-Molina, B. Monge-Maillo, P. Zamarron, R. Lopez-Velez, Neglected tropical diseases outside the tropics, PLoS Negl Trop Dis 4 (2010) e762.
[171] P. Trouiller, E. Torreele, P. Olliaro, N. White, S. Foster, D. Wirth, B. Pecoul, Drugs for neglected diseases: a failure of the market and a public health failure?, Trop Med Int Health 6 (2001) 945-951.
[172] P. Trouiller, P. Olliaro, E. Torreele, J. Orbinski, R. Laing, N. Ford, Drug development for neglected diseases: a deficient market and a public-health policy failure, Lancet 359 (2002) 2188-2194.

[173] T. Oka, T. Toyomura, K. Honjo, Y. Wada, M. Futai, Four subunit a isoforms of Caenorhabditis elegans vacuolar H+-ATPase. Cell-specific expression during development, J Biol Chem 276 (2001) 33079-33085.
[174] K.E. Tripodi, S.M. Menendez Bravo, J.A. Cricco, Role of heme and heme-proteins in trypanosomatid essential metabolic pathways, Enzyme Res 2011 (2011) 873230.
[175] C. Merritt, D. Rasoloson, D. Ko, G. Seydoux, 3' UTRs are the primary regulators of gene expression in the C. elegans germline, Curr Biol 18 (2008) 1476-1482.
[176] L.P. Keegan, A. Leroy, D. Sproul, M.A. O'Connell, Adenosine deaminases acting on RNA (ADARs): RNA-editing enzymes, Genome Biol 5 (2004) 209.